

Classical-Quantum Combs, their Min-Entropy and their Measurement-Based Applications

Isaac D. Smith, Marius Krumm, Lukas J. Fiderer, Hendrik Poulsen Nautrup, and Hans J. Briegel

Institute for Theoretical Physics, UIBK, 6020 Innsbruck, Austria

Learning a hidden property of a quantum system typically requires a series of interactions. In this work, we consider a formalisation of such multi-round learning processes that uses a generalisation of classical-quantum states, called classical-quantum combs. Here, “classical” refers to a random variable encoding the hidden property to be learnt, and “quantum” refers to the quantum comb describing the behaviour of the system. By using the quantum combs formalism, the optimal strategy for learning the hidden property can be quantified via the comb min-entropy (Chiribella and Ebler, *NJP*, 2016). With such a tool on hand, we focus attention on an array of combs derived from measurement-based quantum computation (MBQC) and related applications. Specifically, we describe a known blind quantum computation (BQC) protocol using the combs formalism and thereby leverage the min-entropy to provide a proof of single-shot security for multiple rounds of the protocol, extending the existing result in the literature. Furthermore, we introduce novel connections between MBQC and quantum causal models and quantum causal inference, which allows for the use of the min-entropy to quantify the optimal strategy for causal discovery. We consider further operationally motivated examples, including one associated to learning a quantum reference frame.

1 Introduction

With the rapid development of quantum technology, a plethora of increasingly complex quantum devices has become available. Already, a range of noisy-intermediate scale quantum computers (NISQ) [1] are accessible via the internet. Year on year, these devices increase in size and quality, as evidenced by the growing number of addressable qubits, the lengthening coherence times and improving gate fidelity.

An important parallel development to that of the devices themselves, is in how they interconnect. The current and future progress of quantum communication networks [2–11] aims to create a global quantum internet of networked

quantum computers [12, 13], with the attendant benefits in communication and cryptography. Current implementations of such networks largely focus on protocols for quantum key distribution, however a variety of other significant applications appear to be feasible in the near-term, including distributed quantum computation [14, 15], quantum position verification [16], and blind quantum computation [17].

With the increasing sophistication of quantum networks, a full description using the usual quantum formalism becomes intractable. Consequently, other formalisms are being developed that allow for the description of the relevant parts of complex networks whilst remaining numerically and analytically manageable. One particularly promising such formalism represents networks as *quantum causal models* [18–20], in which the connectivity of the network is faithfully represented but the nodes are freely described by any quantum device. This allows for investigating the statistics of the network under varying quantum protocols at the nodes. The quantum causal modelling formalism is a quantum generalisation of the sub-field of statistics and machine learning known as (classical) causal modelling, which has been successfully applied to modelling complex systems in various classical domains, such as medicine, social science, and engineering [21, 22].

One key object of study in the quantum causal networks literature [23, 24] is known as a *quantum comb*. Quantum combs naturally model multi-round quantum communication protocols, and can be understood as a concatenation of quantum channels where some information may be input and output from the comb at each time-step and some may remain within the comb (and inaccessible) between time-steps. These combs are represented by operators acting on the input and output spaces only, which constitutes a distinct advantage of their use: any forwarding of information between time-steps is modelled by an operator of the same size. As such, they can model arbitrary sequential interactions with a quantum environment, and have consequently become a fruitful tool to describe e.g. non-Markovian noise [25].

A crucial discovery of the field of quantum causal networks is that the optimisation of multi-round quantum communication protocols can be framed as a *semi-definite program* [26], where the optimisation can be with respect to a range of different performance measures. For

a given measure, the resultant optimal success probability leads to a notion of min-entropy for quantum combs, which generalises the min-entropy of quantum states [27] in quantum cryptography. In this work, we consider a performance measure based on learning a hidden classical parameters of quantum networks, which are modelled as classical-quantum combs: generalisations of classical-quantum states [28] where a series of quantum combs are indexed by a classical parameter. We analyse properties of combs of this form and investigate a range of examples based on measurement-based quantum computation.

Measurement-based quantum computing (MBQC) [29–34] is a well-known paradigm for quantum computation distinct from the circuit model formalism. It consists of a sequential interaction with a quantum state (via time-ordered single qubit measurements) and forms the basis of a range of cryptographic computation protocols within the sub-field of quantum cryptography known as blind quantum computation (BQC) [17, 35–38]. Due to existing characterisations of the components of MBQC, such as graph states [39–42] (see also [43]) and the sequence of measurements [32, 44–47], as well as to the connection with stabiliser quantum mechanics [48, 49], investigations into certain aspects of MBQC remain tractable despite its multi-partite, high-dimensional nature. As such, MBQC provides an exemplary test-bed for the application of the quantum causal networks framework.

The first comb we consider models a specific BQC protocol, that of Mantri et al. [36]. This protocol consists of entirely classical communication between a client and a (quantum) server, allowing the client to obtain the results of a quantum computation while maintaining no quantum capabilities. The classical parameter in this context encodes the secret choice of computation by the client which an untrustworthy server may attempt to discover. Due to the restriction to classical communication, the quantum comb part of the classical-quantum comb, the part that models a round of the protocol, is actually classical (i.e. we consider a classical-classical comb). The security of the protocol is analysed by calculating the min-entropy of this comb, which has the interpretation of quantifying how much information the server has yet to learn about the choice of computation when using the most informative strategy. We provide a security analysis both for a single round and for multiple rounds, thereby extending the analysis of the original paper [36].

We then consider a range of classical-quantum combs where the comb component is truly quantum. In particular, we investigate a variety of related scenarios where an unknown device performing a measurement-based computation is interacted with in order to gain some piece of information regarding its internal functioning. In all these scenarios, the classical-quantum combs are built from a comb based upon the method of measurement adaptation required for MBQC [44, 45]. We demonstrate that this base comb satisfies the conditions of a quantum causal model [20] and moreover, we explicate an interpretation of MBQC in the context of quantum

causal inference [50], thereby establishing novel connections between MBQC and quantum causality [18–20, 50–53]. One classical-quantum comb we consider explicitly utilises this connection: the classical parameter encodes the different possible causal structures and the comb min-entropy quantifies the optimal causal inferential strategy. Finally, two examples are considered, each concerned with learning an aspect of the MBQC device required for its proper use: in one case, learning the types of measurement that ensure deterministic computation, and in the other, calibrating measurement devices to ensure the correct computation is performed. The latter has an interesting interpretation as learning a quantum reference frame [54].

The remainder of this paper is structured as follows. The next subsection provides a brief and informal presentation of the key results in this work. In Section 2, the required background knowledge regarding the formalisms of MBQC and quantum combs is presented. We introduce and motivate the comb min-entropy in Section 3, including some results regarding the min-entropy for classical-classical combs in Section 3.1. Section 4 outlines the BQC protocol of [36] (Section 4.1), defines the corresponding classical comb (Section 4.2), and conducts an analysis of the security of the protocol (Section 4.3 and Section 4.4). Section 5 contains the definition of the comb describing the corrections required for MBQC (Section 5.1), a discussion of the connection to quantum causal models and inference (Section 5.2), and an analysis of a series of examples (Section 5.3, Section 5.4 and Section 5.5). Section 6 discusses the future applications and limitations of the methods presented in this work and concludes.

1.1 Our Contributions

The following is a more specific, but informal, summary of the key contributions of this paper.

- Proposition 3.2 establishes upper and lower bounds for the min-entropy for classical-quantum combs where the quantum combs are all diagonal in the same basis (i.e. classical-classical combs). These bounds have an interpretation in terms of maximal Bayesian updating, an interpretation which extends from the analogous case for the state min-entropy (i.e. classical-classical states). These bounds play a role in the security proof of the BQC protocol in Section 4.
- Theorem 4.2 establishes that the BQC protocol of [36] is (partially) secure in a single-round by proving a general lower bound on the min-entropy of the secret choice of computation given the interactions via the protocol. This lower bound is strictly positive, indicating that the secret computation cannot be known with certainty after only a single round, even if the optimal strategy is used. This result extends the existing result [Theorem 2, 36] via use of

the min-entropy as opposed to the Shannon entropy. Furthermore, we give a simple example that obtains the lower bound, which gives some indication of its tightness.

- Similarly, Theorem 4.3 provides a positive lower bound for the min-entropy under any number of rounds of the protocol, demonstrating that the server will remain uncertain about at least some aspect of the computation even if the protocol is repeated. We use the same example as for the single-round case to demonstrate that the min-entropy can strictly decrease between rounds, indicating that more information is leaked in the multi-round case in general.
- Proposition 5.1 establishes the connection between MBQC and quantum causal models, by demonstrating that the conditional adaptation channels defined by gflow [44] satisfy the required commutation conditions of the channels defining a quantum causal model.
- The above connection allows us, via the min-entropy, to frame quantum causal discovery as a semi-definite program, thereby establishing a new tool in the quantum causal inference toolbox. We use this approach to numerically quantify the optimal causal inferential strategy for a given example.
- We demonstrate that in certain circumstances, not even the optimal strategy can learn anything about the causal structure such as when the possible causal structures are related by symmetries. Proposition 5.2 establishes this fact for when the causal structures are given by gflows that are related by symmetries of the underlying graph state.

2 Preliminaries

This section introduces the background information regarding quantum combs and measurement-based quantum computation as required for the introduction of the comb min-entropy in Section 3 and the applications presented in Section 4 and Section 5. Some emphasis is placed on aspects of the discourse deemed important for the sequel, otherwise the aim is for brevity without sacrificing completeness.

2.1 Multi-round Quantum Protocols: Quantum Combs

The standard framework for quantum information theory typically consists of density matrices, positive operator-valued measures (POVMs) and quantum channels (completely positive trace-preserving maps) to describe the processing of quantum information. Each of these can be defined for or act upon multiple quantum systems, can

be composed, and moreover, can be composed on subsystems, such as when two quantum channels are composed over the domain of the latter and a subsystem of the co-domain of the former. Quantum networks, separated nodes with quantum processing capabilities and interconnected via quantum communication, can be modelled via an array of such compositions of quantum channels. In fact, it was realised [23, 24] that it is always possible to represent a quantum network in a canonical form, namely as a sequence of channels with memory, where some of the output of each channel is passed directly as input to the next, and some is available for arbitrary processing as depicted in Figure 1. Such a sequence comes with an explicit ordering on inputs and outputs of the network, from which the interpretation of interacting with a quantum system over multiple time steps can be naturally understood. Throughout this work, we use standard notation: \mathcal{H}_A denotes a Hilbert space for system A , $\mathcal{L}(\mathcal{H}_A)$ the space of linear operators on that space, ρ_A a state of \mathcal{H}_A , $\mathcal{E} : \mathcal{L}(\mathcal{H}_A) \rightarrow \mathcal{L}(\mathcal{H}_B)$ for a CPTP map, and so on.

Instead of explicitly working with a quantum network as a sequence of channels, it is convenient to work with the corresponding operator, a quantum comb, which is a generalisation of the Choi operator [55, 56] to a sequence of quantum channels. A quantum comb is an operator on a Hilbert space consisting of the tensor product of all input spaces $\mathcal{H}_j^{\text{in}}$ and output spaces $\mathcal{H}_j^{\text{out}}$. Each interaction with the system is associated to an input-output pair of Hilbert spaces, between which a quantum instrument can be inserted specifying the interaction. The distinction between input and output is indicated by superscripts in the notation, with time-steps indicated by subscripts. We take the following as our definition of quantum comb, which is sometimes presented as a theorem establishing the connection to quantum networks instead (see e.g. [Theorem 1, 24], [Theorem 3, 23]):

Definition 2.1. A **quantum comb** is a positive semi-definite operator $D \in \mathcal{L}\left(\bigotimes_{j=1}^n \mathcal{H}_{A_j^{\text{in}}} \otimes \mathcal{H}_{A_j^{\text{out}}}\right)$ for which there exists a sequence of positive semi-definite operators $D_k \in \mathcal{L}\left(\bigotimes_{j=1}^k \mathcal{H}_{A_j^{\text{in}}} \otimes \mathcal{H}_{A_j^{\text{out}}}\right)$, $k = 0, \dots, n$ which satisfy

$$\text{Tr}_{A_k^{\text{out}}} [D_k] = I_{A_k^{\text{in}}} \otimes D_{k-1} \quad \forall k \in \{1, \dots, n\}, \quad (1)$$

with $D_n = D$ and $D_0 = 1$. A comb D is called **un-normalised** if D_0 instead satisfies the relaxed constraint $D_0 > 0$.

The partial trace conditions in the above definition correspond to enforcing trace preservation of the individual component channels and positive semi-definiteness enforces complete positivity (for a more thorough explanation, see Appendix A.1 or [23, 24]). Since we also consider combs in this work that are classical, which is to say diagonal, it is useful to have an explicit definition for later reference:

Definition 2.2. A positive semi-definite operator $C \in \mathcal{L}\left(\bigotimes_{j=1}^n \mathcal{H}_{A_j^{\text{in}}} \otimes \mathcal{H}_{A_j^{\text{out}}}\right)$ is a **classical comb** if it can be

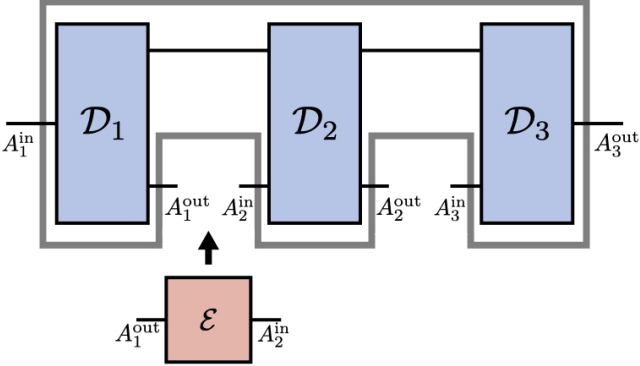


Figure 1: A quantum comb is a representation of a quantum system evolving over multiple time-steps. An example of a comb D (grey outline) is shown, corresponding to the sequence of quantum channels $\mathcal{D}_1, \mathcal{D}_2, \mathcal{D}_3$, each representing the evolution of the system between adjacent time-steps. Interaction with the system at a given time-step can also be represented by a quantum channel, here denoted \mathcal{E} .

written as

$$C = \sum_{\mathbf{a}^{\text{in}}, \mathbf{a}^{\text{out}}} f(\mathbf{a}^{\text{out}}, \mathbf{a}^{\text{in}}) |\mathbf{a}^{\text{in}}, \mathbf{a}^{\text{out}}\rangle \langle \mathbf{a}^{\text{in}}, \mathbf{a}^{\text{out}}| \quad (2)$$

where $\{|\mathbf{a}^{\text{in}}, \mathbf{a}^{\text{out}}\rangle\}$ is an orthonormal basis for the Hilbert space and where f is a non-negative function for which there exists a sequence of non-negative functions $f^{(k)}$, $k = 0, \dots, n$ that satisfy, for all $j = 2, \dots, n$:

$$\begin{aligned} \sum_{a_j^{\text{out}}} f^{(j)}(a_1^{\text{out}}, \dots, a_j^{\text{out}}, a_1^{\text{in}}, \dots, a_j^{\text{in}}) \\ = f^{(j-1)}(a_1^{\text{out}}, \dots, a_{j-1}^{\text{out}}, a_1^{\text{in}}, \dots, a_{j-1}^{\text{in}}) \end{aligned} \quad (3)$$

with $f^{(n)} = f$ and $f^{(0)} := \sum_{a_1^{\text{out}}} f^{(1)}(a_1^{\text{out}}, a_1^{\text{in}}) > 0$. If $f^{(0)} = 1$ then the comb is normalised, otherwise it is unnormalised.

The conditions described in Equation (3) are a simple rewriting of the trace conditions in Equation (1). In the case where the classical comb is normalised, it is most intuitive to write $f(\mathbf{a}^{\text{out}}, \mathbf{a}^{\text{in}})$ as a conditional probability distribution $P(\mathbf{a}^{\text{out}}|\mathbf{a}^{\text{in}})$ and the conditions of Equation (3) then detail independence conditions on this distribution under sequential marginalisation of the a_j^{out} . Note that these distributions can be understood as observable quantities by using C simply as a channel, i.e. by inputting all \mathbf{a}^{in} at once and collecting statistics of the outputs.

We use the notation $\text{Comb}(A_1^{\text{in}} \rightarrow A_1^{\text{out}}, \dots, A_n^{\text{in}} \rightarrow A_n^{\text{out}})$ to denote the set of all combs on $\bigotimes_{j=1}^n \mathcal{H}_{A_j^{\text{in}}} \otimes \mathcal{H}_{A_j^{\text{out}}}$, including unnormalised combs. It will be clear from context, whether we are considering classical combs only for a specific example. If a given input or output space is 1-dimensional, the corresponding $A_j^{\text{in}/\text{out}}$ is replaced with \mathbb{C} . For example, we will often consider combs where the first input space is 1-dimensional, that is, elements of $\text{Comb}(\mathbb{C} \rightarrow A_1^{\text{out}}, \dots, A_n^{\text{in}} \rightarrow A_n^{\text{out}})$.

For later sections, particularly Section 5, it is useful to use the following notation, which provides a convenient way of writing the contraction of a comb with a compatible operator (for example, for contracting \mathcal{E} with the comb in Figure 1).

Definition 2.3 ([23]). For two operators $M \in \mathcal{L}(\mathcal{H}_A \otimes \mathcal{H}_B)$ and $N \in \mathcal{L}(\mathcal{H}_B \otimes \mathcal{H}_C)$, the **link product** is defined as:

$$M * N := \text{Tr}_B [(M^{T_B} \otimes I_C) \cdot (I_A \otimes N)], \quad (4)$$

where T_B denotes the partial transpose over the system B .

In this work, we consider the comb extension of classical-quantum states, called classical-quantum combs, which consist of a series of combs indexed by a classical random variable. Explicitly, we consider operators of the form

$$D = \sum_{x \in X} P(x) |x\rangle\langle x| \otimes \sigma_x \quad (5)$$

which is an element in $\text{Comb}(A_1^{\text{in}} \rightarrow A_1^{\text{out}}, \dots, A_n^{\text{in}} \rightarrow A_n^{\text{out}}, \mathbb{C} \rightarrow X)$ where X is a (finite, discrete) random variable with outcomes defining an orthonormal basis $\{|x\rangle\}_x$ of the $|X|$ -dimensional Hilbert space \mathcal{H}_X , and where the σ_x are in combs in $\text{Comb}(A_1^{\text{in}} \rightarrow A_1^{\text{out}}, \dots, A_n^{\text{in}} \rightarrow A_n^{\text{out}})$. Note that, even though the state corresponding to \mathcal{H}_X is written on the left in D , \mathcal{H}_X is always taken to be the last output space of quantum comb, in order to be compatible with the comb min-entropy defined below.

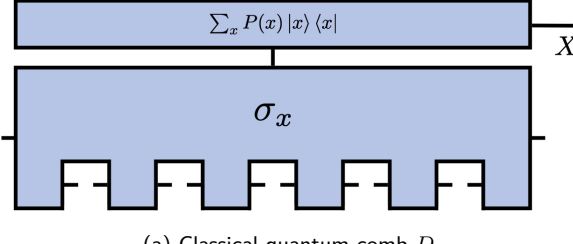
The appropriate perspective to take of D for the remainder of this work, which is elaborated upon below, is that we aim to learn something about the classical state on X by interacting only with the σ_x , i.e. we only have access to the spaces $\mathcal{H}_{A_1^{\text{in}}}, \dots, \mathcal{H}_{A_n^{\text{out}}}$ and not \mathcal{H}_X . This is portrayed in the pictorial representation of D in Figure 2a, where the lower part of the comb is accessible and the upper part is not.

It is important to note that, due to the special form that D takes, it is both an element of $\text{Comb}(A_1^{\text{in}} \rightarrow A_1^{\text{out}}, \dots, A_n^{\text{in}} \rightarrow A_n^{\text{out}}, \mathbb{C} \rightarrow X)$ and an element of $\text{Comb}(\mathbb{C} \rightarrow X, A_1^{\text{in}} \rightarrow A_1^{\text{out}}, \dots, A_n^{\text{in}} \rightarrow A_n^{\text{out}})$, as demonstrated by the proof of the following result (given in Appendix A.1).

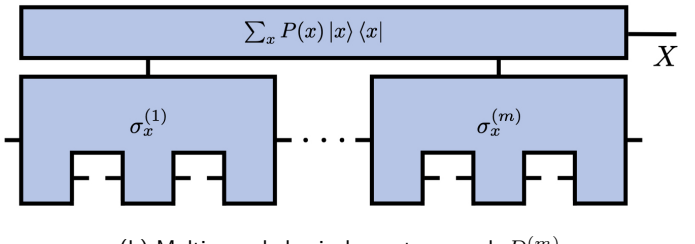
Proposition 2.1. *The operator D as above is an element of both $\text{Comb}(A_1^{\text{in}} \rightarrow A_1^{\text{out}}, \dots, A_n^{\text{in}} \rightarrow A_n^{\text{out}}, \mathbb{C} \rightarrow X)$ and $\text{Comb}(\mathbb{C} \rightarrow X, A_1^{\text{in}} \rightarrow A_1^{\text{out}}, \dots, A_n^{\text{in}} \rightarrow A_n^{\text{out}})$.*

This result is significant for our purposes since the latter inclusion highlights that there is no back-in-time signalling from the inputs of the σ_x to the output at X (cf. [Section III.C, 23]), a fact that is explicitly used in Section 3.1.

At times, we consider interactions with a system that occur in a series of rounds, where the evolution of the system between rounds is independent except for a common



(a) Classical-quantum comb D



(b) Multi-round classical-quantum comb $D^{(m)}$

Figure 2: In this work, we consider an extension to classical-quantum states, called classical-quantum combs, where a classical random variable X indexes a set of quantum combs σ_x (rather than quantum states). (a) The variable X is considered to be unknown and as such is represented as an inaccessible system (upper part). The combs σ_x are contingent on the value of X and describe the dynamics of a system which can be interacted with (lower part) over a series of time-steps. By interacting with the accessible system, updated knowledge of X can be obtained. (b) Some interactions are naturally modelled as a series of separate rounds, which are independent apart from the dependence on X . This is represented by taking each round to be a separate comb $\sigma_x^{(j)}$ which have no direct influence on later rounds. An example of such a multi-round interaction is the BQC protocol presented in Section 4.

dependence on the parameter X (this is represented in Figure 2b). For example, repeated instances of a multi-step cryptographic protocol can be considered in this way (see Section 4). Despite being able to represent these interactions using D above, where independence of rounds is merely an extra constraint on the σ_x , we find it more convenient to use σ_x to denote a single round, and write the multi-round operator as follows (the round number is indicated by the superscript in brackets):

$$D^{(m)} := \sum_{x \in X} P(x) |x\rangle\langle x| \otimes \bigotimes_{j=1}^m \sigma_x^{(j)} \quad (6)$$

which is an operator in Comb $((A_1^{\text{in}})^{(1)} \rightarrow (A_1^{\text{out}})^{(1)}, \dots, (A_n^{\text{in}})^{(m)} \rightarrow (A_n^{\text{out}})^{(m)}, \mathbb{C} \rightarrow X)$.

2.2 MBQC and Gflow

Measurement-based quantum computation [29–33] is a model for quantum computation distinct from the circuit picture, where, as the name indicates, the computation is driven by measurement operations rather than unitary ones. One can consider MBQC as consisting of three components: a highly entangled state, namely a graph state, which is the substrate that supports the computation; a sequence of single qubit projective measurements parametrised by an angle in a plane of the Bloch sphere, the positive outcomes of which encode the desired computation; and a correction method which ensures the desired computation is performed even when negative outcomes are obtained. The latter refers to the notion of gflow [44, 45] which plays a key role in the blind quantum computing protocol of [36] as well as in Section 4 and Section 5 below. In this subsection, each of these three components is introduced, with emphasis on the latter due to its importance in the sequel.

Graph states take their name from the connection to mathematical graphs. Let G be a (simple, connected) graph on vertex set $V = \{1, \dots, n\}$ and edge set E . One

can define a graph state, denoted $|G\rangle$, as

$$|G\rangle := \prod_{(i,j) \in E} CZ_{ij} |+\rangle^{\otimes n} \quad (7)$$

where each vertex of the graph is assigned a qubit in the $|+\rangle$ state and where each edge (i, j) in the graph is associated to a controlled Pauli-Z gate, denoted CZ_{ij} , between the corresponding qubits. Equivalently, $|G\rangle$ can be specified as the unique stabiliser state of the set of stabilisers [57] generated by

$$\left\{ K_v := X_v \bigotimes_{v' \in N_v^G} Z_{v'} \mid v \in V \right\} \quad (8)$$

where N_v^G denotes the set of neighbours of v in G . The stabiliser picture of graph states is a fruitful one since the correction of negative measurement outcomes relies upon the associated symmetries (see below). We will use the notation ρ_G for $|G\rangle\langle G|$.

The single qubit measurements are restricted to projective measurements defined by states that lie in the intersection of the Bloch sphere with the XY -, XZ - and YZ -planes. When it is necessary to specify a particular measurement, we denote the corresponding projectors as $|+\alpha\rangle\langle +\alpha|_{\text{mp}}$ and $|-\alpha\rangle\langle -\alpha|_{\text{mp}}$ where $\text{mp} \in \{XY, XZ, YZ\}$ and $\alpha \in [0, 2\pi)$ specifies the angle from one of the axes in the plane. For example, $|+\alpha\rangle_{XY} = \frac{1}{\sqrt{2}}(|0\rangle + e^{-i\alpha}|1\rangle)$. If no measurement plane label is given, it should be understood as being an XY -plane measurement, as this is the most commonly treated type of measurement in this work. For a fixed graph state $|G\rangle$, the computation is specified by stipulating an angle α_v and measurement plane for each qubit/vertex v .

The key observation for understanding why the restriction to only these planes is made, and also how the correction procedure given by gflow (outlined below) works, is the following set of relations, which hold for all values

of α :

$$\begin{aligned} |-\alpha\rangle\langle-\alpha|_{XY} &= Z^\dagger |+\alpha\rangle\langle+\alpha|_{XY} Z; \\ |-\alpha\rangle\langle-\alpha|_{XZ} &= (XZ)^\dagger |+\alpha\rangle\langle+\alpha|_{XZ} XZ; \\ |-\alpha\rangle\langle-\alpha|_{YZ} &= X^\dagger |+\alpha\rangle\langle+\alpha|_{YZ} X. \end{aligned} \quad (9)$$

Here, one should note that each of the associated unitaries (X , Z or their product) appears naturally in the K_v stabilisers for $|G\rangle$ (or a product thereof). One can thus interpret the occurrence of a negative outcome as equivalent to first applying a Z (or X or XZ) to the graph state and then receiving the correct (positive) measurement outcome. Applying such a gate to the graph state alone changes the computation, however applying the remainder of a stabiliser, of which the Z , X or XZ term is constituent, completes a symmetry of the graph state and so the negative measurement outcome is effectively transformed into a positive one. Since the evolution of a state to be measured can equivalently be considered as the evolution of the measurement observables themselves, we can in fact apply the remainder of the stabiliser to the other measurement operators, leaving the graph state untouched. This is significant, since, due to the form of the stabiliser operators and the properties of the measurement operators, the application of the stabiliser can be affected by an appropriate change to the measurement angle. For example, the measurement projectors in the XY -plane (the other measurement planes follow similar patterns), we have the following:

$$\begin{aligned} X^\dagger |\pm_\alpha\rangle\langle\pm_\alpha|_{XY} X &\equiv |\pm_{-\alpha \bmod 2\pi}\rangle\langle\pm_{-\alpha \bmod 2\pi}|_{XY}; \\ Z^\dagger |\pm_\alpha\rangle\langle\pm_\alpha|_{XY} Z &\equiv |\pm_{\alpha+\pi \bmod 2\pi}\rangle\langle\pm_{\alpha+\pi \bmod 2\pi}|_{XY}. \end{aligned} \quad (10)$$

So, applying the remainder of a stabiliser to such measurements amounts to applying appropriate reflections or adding π phases to the original measurement angles. We thus have two equivalent perspectives for the correction of measurements, both of which play a role in this paper: corrections can either be implemented via applying (conditional) unitaries to the graph state or via adjustments to the classical measurement parameters. The latter perspective is most relevant for Section 4 where as the former is used in Section 5. Due to the importance of this equivalence for this work, a more thorough explanation is provided in Appendix A.2, which is particularly useful for motivating the discourse in Section 5.

To summarise: computations on a graph state are specified by positive outcomes of single qubit measurements; measurements are restricted to measurement planes that exhibit useful symmetries; and negative outcomes are treated via conditional applications of certain symmetries of the graph state. To ensure deterministic computation, the appropriate symmetries are required for every measurement, and the conditionality of their application induces an order in which the measurements must be performed. However, for any given graph state, not every choice of symmetry and measurements order are consistent (i.e. one cannot adapt a measurement that has already been performed). The definition of gflow below

addresses this point: a gflow assigns to every measured qubit a choice of corrective stabiliser and assigns a (partial) order of measurements which ensures consistency.

Definition 2.4 ([44]). Let $G = (V, E)$ be a graph, I and O be input and output subsets of V respectively, and $\omega : O^c \rightarrow \{XY, XZ, YZ\}$ be a map assigning measurement planes to qubits (the superscript c denotes set complement). The tuple (G, I, O, ω) has **gflow** if there exists a map $g : O^c \rightarrow \mathcal{P}(I^c)$, where \mathcal{P} denotes the powerset, and a partial order over V such that the following hold for all $v \in O^c$:

1. if $v' \in g(v)$ and $v' \neq v$, then $v < v'$;
2. if $v' \in \text{Odd}(g(v))$ and $v' \neq v$, then $v < v'$;
3. if $\omega(v) = XY$, then $v \notin g(v)$ and $v \in \text{Odd}(g(v))$;
4. if $\omega(v) = XZ$, then $v \in g(v)$ and $v \in \text{Odd}(g(v))$;
5. if $\omega(v) = YZ$, then $v \notin g(v)$ and $v \notin \text{Odd}(g(v))$;

where $\text{Odd}(K) := \{\tilde{v} \in V : |N_{\tilde{v}}^G \cap K| = 1 \bmod 2\}$ for any $K \subseteq V$.

It is known that the presence of gflow is both necessary and sufficient for deterministic MBQC [Theorems 2 and 3, 44]. Furthermore, polynomial time algorithms exist for determining whether a given tuple (G, I, O, ω) supports gflow [58, 59]. Many distinct gflows for a given (G, I, O, ω) can exist, and characterising or counting all gflows for a given graph (as the input and output sets vary) in general remains an open problem.

We can understand this definition in light of the discussion preceding it as follows. The map g assigns a (product of) stabiliser(s) to each qubit being measured: $g(v)$ is a subset of V and identifies the stabiliser

$$K_{g(v)} := \prod_{w \in g(v)} K_w.$$

Every element in the set $g(v)$ receives an X -correction from the above product and every element of $\text{Odd}(g(v))$ receives a Z -correction; the vertices in their intersection will receive both. The partial order and the first two conditions enforce that every correction conditioned on the measurement at v happens in the future of that measurement. The remaining three conditions enforce that the component of the product that acts on the qubit v is precisely the required symmetry associated to the measurement plane $\omega(v)$, as given in Equation (9).

Derived from the definition of gflow, it is useful to define, for each $v \in V$, the set of vertices whose corrections induce an X -operation on v and the set whose correction induce a Z -operation:

$$\begin{aligned} \mathcal{X}_v &:= \{v' \in V : v \in g(v') \setminus \{v\}\}; \\ \mathcal{Z}_v &:= \{v' \in V : v \in \text{Odd}(g(v')) \setminus \{v\}\}. \end{aligned} \quad (11)$$

We allow for \mathcal{X}_v or \mathcal{Z}_v to be empty (such as when $v \in I$ for example).

3 Quantum Comb Min-Entropy

In this section, we introduce and motivate the primary tool of analysis used in the remainder of this work: the comb min-entropy [26]. This entropic quantity is an extension of the min-entropy for quantum states (see e.g. [27, 60–62]), a well-understood information-theoretic quantity with interpretations relating to maximal guessing probability of a random variable or the maximal singlet fraction achievable from a quantum state [27]. Below, we consider the operational meaning of the comb min-entropy, with particular emphasis on the cases relevant for subsequent sections, namely for combs of the forms given in Equations (5) and (6).

We commence by stating the definition of the comb min-entropy via three equivalent characterisations, and then contextualise these in the subsequent discussion.

Definition 3.1 ([26]). Let $D \in \text{Comb}(A_1^{\text{in}} \rightarrow A_1^{\text{out}}, \dots, A_n^{\text{in}} \rightarrow A_n^{\text{out}})$. The **min-entropy** relative to D is

$$H_{\min}(A_n | A_1, \dots, A_{n-1})_D := -\log \left[\min_{\Gamma} \min \{ \lambda \in \mathbb{R} : I_{A_n^{\text{in}} A_n^{\text{out}}} \otimes \lambda \Gamma \geq D \} \right] \quad (12)$$

$$\equiv -\log \left[\min_{\substack{\widehat{\Gamma}, \\ I_{A_n^{\text{in}} A_n^{\text{out}}} \otimes \widehat{\Gamma} \geq D}} \frac{\text{Tr}[\widehat{\Gamma}]}{\prod_{j=1}^{n-1} \dim A_j^{\text{in}}} \right] \quad (13)$$

$$\equiv -\log \left[\max_E \text{Tr}[DE^T] \right] \quad (14)$$

where $\Gamma \in \text{Comb}(A_1^{\text{in}} \rightarrow A_1^{\text{out}}, \dots, A_{n-1}^{\text{in}} \rightarrow A_{n-1}^{\text{out}})$ is a normalised comb, $\widehat{\Gamma}$ is an unnormalised comb over the same space, and E ranges over elements of $\text{Comb}(\mathbb{C} \rightarrow A_1^{\text{in}}, A_1^{\text{out}} \rightarrow A_2^{\text{in}}, \dots, A_{n-1}^{\text{out}} \rightarrow A_n^{\text{in}} \otimes A_n^{\text{out}})$.

Each of the three quantities above are equivalent and each can be calculated via semi-definite programming methods. Despite their equivalence, we have chosen to present all three due to the following reasons. The first expression, Equation (12), is consistent with the definition given in [26] (cf. Definition 4). The third expression as written has a nice interpretation in terms of the generalised Born rule: the term inside the logarithm is the maximum probability given by the Born rule for any comb dual to D , that is, a strategy for interacting with D . Equivalently, it can be interpreted as maximising over dual combs on a slightly different space that generate correlations with the output space of the comb D . This perspective is particularly useful when D is a classical-quantum comb where the output is the variable we aim to learn about, and hence we elaborate upon it below (see also Figure 3b). The third expression is equivalent to the first expression via e.g., Theorem 2 in [26], and reflects the strong duality in the associated semi-definite programs. The second expression is the form of the comb min-entropy that is most used throughout this paper for

both analytical and numerical results (such as in Section 3.1, Section 4 and Section 5), due in part to its suitability for implementation in code. This expression is equivalent to the first by combining λ and Γ into one operator.

In the present context, the expression for the min-entropy given in Equation (14) is particularly valuable conceptually. Above, E is defined to be a dual operator on the exact same Hilbert spaces as D , since this provides a closed expression for the probability given by $\text{Tr}[DE^T]$. As dual operators, the E can be understood as multi-timestep, adaptive strategies for interacting with the system. However, by considering operators $\widehat{E} \in \text{Comb}(\mathbb{C} \rightarrow A_1^{\text{in}}, A_1^{\text{out}} \rightarrow A_2^{\text{in}}, \dots, A_{n-1}^{\text{out}} \rightarrow A_n^{\text{in}} \otimes \widehat{A}_n^{\text{out}})$ instead, where $\mathcal{H}_{A_n^{\text{out}}} \cong \mathcal{H}_{A_n^{\text{out}}}$, the min-entropy can equivalently be understood as optimising over strategies \widehat{E} that produce maximal correlations between two different spaces, namely $\mathcal{H}_{A_n^{\text{out}}}$ and $\mathcal{H}_{A_n^{\text{out}}}$. We find this perspective of maximising correlations between *separate* spaces especially appropriate for our purposes, since, for the classical-quantum combs considered here, the output space of D (the classical parameter space) is deemed to be inaccessible, and we thus aim to learn the classical parameter via strategies with an output space available to us.

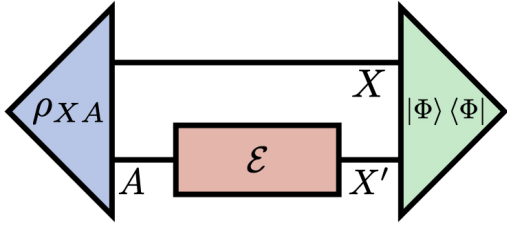
To begin to formalise these equivalent perspectives, it can be shown (a combination of [Proposition 6, 26] and [Theorem 2, 27]), that

$$\max_E \text{Tr}[DE^T] \equiv \max_{\widehat{E}} \dim A_n^{\text{out}} \text{Tr}[D\widehat{E}^T |\Phi^+\rangle\langle\Phi^+|] \quad (15)$$

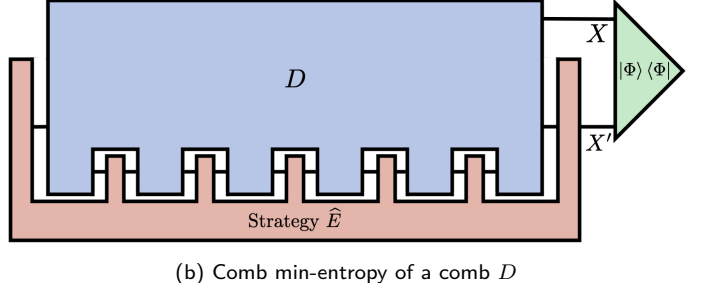
where T is to be understood as denoting the transpose over spaces that D and E (respectively D and \widehat{E}) share, and where

$$|\Phi^+\rangle := \frac{1}{\sqrt{\dim A_n^{\text{out}}}} \sum_i |i\rangle_{A_n^{\text{out}}} |i\rangle_{\widehat{A}_n^{\text{out}}} \quad (16)$$

with $\{|i\rangle\}$ an orthonormal basis. The term $\text{Tr}_{A_1^{\text{in}}, A_1^{\text{out}}, \dots, A_n^{\text{in}}} [D\widehat{E}^T]$ is in particular a state on $\mathcal{H}_{A_n^{\text{out}}} \otimes \mathcal{H}_{\widehat{A}_n^{\text{out}}}$ and thus the full trace term on the right-hand side of Equation (15) is a measure of the overlap with the maximally-entangled state $|\Phi^+\rangle\langle\Phi^+|$. Maximising over \widehat{E} amounts to maximising this overlap. In the case where D is a bipartite quantum state, \widehat{E} is the Choi representation of a CPTP map so Equation (15) is directly related to the operational meaning of the state min-entropy (see the proof of [Theorem 2, 27]). For any comb with classical output, $|\Phi^+\rangle\langle\Phi^+|$ can be replaced by its diagonal part $(\dim A_n^{\text{out}})^{-1} \sum_i |ii\rangle\langle ii|_{A_n^{\text{out}} \widehat{A}_n^{\text{out}}}$. Figure 3 depicts this perspective for both the state and comb cases. Throughout this work, when discussing the maximum formulation of the min-entropy, we will often identify E with \widehat{E} for simplicity (they are in one-to-one correspondence) despite the abuse of notation regarding the constituent Hilbert spaces.



(a) Min-entropy of a quantum state ρ_{XA}



(b) Comb min-entropy of a comb D

Figure 3: The min-entropy can be considered as a measure of the maximal amount of correlation achievable from a given state of two systems by interacting with one system alone. (a) The state min-entropy is calculated if the interaction occurs at a single time step. For a quantum state ρ_{XA} , the min-entropy is calculated via maximising over all quantum channels \mathcal{E} acting on the system A , and comparing the output to a maximally-entangled state $|\Phi\rangle\langle\Phi|_{X'X'}$. If ρ_{XA} is a classical-quantum state instead, one simply maximises over POVMs and compares the output to a maximally classically-correlated state (namely $(\dim X)^{-1} \sum_x |xx\rangle\langle xx|_{X'X'}$). (b) If interactions occur over a series of time steps, the comb min-entropy is calculated instead. For a quantum (respectively, classical-quantum) comb D , the min-entropy is calculated via maximising over strategies \hat{E} (dual combs to D) and again comparing the output to a maximally-entangled (maximally classically-correlated) state. The comb min-entropy given for D a classical-quantum as depicted in Figure 2 are the primary concern of this work.

Let us now consider more closely the classical-quantum combs as presented in Equation (5) and Equation (6). For classical-quantum states, i.e. for $D = \sum_x P(x) |x\rangle\langle x| \otimes \rho_x^A$ where $\rho_x^A \in \mathcal{L}(\mathcal{H}_A)$, the term $\max_E \text{Tr}[DE^T]$ is called the guessing probability [27] since it quantifies the best probability of guessing X after interacting with the state on A . We use the same terminology for the combs case: $P_{\text{guess}}(X|A_1, \dots, A_n)_D$ is the probability of guessing X after interacting with $A_1^{\text{in}}, A_1^{\text{out}}, \dots, A_n^{\text{in}}, A_n^{\text{out}}$ as given by

$$P_{\text{guess}}(X|A_1, \dots, A_n)_D := \max_E \sum_x P(x) \text{Tr}[(|x\rangle\langle x| \otimes \sigma_x) E^T]$$

where E ranges over elements of $\text{Comb}(\mathbb{C} \rightarrow A_1^{\text{in}}, A_1^{\text{out}} \rightarrow A_2^{\text{in}}, \dots, A_n^{\text{out}} \rightarrow X)$. Since $P_{\text{guess}}(X|A_1, \dots, A_n)_D = 2^{-H_{\text{min}}(X|A_1, \dots, A_n)_D}$, we will often use the terms ‘guessing probability’ and ‘min-entropy’ interchangeably.

Later sections will compare the comb min-entropy across different numbers of rounds of interactions, i.e. comparing the min-entropy for $D^{(m)}$ for different values of m . Intuitively, given the specific structure of $D^{(m)}$, one would expect that as the number of rounds increases, the min-entropy should not increase. This is indeed the case, as stated in the following lemma whose proof is given in Appendix B.

Lemma 3.1. *For $D^{(m)}$ and $D^{(l)}$ of the form given in Equation (6), where $m \geq l$,*

$$H_{\text{min}}(X|A_1^{(1)}, \dots, A_n^{(l)})_{D^{(l)}} \geq H_{\text{min}}(X|A_1^{(1)}, \dots, A_n^{(m)})_{D^{(m)}}.$$

For emphasis, we reiterate comments made above: throughout this work, we take the perspective that the min-entropy relates to the maximal guessing probability under the optimal strategy of interacting with a comb, which we find more intuitive, however calculations will largely be done via the expressions involving the minimum (typically Equation (13)), which is easier to work with since the optimisation is over fewer Hilbert spaces.

3.1 Min-Entropy for Classical-Classical Combs

In the previous subsection, we considered the relation between the comb min-entropy and guessing probability for classical-quantum combs D . Due to their relevance for the analysis that will take place in Section 4, we present here a general result regarding the guessing probability for a further restricted class of combs: classical-classical combs. The result is Proposition 3.2 and in particular provides upper and lower bounds for the guessing probability.

Classical-classical are combs of the form

$$D = \sum_x P(x) |x\rangle\langle x| \otimes \sigma_x \quad (17)$$

where $D \in \text{Comb}(A_1^{\text{in}} \rightarrow A_1^{\text{out}}, \dots, A_n^{\text{in}} \rightarrow A_n^{\text{out}}, \mathbb{C} \rightarrow X)$ and where all the $\sigma_x \in \text{Comb}(A_1^{\text{in}} \rightarrow A_1^{\text{out}}, \dots, A_n^{\text{in}} \rightarrow A_n^{\text{out}})$ are normalised and diagonal in the same basis (cf. Definition 2.2). Due to normalisation, we can adopt the probability distribution notation and write

$$\sigma_x := \sum_{x, \mathbf{a}^{\text{in}}, \mathbf{a}^{\text{out}}} P(\mathbf{a}^{\text{out}}|x, \mathbf{a}^{\text{in}}) |\mathbf{a}^{\text{in}}, \mathbf{a}^{\text{out}}\rangle\langle \mathbf{a}^{\text{in}}, \mathbf{a}^{\text{out}}| \quad (18)$$

where $P(\mathbf{a}^{\text{out}}|x, \mathbf{a}^{\text{in}})$ satisfies the required marginalisation conditions (Equation (3)) for each x . This allows D to be rewritten as

$$D = \sum_x P(x) |x\rangle\langle x| \otimes \sum_{\mathbf{a}^{\text{in}}, \mathbf{a}^{\text{out}}} P(\mathbf{a}^{\text{out}}|x, \mathbf{a}^{\text{in}}) |\mathbf{a}^{\text{in}}, \mathbf{a}^{\text{out}}\rangle\langle \mathbf{a}^{\text{in}}, \mathbf{a}^{\text{out}}| \quad (19)$$

$$= \sum_{x, \mathbf{a}^{\text{in}}, \mathbf{a}^{\text{out}}} P(x) P(\mathbf{a}^{\text{out}}|x, \mathbf{a}^{\text{in}}) |x, \mathbf{a}^{\text{in}}, \mathbf{a}^{\text{out}}\rangle\langle \mathbf{a}^{\text{in}}, \mathbf{a}^{\text{out}}|. \quad (20)$$

In the case where all input spaces are trivial, that is, when D is a classical-classical state (all the σ_x are states that are diagonal in the same basis), the guessing probability is known to have a nice interpretation in terms of

a maximal Bayesian update (this interpretation is explained in Appendix B; see also [Section 6.1.4, 62]). In an attempt to arrive at similar interpretation for the case where the inputs are non-trivial, let us consider the conditional version of Bayes' rule, namely:

$$P(X|\mathbf{A}^{\text{in}}, \mathbf{A}^{\text{out}})P(\mathbf{A}^{\text{out}}|\mathbf{A}^{\text{in}}) = P(\mathbf{A}^{\text{out}}|X, \mathbf{A}^{\text{in}})P(X|\mathbf{A}^{\text{in}}) \quad (21)$$

where the capitalised letters denote random variables (as opposed to their values denoted by the lower case letters as above). One notes that the right-hand side is *almost* what appears in the form of D above, except instead of $P(X)$ we have $P(X|\mathbf{A}^{\text{in}})$. A consequence of Proposition 2.1 is that X is independent of \mathbf{A}^{in} , so we do in fact have

$$P(X|\mathbf{A}^{\text{in}}) = P(X). \quad (22)$$

This allows D to be written as

$$D = \sum_{\substack{x, \mathbf{a}^{\text{in}}, \\ \mathbf{a}^{\text{out}}}} P(x|\mathbf{a}^{\text{in}}, \mathbf{a}^{\text{out}})P(\mathbf{a}^{\text{out}}|\mathbf{a}^{\text{in}}) |x, \mathbf{a}^{\text{in}}, \mathbf{a}^{\text{out}}\rangle \langle \dots|. \quad (23)$$

Using this form for D , we can establish the following:

Proposition 3.2. *Let D be as above. Then*

$$\sum_{\substack{\mathbf{a}^{\text{in}}, \\ \mathbf{a}^{\text{out}}}} \max_x P(x|\mathbf{a}^{\text{in}}, \mathbf{a}^{\text{out}})P(\mathbf{a}^{\text{out}}|\mathbf{a}^{\text{in}}) \leq \min_{\substack{\Gamma, \\ I_X \otimes \Gamma \geq D}} \text{Tr}[\Gamma] \quad (24)$$

$$\leq \sum_{\substack{\mathbf{a}^{\text{in}}, \\ \mathbf{a}^{\text{out}}}} \max_{x, \tilde{\mathbf{a}}} P(x|\tilde{\mathbf{a}}, \mathbf{a}^{\text{out}})P(\mathbf{a}^{\text{out}}|\tilde{\mathbf{a}}) \quad (25)$$

where the minimisation is over unnormalised combs Γ .

By normalising each term by the dimension of the input spaces, and in light of the definition of the comb min-entropy (specifically Equation (13)), the above provides bounds for the guessing probability (this is discussed in more depth below). The proof is given in Appendix B and demonstrates the left-hand inequality by showing that every positive semi-definite operator Γ , which clearly includes all unnormalised combs that satisfies $I_X \otimes \Gamma \geq D$, must have trace greater than the left-hand quantity above. The right-hand inequality is obtained by showing that

$$\Gamma := I_{\mathbf{A}^{\text{in}}} \otimes \sum_{\mathbf{a}^{\text{out}}} \max_{x, \tilde{\mathbf{a}}} P(x|\tilde{\mathbf{a}}, \mathbf{a}^{\text{out}})P(\mathbf{a}^{\text{out}}|\tilde{\mathbf{a}}) |\mathbf{a}^{\text{out}}\rangle \langle \mathbf{a}^{\text{out}}| \quad (26)$$

is indeed an unnormalised classical comb. It also is worth noting that, for D classical, the minimum over unnormalised combs can always be achieved by a diagonal Γ (see Lemma B.1 and Lemma B.2).

Explicitly, the consequences for the guessing probability are as follows:

$$P_{\text{guess}}(X|\mathbf{A}^{\text{in}}, \mathbf{A}^{\text{out}}) \geq \sum_{\substack{\mathbf{a}^{\text{in}}, \\ \mathbf{a}^{\text{out}}}} \max_x P(x|\mathbf{a}^{\text{in}}, \mathbf{a}^{\text{out}}) \frac{P(\mathbf{a}^{\text{out}}|\mathbf{a}^{\text{in}})}{\dim \mathbf{A}^{\text{in}}} \quad (27)$$

$$\equiv \sum_{\substack{\mathbf{a}^{\text{in}}, \\ \mathbf{a}^{\text{out}}}} \max_x P(x|\mathbf{a}^{\text{in}}, \mathbf{a}^{\text{out}})P(\mathbf{a}^{\text{out}}|\mathbf{a}^{\text{in}})P_{\text{unif}}(\mathbf{a}^{\text{in}}) \quad (28)$$

where $P_{\text{unif}}(\cdot)$ denotes the uniform probability distribution, and

$$\begin{aligned} P_{\text{guess}}(X|\mathbf{A}^{\text{in}}, \mathbf{A}^{\text{out}}) &\leq \sum_{\mathbf{a}^{\text{in}}, \mathbf{a}^{\text{out}}} \max_{x, \tilde{\mathbf{a}}} P(x|\tilde{\mathbf{a}}, \mathbf{a}^{\text{out}}) \frac{P(\mathbf{a}^{\text{out}}|\tilde{\mathbf{a}})}{\dim \mathbf{A}^{\text{in}}} \\ &= \sum_{\mathbf{a}^{\text{out}}} \max_{x, \tilde{\mathbf{a}}} P(x|\tilde{\mathbf{a}}, \mathbf{a}^{\text{out}})P(\mathbf{a}^{\text{out}}|\tilde{\mathbf{a}}). \end{aligned} \quad (29)$$

If, for each \mathbf{a}^{out} , the factor $\max_x P(x|\mathbf{a}^{\text{in}}, \mathbf{a}^{\text{out}})P(\mathbf{a}^{\text{out}}|\mathbf{a}^{\text{in}})$ is the same for every \mathbf{a}^{in} , then the upper and lower bounds coincide, thus specifying the guessing probability exactly. As discussed in Appendix B, this occurs trivially for the state case since the input space is one-dimensional, but we will see in Section 4.3 a simple comb example with non-trivial input spaces where this also holds.

The above proposition highlights that, even in the entirely classical case, the generalisation of the maximum Bayesian updating interpretation of the guessing probability for states to the classical comb case is more subtle. This aligns with what one would expect: the fact that the comb case allows for inputs to the system plays a non-trivial role in the interpretation of the guessing probability. For the case of quantum combs, further subtleties likely exist, not in the least since certain formulations of conditional quantum Bayesian updating are known to be potentially problematic (see e.g. [Section VII, 63]).

A final comment regarding the multi-round case. Since a classical multi-round comb (recall Equation (6)) can be viewed as a special case of Equation (20) above with extra independence conditions on the distribution $P(\mathbf{a}^{\text{out}}|x, \mathbf{a}^{\text{in}})$, namely that

$$P(\mathbf{a}^{\text{out}}|x, \mathbf{a}^{\text{in}}) = \prod_{j=1}^m P(\mathbf{a}^{\text{out},(j)}|x, \mathbf{a}^{\text{in},(j)}) \quad (31)$$

where $\mathbf{a}^{\text{in},(j)}$ denotes the inputs for round j and similarly for $\mathbf{a}^{\text{out},(j)}$, applying the results of Proposition 3.2 to the multi-round case gives

$$\begin{aligned} P_{\text{guess}}(X|\mathbf{A}^{\text{in},(1)}, \mathbf{A}^{\text{out},(1)}, \dots, \mathbf{A}^{\text{in},(m)}, \mathbf{A}^{\text{out},(m)}) \\ \geq \sum_{\substack{\mathbf{a}^{\text{in},(1:m)}, \\ \mathbf{a}^{\text{out},(1:m)}}} \max_x P(x|\mathbf{a}^{\text{in},(1:m)}, \mathbf{a}^{\text{out},(1:m)}) \prod_{j=1}^m \frac{P(\mathbf{a}^{\text{out},(j)}|\mathbf{a}^{\text{in},(j)})}{\dim \mathbf{A}^{\text{in},(j)}} \end{aligned} \quad (32)$$

and

$$\begin{aligned} P_{\text{guess}}(X|\mathbf{A}^{\text{in},(1)}, \mathbf{A}^{\text{out},(1)}, \dots, \mathbf{A}^{\text{in},(m)}, \mathbf{A}^{\text{out},(m)}) \\ \leq \sum_{\mathbf{a}^{\text{out},(1:m)}} \max_{x, \tilde{\mathbf{a}}^{(1:m)}} P(x|\tilde{\mathbf{a}}^{(1:m)}, \mathbf{a}^{\text{out},(1:m)}) \prod_{j=1}^m P(\mathbf{a}^{\text{out},(j)}|\tilde{\mathbf{a}}^{(j)}) \end{aligned} \quad (33)$$

where the shorthand $\mathbf{a}^{\text{in},(1:m)}$ has been used for the inputs for all rounds and similarly for $\mathbf{a}^{\text{out},(j)}$.

4 Blind Quantum Computing Protocol Analysis

Blind quantum computing is a term that encompasses an array of cryptographic quantum computational protocols (see e.g. [35–38] and the review [17]), many of which build upon, or are inspired by, aspects derived from MBQC. In very broad terms, a BQC protocol consists of a client, who has limited computational power, interacting with a server (multi-party variants also exist), who has quantum computational capabilities, in order to carry out a desired computation in such a way that the latter is “blind” to the details. A range of theoretical tools for modelling quantum cryptographic protocols and analysing their security exist (see e.g. [64, 65] and the review [66]).

In this work, we consider one specific BQC protocol, that of Mantri et al. [36] (discussed in the next subsection), and our main method of security analysis consists of calculating the comb min-entropy applied to the corresponding classical comb, D_{client} , which we define below (Section 4.2). In Section 4.3, by establishing a strictly positive lower bound for the min-entropy of D_{client} , which means the server must still learn more information in order to know the client’s choice of computation with certainty, we prove the partial security of the protocol for a single round. We further provide a simple example of the protocol run on a three-qubit graph state that obtains the lower bound. In Section 4.4, we extend the security analysis to multiple rounds by considering a comb $D_{\text{client}}^{(m)}$, where a positive lower bound is again shown for all rounds m , and comment on the consequences for the blindness of the protocol in this case.

4.1 A Classically Driven BQC Protocol

The protocol of [36] is distinct from many other BQC proposals in that it considers purely classical communication between client and server. At its core, the protocol leverages various properties of gflow and MBQC outlined in Section 2.2, such as the non-uniqueness of gflows existing for a given graph state and the symmetries of measurement projections as in Equation (10), along with

cryptographic primitives such as the use of random bits as one-time pads. The protocol parameters consist of a choice of graph G along with a total order on vertices, and a discrete set of angles \mathcal{A} which satisfies the following property:

$$\mathcal{A} = \{(-1)^x \alpha + z\pi \bmod 2\pi : \alpha \in \mathcal{A}; x, z \in \mathbb{Z}_2\}. \quad (34)$$

All measurements are made in the XY -plane (which is no restriction on the universality of the resulting computations - see [67]) and so the above property enforces that \mathcal{A} is closed under the angle transformations given in Equation (10). The specific graph, total order and angle set are agreed upon collectively by both the client and server prior to the commencement of a specific computation. In secret, the client also chooses their desired computation, that is, a list of measurement angles $\alpha \in \mathcal{A}^n$ (where n is the number of vertices in G) and designated input and output sets I and O , a bit-string one-time pad $\mathbf{r} \in \mathbb{Z}_2^n$ uniformly at random, and a gflow compatible with (G, I, O) and the total order.

One round of computation proceeds as follows:

1. The server initialises the graph state ρ_G .
2. For $i = 1, \dots, n$ according to the total order, the following sequence is repeated:
 - (a) The user reports a measurement angle α'_i to the server, where
$$\alpha'_i := (-1)^{\bigoplus_{j \in \mathcal{X}_i} c_j} \alpha_i + \left(r_i \oplus \bigoplus_{j \in \mathcal{Z}_i} c_j \right) \pi \bmod 2\pi \quad (35)$$

where c_j denotes the measurement outcome for qubit $j < i$ recorded by the user based on the outcome reported by the server and where \mathcal{X}_i and \mathcal{Z}_i are the corrections sets defined by the gflow (as in Equation (11)).
- (b) The server measures $\mathcal{M}_{\alpha'_i}$ and reports $c'_i = 0$ for a positive outcome and $c'_i = 1$ for a negative outcome.
- (c) The user records $c_i = c'_i \oplus r_i$.
3. The outcomes pertaining to the output qubits (which are known only to the user) are processed to obtain the results of the computation.

There are two things worth noting about the one-time pads. Firstly, their utility for obscuring angles is a direct consequence of the Z -relation given in Equation (10) (i.e. a positive measurement outcome for α and negative measurement outcome for $\alpha + \pi$ are equivalent). Secondly, the presence of r_i in both the equation for α'_i as well as for any α'_k for which $i \in \mathcal{X}_k$ or $i \in \mathcal{Z}_k$ places constraints on the set of possible reported angles α' for a given choice of true angles α .

The protocol is known to be correct if both the client and server behave accordingly [Theorem 1, 36], however it also known that this protocol is not verifiable: the client has no way of knowing whether the server actually prepares a graph state, measures according to the reported angles, and communicates the actual measurement outcomes. The server could in fact do none of these and report random outcomes c' instead, with the client only being aware of this fact if they could compute the measurement statistics of the final state themselves anyway. We review the proof of blindness for a single round of the protocol [Theorem 2, 36] and provide our own analysis in Section 4.3 after introducing the classical comb that models the protocol.

Some final remarks regarding minor differences between the analysis in [36] and the one below. Mantri et al. place a further condition on the definition of gflow, largely for the purpose of simplifying a counting argument (see [Theorem 3, 36]), which effectively singles out one gflow for every pair (I, O) given G and they thus identify a choice of computation with a choice of angles and choice of gflow. Here, we work with the unconstrained definition of gflow and so identify a choice of computation as a choice of α and (I, O) (again for fixed G), for which any of the compatible gflows can be chosen. Moreover, since the protocol is entirely classical, the client can only prepare an input state on the qubits in I via measurement-based state preparation, which is thus indistinguishable from the part of the measurement sequence implementing the unitary. As such, computations are specified here purely by angles α and a choice of output set O for which (G, I, O) supports gflow for some I .

4.2 The Classical BQC Protocol as a Classical Comb

The protocol parameters outlined in the previous section also form the starting point for defining the corresponding classical comb: we fix a choice of graph G , say on n vertices, a total order on the vertices $1 < 2 < \dots < n$, and a set of allowed angles \mathcal{A} satisfying Equation (34). Since all communication in the protocol is classical, we represent the reported angles and measurement outcomes as basis states in corresponding Hilbert spaces: $|\alpha'_i\rangle\langle\alpha'_i| \in \mathcal{H}_{A'_i}$ for the reported angle at step i and $|c'_i\rangle\langle c'_i| \in \mathcal{H}_{C'_i}$ for the reported measurement outcome, where $\dim \mathcal{H}_{A'_i} = |\mathcal{A}|$ and $\dim \mathcal{H}_{C'_i} = 2$.

Prior to the commencement of the protocol, the client selects the output space O , the “true” angles for the computation $\alpha \in \mathcal{A}^n$, the one-time pads $r \in \mathbb{Z}_2^n$, and a gflow g compatible with the graph and total order and chosen output set. We denote compatibility with an output set O as $g \sim O$. We define the classical comb corresponding to the protocol for the specific choice of α, r and g as

$$\sigma_{\text{BQC}}^{\alpha, r, g} := \sum_{\substack{\alpha' \in \mathcal{A}^n, \\ c' \in \mathbb{Z}_2^n}} P(\alpha' | c', \alpha, r, g) |\alpha' c'\rangle\langle\alpha' c'| \quad (36)$$

where $P(\alpha' | c', \alpha, r, g)$ is simply a deterministic distribution that encodes the angle adaptations:

$$P(\alpha' | c', \alpha, r, g) = \begin{cases} 1, & \text{if Equation (35) holds for all } i \\ 0, & \text{otherwise} \end{cases} \quad (37)$$

Note that Equation (35) contains the notation c_i , but since $c_i := c'_i \oplus r_i$, we use only the c' and r notation instead.

For a given computation, that is, for a given α and O , any choice of $g \sim O$ and r produce the desired result. Since these choices are made in secret, the protocol for a given computation is modelled as

$$\sum_{g \sim O, r} P(g | O) P(r) \sigma_{\text{BQC}}^{\alpha, r, g} \quad (38)$$

where $P(g | O)$ is the probability that the gflow g is chosen and $P(r)$ is the probability of the one-time pad r is chosen. According to the above protocol, the latter distribution is taken to be uniform, $P(r) = \frac{1}{2^n}$, and independent of all other variables (see [Lemma 4, 36]). Since the specific choice of gflow is irrelevant for the computation once O is fixed, we take $P(g | O)$ to have uniform weight for all $g \sim O$ and 0 otherwise, and moreover we take $P(g | O) = P(g | \alpha, O)$. We thus have the following:

$$P(\alpha' | c', \alpha, r, g) = P(\alpha' | c', \alpha, r, g, O) \quad \forall g \sim O \quad (39)$$

$$P(r, g | c', \alpha, O) = P(r) P(g | O) \quad (40)$$

where Equation (40) has used the independence of g and r from c' which follows from similar reasoning as for Equation (22) in the previous section. We can thus expand Equation (38) as follows:

$$\begin{aligned} & \sum_{g \sim O, r} P(g | O) P(r) \sigma_{\text{BQC}}^{\alpha, r, g} \\ &= \sum_{\substack{\alpha', c', \\ g \sim O, r}} P(\alpha' | c', \alpha, r, g, O) P(r, g | c', \alpha, O) |\alpha' c'\rangle\langle\alpha' c'| \end{aligned} \quad (41)$$

$$= \sum_{\alpha', c'} P(\alpha' | c', \alpha, O) |\alpha' c'\rangle\langle\alpha' c'| \quad (42)$$

$$=: \sigma_{\alpha, O} \quad (43)$$

where we have used $\langle..|$ when its contents are the same as the accompanying ket.

Having summed over $g \sim O$ and r , the probability distribution $P(\alpha' | c', \alpha, O)$ is no longer a simple deterministic distribution, but in general a more complicated one. In particular, it depends on the set of gflows compatible with O and the set of angles they can mutually report.

The final step to arrive at a comb of the form of Equation (5) is to include the random variable. In this case, the random variable encodes the choice of computation

made by the client. Denoting the set of all possible output sets for the fixed graph by \mathcal{O} , the values that the computation random variable can take are given by $|\alpha, O\rangle\langle\alpha, O| \in \mathcal{H}_{\mathcal{A}^n} \otimes \mathcal{H}_{\mathcal{O}}$. We can now write down the classical comb that fully represents the BQC protocol for a fixed G and \mathcal{A} as:

$$D_{\text{client}} = \sum_{\alpha \in \mathcal{A}^n, O \in \mathcal{O}} P(\alpha, O) |\alpha, O\rangle\langle\alpha, O| \otimes \sigma_{\alpha, O}. \quad (44)$$

This is a classical comb in $\text{Comb}(\mathbb{C} \rightarrow A'_1, C'_1 \rightarrow A'_2, \dots, C'_n \rightarrow \mathbb{C}, \mathbb{C} \rightarrow \mathbf{A} \times \mathbf{O})$ and as such the results of Section 3.1 regarding the min-entropy apply, a fact that will be used in the blindness proof in the next section.

4.3 Blindness in a Single Round

We begin this subsection with a discussion of the security proof given in [36] for the protocol. The proof proceeds by showing that, for a single round, the mutual information between the information received by the server and the client's choice of computation is bounded away from the required amount to learn the computation with certainty. We state their blindness theorem below, using notation as close to the original as possible, and then consider a related form more suitable for comparison with our analysis using the min-entropy.

Recalling the comments at the end of Section 4.1, since in [36] a restricted version of gflow was used, a computation is stipulated by a choice of angles and a choice of restricted gflow (instead of the choice of O as above). We let \mathbf{A} denote the random variable for the angles, which takes values in \mathcal{A}^n , and let \mathbf{F} denote the random variable which takes values in the set of restricted gflows. The random variables for the reported angles and measurement outcomes are denoted \mathbf{A}' and \mathbf{C}' respectively. With this notation, the blindness theorem is:

Theorem 4.1 (Theorem 2, [36]). *In a single instance of the protocol, the mutual information between the client's secret input $\{\alpha, \mathbf{f}\}$ and the information received by the server is bounded by*

$$I(\mathbf{C}', \mathbf{A}'; \mathbf{A}, \mathbf{F}) \leq H(\mathbf{A}') \quad (45)$$

where $I(\cdot; \cdot)$ denotes the mutual information and $H(\cdot)$ denotes the Shannon entropy.

Using part of the proof of the above theorem which in particular shows that $H(\mathbf{A}', \mathbf{C}' | \mathbf{A}, \mathbf{F}) \geq n$ (see [Lemma 4, 36]) along with the properties of the mutual information and Shannon entropy, it is possible to arrive at a related entropic inequality which indicates the at least partial security of the protocol ('partial' because some information is leaked about the choice of angles in a given round):

$$H(\mathbf{A}, \mathbf{F} | \mathbf{C}', \mathbf{A}') \geq \log_2 |\mathbf{F}| > 0. \quad (46)$$

One important aspect that we want to emphasise is that the Shannon entropy is not a single-shot entropy and therefore only provides limited insight about the security of the protocol in a single round. The min-entropy however, is a single-shot quantity, and since it deals with optimal learning strategies (optimal from the inquisitive server's perspective), it provides a more appropriate measure of security in this case: if it can be shown that the min-entropy equivalent of the quantity $H(\mathbf{A}, \mathbf{F} | \mathbf{C}', \mathbf{A}')$ is bounded above zero, then the server is guaranteed to retain some uncertainty about the true computation. This is the content of the following theorem. It should first be noted that, in deriving Equation (46), the assumption is made that the computation is chosen uniformly at random (i.e. $H(\mathbf{A}, \mathbf{F}) = \log_2 |\mathbf{A}| + \log_2 |\mathbf{F}|$) and we make the equivalent assumption here (however for the corresponding change in variable from \mathbf{F} to \mathbf{O} ; explicitly, we assume $P(\alpha, O) = \frac{1}{|\mathcal{A}|^n |\mathcal{O}|}$).

Theorem 4.2. *For D_{client} as above, and under the given assumptions, the following holds for any choice of graph G and angle set \mathcal{A} that satisfy the required conditions:*

$$H_{\min}(\mathbf{A}, \mathbf{O} | \mathbf{A}', \mathbf{C}')_{D_{\text{client}}} \geq n + \log_2(|\mathcal{O}|). \quad (47)$$

The proof of this theorem is given in Appendix C.1. The key step of the proof consists of providing an upper bound for the guessing probability (which provides a corresponding lower bound for the min-entropy) via the upper bound of Proposition 3.2 applied to the comb D_{client} . Due to the specific form of D_{client} , this bound has an interpretation in terms of the number of different ways each α' can be reported for a given classical message (that is, for different gflows g and one-time pads \mathbf{r}) with a larger number corresponding to a lower min-entropy bound (this is explained further after the proof of the theorem in Appendix C.1).

One can rightfully ask how good this bound is in practice. To conclude this subsection, we consider a simple example for which the gflows are characterised and the min-entropy is in fact given exactly by the right-hand side of Equation (47). Let G be the three-vertex graph as shown in Figure 4 with total order given by the natural order on vertex labels. As demonstrated in Appendix C.2, there is exactly one non-trivial output set ($O = \{2, 3\}$) that supports gflow for this example, and exactly two corresponding gflows exist. It can further be shown that the upper and lower bounds of Proposition 3.2 for D_{client} coincide, which establishes $n + \log_2(|\mathcal{O}|)$ as the true min-entropy value. For this example, $n = 3$ and $|\mathcal{O}| = 1$, so $H_{\min}(\mathbf{A}, \mathbf{O} | \mathbf{A}', \mathbf{C}')_{D_{\text{client}}} = 3$, which is corroborated by the numerical results (for two choices of \mathcal{A} , one such that $|\mathcal{A}| = 4$ and the other such that $|\mathcal{A}| = 8$).

4.4 Regarding Multi-Round Blindness

In this subsection, we extend the blindness analysis to the situation where the client and server engage in multiple rounds of the protocol, for example, in order to collect

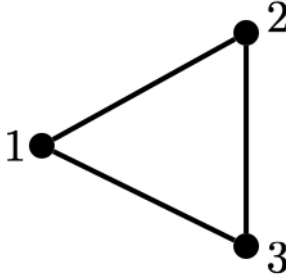


Figure 4: An example graph state for which the security for a single round of the BQC protocol considered here is maximally bad (that is, the min-entropy for the associated quantum comb obtains the lower bound given in Theorem 4.2). All potential gflows for the protocol are required to be compatible with the order $1 < 2 < 3$ on vertices. The only output set that supports such gflows is $O = \{2, 3\}$.

measurement statistics of the output. It is not clear that the protocol does indeed stay secure in this case (multi-round security was not treated in the original work [36]). As an extension of Theorem 4.2 above, we demonstrate that the min-entropy is bounded away from zero for all rounds.

We use similar assumptions to Theorem 4.2, namely that $P(g|O)$ and $P(r)$ are uniform, however we make a slightly weaker assumption on $P(\alpha, O)$: we take $P(\alpha, O) = \frac{P(O)}{|\mathcal{A}|^n}$ for $P(O)$ an arbitrary distribution over the output sets. Furthermore, we make the additional assumptions that the gflow and one-time pads are chosen independently for each round, allowing the multi-round protocol to be represented as

$$D_{\text{client}}^{(m)} = \sum_{\alpha, O} \frac{P(O)}{|\mathcal{A}|^n} |\alpha, O\rangle\langle\alpha, O| \bigotimes_{j=1}^m \sigma_{\alpha, O}^{(j)}. \quad (48)$$

We have the following theorem:

Theorem 4.3. *For any m , the following holds:*

$$\begin{aligned} H_{\min}(\mathbf{A}, \mathbf{O} | \mathbf{A}'^{(1)}, \mathbf{C}'^{(1)}, \dots, \mathbf{A}'^{(m)}, \mathbf{C}'^{(m)})_{D_{\text{client}}^{(m)}} \\ \geq -\log \left(\sum_{O \in \mathcal{O}} \frac{P(O)}{2^{|O|}} \right). \end{aligned} \quad (49)$$

A key point of the proof, given in Appendix C.3, consists of the observation that, for any choice of output set O , the one-time pads assigned to the qubits in the output set cannot be learnt by the server since they do not appear in the adaptation of any other angle (in contrast to the one-time pads assigned to non-output qubits). The consequence is that the server can, at best, only learn the output angles of α up to a π phase. However, the server may be able to learn all other measurement angles with certainty, which correspond to the computation proper, in which case the only remaining uncertainty consists of not knowing how to interpret the measurement outcomes on the output state. This level of uncertainty is likely

insufficient to deem the protocol as secure in multiple rounds.

The above theorem does not say anything about whether the min-entropy does in fact change from round to round, let alone whether the above bound can ever be reached. To provide an answer to the former, we conclude by returning to the minimal example presented above and consider the associated min-entropy for two rounds. As outlined in Appendix C.2, for a specific choice of angle set \mathcal{A} , the two round entropy is upper bounded by $-\log_2(0.140625) \approx 2.830(0)$ and thus the min-entropy value does indeed decrease from the single round to the two round case.

5 Grey Box MBQC

In this section, we consider a set of combs that are once again defined via gflow, however there is now a mixture of quantum and classical interactions. The inputs to the combs defined here are the same as for the BQC case (measurement outcomes), but the outputs are now single qubit states of the graph state, potentially acted upon by correction operators. We demonstrate that these combs can be understood as quantum causal models in the style of [20]. Moreover, the measurement channels inserted into the comb to perform a measurement-based computation bear close resemblance to the notion of observation put forward in [50] in the context of quantum causal inference. As such, a key goal of this section is to explicate a novel connection between measurement-based quantum computation and quantum causal models and causal discovery.

In keeping with the rest of this work, we again apply the comb min-entropy to quantify optimal learning of an unknown property, now of a “grey box MBQC device” - a device which both prepares the graph state and conducts measurement corrections (so that we simply need to insert measurement channels) and for which we have only partial knowledge. Specifically, we consider an example where the graph state and designated input and output vertex sets are known but the particular gflow defining the corrections is not. In light of the above connection, learning the gflow corresponds to learning the causal structure of the device, i.e. a type of causal discovery. The min-entropy for this example provides a benchmark for optimal causal learning to which e.g. a learning strategy involving only observations (defined below) can be compared.

In the final two subsections, we introduce two further pragmatic examples that continue to demonstrate the utility of the quantum comb and min-entropic approach to the type of partial-information analysis considered here. The first considers the same specific graph as the causal discovery example, however instead of learning the gflow itself, we aim now only to learn the required measurement planes for which the gflow is compatible. For the given level of knowledge about the device, i.e. know-

ing the graph state being prepared and the input and output sets, this represents the minimal information required to use the MBQC device for deterministic computation - knowing the full details of the specific gflow is not required. However, to ensure that any *particular* computation can be correctly performed, we also need to calibrate the frame of reference of our measurement channels (outside the device) with the frame of reference of the graph state preparation (inside the device). Said another way, we want to ensure that measuring in, say, the XY -plane at an angle α to the positive X -axis in our measuring device does indeed correspond to an angle α with respect to the positive X -axis implicit in the preparation of $|G\rangle$. The final example is concerned with this scenario by aiming to learn the angle discrepancy between the positive X -axes in the internal and external frame of references under the assumption that the Z -axis is known. This can be considered as an example of correlating reference frames in the quantum reference frames literature [54].

5.1 Gflow Quantum Combs

In Section 2.2, and reinforced by the discourse in Appendix A.2, much emphasis was placed on the two equivalent ways of correcting for a negative measurement outcome at a given qubit in an MBQC: by classically adapting measurement angles for measurement on other qubits or by applying a partial stabiliser on the graph state. The latter perspective is the relevant one for our present purposes. An MBQC on a graph state ρ_G that prepares an output (quantum) state on the output set O can be written as

$$\text{Tr} \left[\left(\bigotimes_{v \in V \setminus O} |\pm_{\alpha_v}\rangle\langle\pm_{\alpha_v}|_v \right) \rho_G \right] \quad (50)$$

where the trace is over all qubits in $V \setminus O$ and the measurement planes can be considered as all XY for simplicity. For a given vertex $v_0 \in V \setminus O$, there are two possibilities: either a positive measurement outcome obtains in which case no corrections are required, or a negative outcome obtains, for which corrections can be performed by applying a partial stabiliser to ρ_G :

$$\begin{aligned} & \text{Tr} \left[\left(|\pm_{\alpha_{v_0}}\rangle\langle\pm_{\alpha_{v_0}}|_{v_0} \bigotimes_{v \in V \setminus (O \cup v_0)} |\pm_{\alpha_v}\rangle\langle\pm_{\alpha_v}|_v \right) \rho_G \right] \\ & \equiv \text{Tr} \left[\left(|\pm_{\alpha_{v_0}}\rangle\langle\pm_{\alpha_{v_0}}|_{v_0} \bigotimes_{v \in V \setminus (O \cup v_0)} |\pm_{\alpha_v}\rangle\langle\pm_{\alpha_v}|_v \right) \right. \\ & \quad \left. \cdot K_{g(v_0)}|_{\setminus v_0} \rho_G K_{g(v_0)}^\dagger|_{\setminus v_0} \right] \quad (51) \end{aligned}$$

where $K_{g(v_0)}$ is the (product of) stabiliser(s) assigned by a gflow g to correct for measurements at v_0 and the notation $K_{g(v_0)}|_{\setminus v_0}$ denotes the operator derived from $K_{g(v_0)}$ with the v_0 tensor factor replaced with the identity.

So, for each measurement and conditional on the measurement outcome, we are applying an operator on the graph state, either the identity (no correction implemented) or the partial stabiliser (correction implemented). The ability to correct for a negative outcome at every qubit via stabilisers only works if each measurement is performed in the assigned plane for which the graph and measurement plane assignment has gflow. If gflow exists and the restriction on the measurement planes is followed, one can take the perspective that the correction method defined from gflow is a mapping from measurement channels to unitary channels, i.e. a higher order quantum map (a quantum comb).

To make this perspective precise, let us consider a tuple (G, I, O, ω) for which a gflow g exists. Our aim is then to write down an operator σ_{MBQC}^g corresponding to the correction method induced by g such that the following quantity is the same for every set of measurement outcomes (which in particular includes the all positive outcome instance, and thus is equivalent to the desired computation):

$$\left(\bigotimes_{v \in V \setminus O} \mathcal{M}_{v, \alpha_v, \omega(v)} \right) * \sigma_{\text{MBQC}}^g * \rho_G \quad (52)$$

where the projections $|\pm_{\alpha_v}\rangle\langle\pm_{\alpha_v}|$ in measurement plane $\omega(v)$ are now described by appropriately defined measurement channels $\mathcal{M}_{v, \alpha_v, \omega(v)}$ (see below) and where $*$ denotes the link product (Definition 2.3) which in particular includes the trace over all spaces not related to the output space. The next few paragraphs are devoted to defining the operator σ_{MBQC}^g .

Let g be a gflow for (G, I, O, ω) , where G is a graph on n vertices and as such we identify V with $\{1, \dots, n\}$. The operator σ_{MBQC}^g is defined on the Hilbert spaces $\bigotimes_{i=1}^n \mathcal{H}_{A_i} \otimes \mathcal{H}_{C_i} \otimes \mathcal{H}_{A'_i}$, where $\mathcal{H}_{A_i} \cong \mathcal{H}_{C_i} \cong \mathcal{H}_{A'_i} \cong \mathbb{C}^2$ for each i . Recalling from Equation (11) that g defines the correction sets \mathcal{X}_i and \mathcal{Z}_i for each $i \in V$, we define the correction operator for i as

$$U_{\text{corr}(\mathbf{c}), i} := X_{A_i}^{\bigoplus_{j \in \mathcal{X}_i} c_j} Z_{A_i}^{\bigoplus_{j \in \mathcal{Z}_i} c_j} \quad (53)$$

and for notational simplicity in the following, we take

$$U_{\text{corr}(\mathbf{c})} := \bigotimes_{i=1}^n U_{\text{corr}(\mathbf{c}), i}. \quad (54)$$

We can then define σ_{MBQC}^g as

$$\sigma_{\text{MBQC}}^g := \sum_{\mathbf{a}, \mathbf{b}, \mathbf{c}} U_{\text{corr}(\mathbf{c})} |\mathbf{a}\rangle\langle\mathbf{b}|_A U_{\text{corr}(\mathbf{c})}^\dagger \otimes |\mathbf{c}, \mathbf{a}\rangle\langle\mathbf{c}, \mathbf{b}|_{CA'} \quad (55)$$

where the subscripts A , C and A' denote that the corresponding state is in $\mathcal{H}_A := \bigotimes_{i=1}^n \mathcal{H}_{A_i}$, $\mathcal{H}_C := \bigotimes_{i=1}^n \mathcal{H}_{C_i}$ or $\mathcal{H}_{A'} := \bigotimes_{i=1}^n \mathcal{H}_{A'_i}$ respectively, and where the sum is

over the computational basis of these spaces. The space $\mathcal{H}_{A'}$ receives the graph state ρ_G via the link product as in Equation (52). To connect back to the discussion above, σ_{MBQC}^g is the Choi operator of the channel that conditionally applies the appropriate corrections via partial stabiliser to the graph state. See Figure 5a for a depiction of σ_{MBQC}^g for one of the gflows considered in the example in Section 5.3.

It remains then only to define the measurement channels $\mathcal{M}_{\alpha_i, i, \omega(i)}$. Previously, we denoted measurements simply via projection operators $|\pm_\alpha\rangle\langle\pm_\alpha|_{\text{mp}}$ for $\text{mp} \in \{XY, XZ, YZ\}$, however for our present purposes we would like to consider channels from \mathcal{H}_{A_i} to \mathcal{H}_{C_i} which moreover prepare classical measurement outcomes ($|0\rangle\langle 0|$ or $|1\rangle\langle 1|$) at \mathcal{H}_{C_i} . We define $\mathcal{M}_{\alpha_i, i, \omega(i)} : \mathcal{H}_{A_i} \rightarrow \mathcal{H}_{C_i}$ via its Choi representation:

$$\begin{aligned} \mathcal{M}_{\alpha_i, i, \omega(i)} := & |0\rangle\langle 0|_{C_i} \otimes |+\alpha_i\rangle\langle +\alpha_i|_{\omega(i), A_i}^T \\ & + |1\rangle\langle 1|_{C_i} \otimes |-\alpha_i\rangle\langle -\alpha_i|_{\omega(i), A_i}^T. \end{aligned} \quad (56)$$

It should be noted that, since quantum combs are typically considered with a total order, we endow σ_{MBQC}^g with a choice of total order for which the partial order given by the gflow is compatible. Any such total order is sufficient and we leave it implicit in the labelling of the Hilbert spaces. Explicitly, we consider $\sigma_{\text{MBQC}}^g \in \text{Comb}(\mathcal{H}_{A'} \rightarrow \mathcal{H}_{A_1}, \mathcal{H}_{C_1} \rightarrow \mathcal{H}_{A_2}, \dots, \mathcal{H}_{C_{|V \setminus O|}} \rightarrow \bigotimes_{i \in O} \mathcal{H}_{A_i})$.

A proof that σ_{MBQC}^g is indeed correct in the sense of ensuring that Equation (52) is equivalent for all measurement outcomes is given in Appendix D.1. This proof is related to the existing theorem establishing sufficiency of gflow for deterministic computation [Theorem 2, 44] and also provides justification for why the ordering of operators in Equation (53) is valid.

5.2 Quantum Causal Models and Inference

Having defined σ_{MBQC}^g for an arbitrary g , we can now make two connections to the literature of quantum causal models [19, 20, 68] and quantum causal inference [50–52]. Quantum causal models (QCMs) are an extension to the classical causal modelling literature (see e.g. [21, 22, 69]) due, in part, to the realisation that the classical methodology is insufficient for treating quantum correlations [70], and are typically represented in the process matrix formalism [71]. In the first part of this subsection, we show that each σ_{MBQC}^g satisfies the conditions required for being a quantum causal model as per [20].

A key aspect of the classical causality literature consists of regarding the differences between the probability distribution obtained under observations and that obtained under an intervention on one or more of the causal mechanisms generating the distribution. A full introduction and treatment of these notions is beyond the scope of this work, however suffice it to say that their counterparts for quantum causal inference are far more nuanced [50–52]. For our present purposes, we focus on the no-

tion of observation as given in [50] (discussed below) and showcase in the second part of this subsection the close resemblance between this perspective of observation and the measurement channels $\mathcal{M}_{\alpha_i, i, \omega(i)}$ defined in the previous subsection for MBQC.

As a first step towards the upcoming definition of quantum causal models, it is worthwhile to briefly review the main components of their classical counterparts. Classical causal models are specified by a directed acyclic graph (DAG), with each node assigned a random variable, and functional equations relating the value of a given node to the values of its parents. In the quantum case, random variables are replaced by quantum nodes B_i , which consist of two Hilbert spaces \mathcal{H}_{B_i} and $\mathcal{H}_{B_i}^*$ specifying incoming and outgoing state spaces of the node (just as for combs), and with functional equations replaced by quantum channels.

Definition 5.1 (Definition 3.3, [20]). A **quantum causal model** is given by a directed acyclic graph over quantum nodes B_1, \dots, B_n and for each node B_i , a quantum channel $\rho_{B_i | \text{Pa}(B_i)} \in \mathcal{L}(\mathcal{H}_{B_i} \otimes \mathcal{H}_{\text{Pa}(B_i)}^*)$ (where $\text{Pa}(B_i)$ denotes the set of parent nodes to B_i with respect to the DAG) such that all channels mutually commute. This defines a process operator

$$\sigma_{B_1, \dots, B_n} := \prod_{i=1}^n \rho_{B_i | \text{Pa}(B_i)}.$$

A note regarding notation: the asterisk on the $\mathcal{H}_{B_i}^*$ is not (necessarily) to indicate that this is the dual space of \mathcal{H}_{B_i} . It is merely to differentiate the outgoing space of the node from the incoming one. We are avoiding using superscripts involving “in” and “out” since the convention here would clash with that used in the combs notation (ingoing to the node is outgoing from the comb and vice versa).

To show that σ_{MBQC}^g is a valid QCM, we first realise that each gflow g (including the partial order) induces a DAG on the vertices of the corresponding graph G (see Proposition D.2). In particular, for each $i \in V$, the parents of i are given by the union of the correction sets:

$$\text{Pa}(i) := \mathcal{X}_i \cup \mathcal{Z}_i. \quad (57)$$

Using this notation, one can see how to write σ_{MBQC}^g as given in Equation (55) as a product of channels as in the definition above and what those channels are:

$$\sigma_{\text{MBQC}}^g = \prod_{i=1}^n \rho_{A_i | C_{j:j \in \text{Pa}(i)}, A'_i} \quad (58)$$

where

$$\begin{aligned} \rho_{A_i | C_{j:j \in \text{Pa}(i)}, A'_i} := & \sum_{\substack{a_i, b_i \\ \mathbf{c}_{\text{Pa}(i)}}} U_{\text{corr}(\mathbf{c}_{\text{Pa}(i)}, i)} |a_i\rangle\langle b_i| U_{\text{corr}(\mathbf{c}_{\text{Pa}(i)}, i)}^\dagger \\ & \otimes |\mathbf{c}_{\text{Pa}(i)} a_i\rangle\langle \mathbf{c}_{\text{Pa}(i)} b_i| \end{aligned} \quad (59)$$

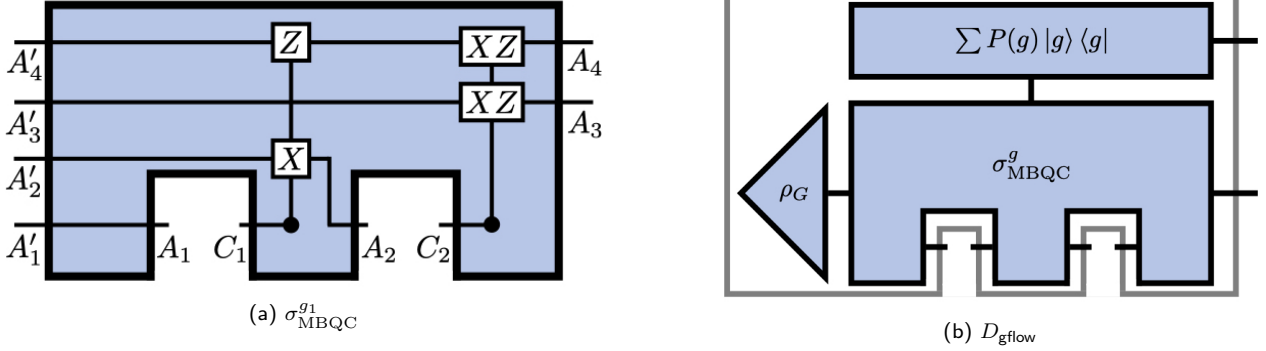


Figure 5: The classical-quantum combs defined here for the consideration of an MBQC device have quantum comb component based on the flow of corrections required for measurement-based computation (known as gflow). (a) An example of such a quantum comb is $\sigma_{\text{MBQC}}^{g_1}$ corresponding to a gflow g_1 for a four-qubit graph state (see the example in Section 5.3 for more details). The graph state is input on the left and passed through the conditional correction channels to each of the output spaces on the right. Measurement channels performing single qubit measurements can be inserted into the gaps (such as between A_1 AND C_1) (b) An example of the full MBQC device (the grey outline) is modelled as a classical-quantum comb built from the classical parameter that takes values g denoting the gflow (equivalently causal structure) and quantum comb σ_{MBQC}^g along with the preparation of the graph state ρ_G . As with all classical-quantum combs in this work, only the lower systems (those extending out of σ_{MBQC}^g) can be interacted with, and the upper system is to be learnt about.

with $c_{\text{Pa}(i)}$ denoting the classical message that are input into σ_{MBQC}^g for the vertices in $\text{Pa}(i)$. The channel $\rho_{A_i|C_{j:j \in \text{Pa}(i)}, A'_i}$ clearly has a very similar structure to Equation (55), but contains only the relevant spaces and corrections pertaining to A_i .

It is immediate to see that the remaining condition, that the $\rho_{A_i|C_{j:j \in \text{Pa}(i)}, A'_i}$ commute, is satisfied: the only overlap between any two such channels occurs on the classical message spaces, upon which the operators are diagonal. We have thus shown:

Proposition 5.1. *For each gflow g , σ_{MBQC}^g is a quantum causal model.*

Having demonstrated the first connection between MBQC and quantum causality, we return to the common theme running through this work: learning about a random variable via interactions with a comb. Let the random variable X take values in the set of all gflows for a given graph G (or perhaps a given tuple (G, I, O) or (G, I, O, ω)) and consider

$$D_{\text{gflow}} := \sum_{g \in X} P(g) |g\rangle\langle g| \otimes \sigma_{\text{MBQC}}^g * \rho_G. \quad (60)$$

In this case, we can understand learning about X as a type of quantum causal discovery: X encodes information about g and g corresponds to a unique QCM, so learning about X , via interactions with the $\sigma_{\text{MBQC}}^g * \rho_G$, is equivalent to learning the causal structure. In the classical literature, a distinction is made between learning the causal structure via observations and via interventions. For the quantum case, Ried et al. [50] (see also [53]) define an observation as a standard projective measurement channel (i.e. one that performs a projective measurement and then prepares the post-measurement state according to the standard update rule) which takes a maximally mixed state as input. The requirement of a maximally

mixed input is necessary and sufficient to enforce an “informational symmetry” between the updated belief of the input state and the knowledge of the output state of the channel (see Section III.A in the supplementary information of [50]).

The measurement channels $\mathcal{M}_{\alpha_i, i, \omega_i}$ defined in Section 5.1 are not *exactly* the measurement channels as stipulated above, but the difference is only cosmetic: the standard projective measurement channel can be recovered simply by post-composing $\mathcal{M}_{\alpha_i, i, \omega_i}$ with a unitary channel (that depends on α_i and ω_i). In particular, the guiding principle of informational symmetry between input and output is preserved. Regarding the requirement of a maximally mixed input state, this is indeed ensured provided that a graph state is input into σ_{MBQC}^g (each single qubit reduced state of a graph state is maximally mixed). Thus, using the present terminology, one could consider a measurement-based computation, such as that described by Equation (52), as a specific set of observations of a particular quantum causal model.

For the reader familiar with the classical causality literature, in particular the work of Pearl (eg., [21]), the A'_i are analogous to the exogenous variables for a classical causal model, and thus ρ_G can be considered as the equivalent of a distribution over the exogenous variables and moreover one that does not factorise into a product distribution as is often assumed. The last sentence of the previous paragraph can then be more thoroughly reformulated as MBQC being a specific set of observations of a particular quantum causal model for a certain state of the exogenous nodes. See Appendix D.2 for more details of this correspondence.

5.3 Causal Discovery Example

Let us now consider a concrete example, which acts both as an explanatory aid to the preceding subsection and as a vehicle to discuss the comparison between the optimal strategy for causal discovery and an observational strategy. We fix a graph and input and output sets for which all corresponding gflows are characterised, and thereafter numerically calculate the min-entropy for D_{gflow} (Equation (60)) as well as for a related comb with a restriction on the included gflows. With this benchmark for the optimal causal learning, we optimise over a restricted set of strategies constrained to consist of observations only (as per the above notion of observation) thereby quantifying the difference between the best such observational strategy and the best overall strategy. We further demonstrate that, for cases where the causal structures (gflows) differ only by symmetries of the input state (graph state), even the optimal strategy is completely uninformative for causal discovery.

Figure 6a depicts the four-vertex graph and choice of input and output sets that forms the basis for our example. For this (G, I, O) there are 15 different possible gflows, which are catalogued in Appendix D by stipulating the map g and corresponding DAG for each (an example is depicted in Figure 6b for g_1 ; the labelling is given in the appendices).

We write the D_{gflow} for this example as

$$D_{\text{gflow}} = \sum_{j=1}^{15} P(g_j) |j\rangle\langle j| \otimes \sigma_{\text{MBQC}}^{g_j} * \rho_G \quad (61)$$

which is a comb in $\text{Comb}(\mathbb{C} \rightarrow A_1, C_1 \rightarrow A_2, C_2 \rightarrow A_{3,4}, \mathbb{C} \rightarrow X)$ where A_1 and A_2 label the Hilbert spaces for graph state qubits 1 and 2 respectively, $A_{3,4}$ labels the two-qubit Hilbert space for the remaining graph state qubits, and X labels a 15-dimensional Hilbert space for which the elements of a choice of orthonormal basis $\{|j\rangle\}_{j=1}^{15}$ correspond to the different gflows. Note that no measurement outcomes on the output qubits are input into D_{gflow} . In this example, we once again assume a uniform prior: $P(g_j) = \frac{1}{15}$.

We will also consider a related comb to D_{gflow} , but instead of including all 15 gflows that exist for the choice of graph and input and output sets, we consider only those for which the assigned measurement planes for qubits 1 and 2 are both in the XY -plane and moreover only the gflows which have partial order such that $1 < 2$. Using the labelling convention of Appendix D, the gflows g_1, g_2, g_4 and g_5 satisfy these criteria. We define

$$D_{XY,1 < 2} := \sum_{j \in \{1,2,4,5\}} P(g_j) |j\rangle\langle j| \otimes \sigma_{\text{MBQC}}^{g_j} * \rho_G \quad (62)$$

with $P(g_j) = \frac{1}{4}$. This is a comb in $\text{Comb}(\mathbb{C} \rightarrow A_1, C_1 \rightarrow A_2, C_2 \rightarrow A_{3,4}, \mathbb{C} \rightarrow X)$ where \mathcal{H}_X is 4-dimensional in this case (we overload X for notational simplicity).

The guessing probability for each of these combs is given below, and, as for all numerical calculations of guessing probabilities in this work, it is calculated via the minimisation over unnormalised combs (recall Equation (13)). However, to conduct the comparison with an optimal observational strategy, it is more convenient to use the maximisation form instead (c.f. Equation (14)):

$$P_{\text{guess}} = \max_E \text{Tr}[DE^T] \quad (63)$$

where D is replaced by D_{gflow} or $D_{XY,1 < 2}$ for the relevant calculation, and E is an element of $\text{Comb}(A_1 \rightarrow C_1, A_2 \rightarrow C_2, A_{3,4} \rightarrow X)$ with X the appropriate space for each case. The guessing probability under observational strategies only is given by an analogous quantity to Equation (63) except that E is now restricted to having the form

$$E := \sum_{c_1, c_2} \mathcal{M}_{C_1|A_1}^{c_1}(|\psi\rangle) \otimes \mathcal{M}_{C_2|A_2}^{c_2}(\phi) \otimes \mathcal{E}_{X|A_{3,4}}^{c_1 c_2} \quad (64)$$

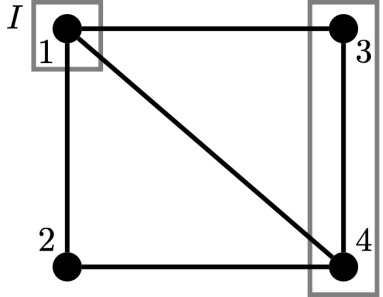
where

$$\begin{aligned} \mathcal{M}_{C_i|A_i}^0(|\psi\rangle) &:= |0\rangle\langle 0|_{C_i} \otimes |\psi\rangle\langle\psi|_{A_i} \\ \mathcal{M}_{C_i|A_i}^1(|\psi\rangle) &:= |1\rangle\langle 1|_{C_i} \otimes (I - |\psi\rangle\langle\psi|)_{A_i} \end{aligned} \quad (65)$$

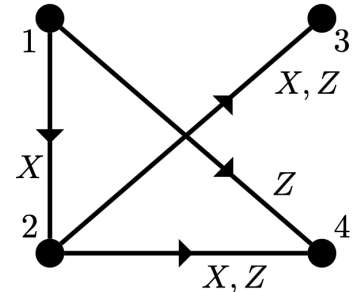
denote the observations, i.e. measurement channels $\mathcal{M}_{C_i|A_i}(\psi) = \mathcal{M}_{C_i|A_i}^0(\psi) + \mathcal{M}_{C_i|A_i}^1(\psi)$, and $\mathcal{E}_{X|A_{3,4}}^{c_1 c_2}$ denotes the Choi state for a CPTP map $\mathcal{E} : \mathcal{H}_{A_{3,4}} \rightarrow \mathcal{H}_X$ for the relevant \mathcal{H}_X for the corresponding D . We allow for the choice of CPTP map to depend on the measurement outcomes, hence the c_1, c_2 in the superscript.

Numerically, the optimal guessing probability for D_{gflow} , which is to say, for selecting the correct causal structure after a single round of interaction with the device, stands at 0.373(2) (see Appendix E for details of the numerical implementation). This is a clear improvement over the uniform distribution prior to interacting with the device ($\frac{1}{15} \approx 0.067(1)$). To calculate the guessing probability with the restriction to observational strategies, a different approach is required since the extra restriction on the set of operators that is maximised over imposes nonlinear constraints on the problem, so SDP methods no longer apply. Namely, a brute force search was conducted over a mesh lattice of single qubit projectors. Using this method, an approximate value for the guessing probability under the optimal observational strategy is 0.199(1) which indicates that there exist strategies for causal discovery that are more informative than any observational strategy for this case.

For $D_{XY,1 < 2}$, the situation is different and rather interesting: the guessing probability is 0.250(0). That is, in a single round even the optimal learning strategy can not distinguish between the four different causal structures. A trivial consequence of this fact is that, in this case, any observational strategy is optimal (but still completely uninformative). In fact, one can understand why the lack of distinguishability is to be expected by considering the following proposition.



(a) (G, I, O)



(b) DAG for g_1

Figure 6: To give a concrete example, we consider a specific graph state and the set of all corresponding gflows. (a) The four qubit graph G and choice of input set $I = \{1\}$ and output set $O = \{3, 4\}$. There are 15 gflows compatible with this choice of (G, I, O) which are catalogued in Appendix D.4 including the corresponding directed acyclic graph and correction operators. (b) The DAG for gflow g_1 , which measures qubits 1 and 2 in the XY -plane following the order $1 < 2$. The labels on the directed arrows depict the conditional correction operators, with the head and tail of the arrow denoting the target and control of the operation respectively.

Proposition 5.2. For any $c_j \in \{0, 1\}$ for $j = 1, \dots, |V \setminus O|$,

$$\left(\bigotimes_{j=1}^{|V \setminus O|} |c_j\rangle\langle c_j|_{C_j} \right) * \sigma_{\text{MBQC}}^g * \rho_G \quad (66)$$

is the same state for each gflow g compatible with (G, I, O, ω) and have mutually compatible partial orders.

The proof is given in Appendix D.3, but the key point is that for any given measurement outcomes, the correction operators induced by each $g \sim (G, I, O, \omega)$ are related to each other by some stabiliser and hence are in fact equivalent.

There are a number of conclusions one can draw from the above analysis. Firstly, as expected, an observational strategy for quantum causal discovery is typically not optimal in general (at least in a single round). Secondly, in certain cases, it is not guaranteed that *anything* about the causal structure can be learnt in a single round by any strategy. This arises due to the fine-tuned situation where the possible causal structures coincide precisely with symmetries of the particular prepared state. This serves to highlight the important role that noise likely plays in the ability to learn a causal structure (a topic for future work). Finally, we must emphasise that the numerical results here are for a single round of interaction only, largely due to implementation constraints (see Appendix E).

5.4 Learning Measurement Planes

The example of $D_{XY,1 < 2}$ above demonstrates that barriers to learning the exact flow of corrections exist, but fortunately, these details are not required if our objective is to use the device to perform computations. In this subsection, we consider the same example as given above, however we are no longer concerned with learning the causal structure of the device but rather learning

enough information about the gflow being implemented in order to ensure deterministic computation.

Specifically, we consider the case where the assignment of measurement planes is unknown: that is, we know (G, I, O) and need to learn ω . We continue with the same graph (G, I, O) as in Figure 6 which has gflows catalogued in Appendix D. Due to the properties of gflow, the input qubits are always assigned the XY -plane by ω , so for our example $\omega(1) \equiv XY$. Since we allow for any measurements on the output qubits, it remains only to learn the value of $\omega(2)$. It turns out that, for the current choice of (G, I, O) , all three measurement planes on qubit 2 are possible, with an equal number of gflows (5) for each. Under the labelling as given in Appendix D, gflows g_1, \dots, g_5 correspond to $\omega(2) = XY$, g_6, \dots, g_{10} to $\omega(2) = XZ$ and g_{11}, \dots, g_{15} to $\omega(2) = YZ$. For this example, we let X be the random variable that encodes the measurement plane choice for the second qubit, i.e. takes values in $\{XY, XZ, YZ\}$, and we denote an arbitrary measurement plane by mp . The notation $g \sim mp$ indicates the gflow g is defined for (G, I, O, ω) where $\omega(2) = mp$.

We consider the comb

$$D_{mp} := \sum_{mp \in X} P(mp) |mp\rangle\langle mp| \otimes \sum_{g \sim mp} P(g|mp) \sigma_{\text{MBQC}}^g * \rho_G \quad (67)$$

in $\text{Comb}(\mathbb{C} \rightarrow A_1, C_1 \rightarrow A_2, C_2 \rightarrow A_{3,4}, \mathbb{C} \rightarrow X)$ where $\dim \mathcal{H}_X = 3$. For simplicity, we once again make uniformity assumptions on the distributions: $P(mp) = \frac{1}{3}$ and $P(g|mp) = \frac{1}{5}$. Under these assumptions, the guessing probability for D_{mp} reaches 1.000(0) indicating that the measurement planes can in fact be determined with certainty after just a single use of the device. This is perhaps unsurprising since the correction operators of gflows that differ in the measurement plane assignment for the second qubit (e.g. for g_1 and g_6) are not related by a stabiliser and so the type of indistinguishability problem that arose for $D_{XY,1 < 2}$ does not apply here.

5.5 Calibrating Measurements

In the previous example, the aim was to learn the correct measurement planes for the proper functioning of the device, which in particular allows the user to insert measurement channels $\mathcal{M}_{\alpha_v, v, \text{mp}_v}$ for the correct mp_v for each v (i.e. $\text{mp}_v = \omega(v)$), thereby performing deterministic computation. However, this is not yet enough to ensure the correctness of a *specific* computation: we need to ensure that the α_v are also correct for each v . To explain this further, consider a computation where all measurements are in the XY -plane, meaning that the projection operators are given by

$$|\pm_{\alpha_v}\rangle\langle\pm_{\alpha_v}| = R_Z(\alpha_v) |\pm\rangle\langle\pm| R_Z(\alpha_v)^\dagger \quad (68)$$

for each v . The $|\pm\rangle$ denote the eigenvectors of the X operator and moreover, there is an implicit assumption that the $|+\rangle$ state is the same as that used in the graph state preparation (recall Equation (7)). This assumption is typically a very reasonable one, however, since in this case the state preparation occurs inside the device and the measurement channels occur outside of it, there is no guarantee that this assumption is valid. If a measurement channel $\mathcal{M}_{\alpha_v, v, XY}$, thought to consist of projectors as in Equation (68), instead consists of projectors

$$R_Z(\alpha_v) |\pm_{\text{meas}}\rangle\langle\pm_{\text{meas}}| R_Z(\alpha_v)^\dagger \quad (69)$$

where

$$|\pm_{\text{meas}}\rangle\langle\pm_{\text{meas}}| = R_Z(\theta) |\pm\rangle\langle\pm| R_Z^\dagger(\theta) \quad (70)$$

for some θ , then the effective measurement on the graph state qubit is for an angle $\alpha_v + \theta$ rather than α_v , meaning an incorrect computation is performed. Even if the measurement planes for the device are known, the specific measurement channels required to calibrate the device in order to give the computations as expected (i.e. specifying the computation using $\alpha_v - \theta$ recovers the correct computation). It is interesting to note that this calibration can be considered as correlating two quantum reference frames [54], the one inside the device with the one outside of it.

In this subsection, we consider a simple example along the lines of the explanation above: we consider a scenario where the positive Z -axis of the Bloch sphere is known, but the positive X -axis is not (we assume a right-handed frame meaning that the positive Y -axis is determined if the positive X - and Z -axes are). In other words, we aim to learn θ in Equation (70) above. We assume θ can take values in a discrete set of angles which are evenly spaced between 0 and 2π . We consider here a simple three-vertex linear graph (i.e. with vertices $V = \{1, 2, 3\}$ and edges $\{(1, 2), (2, 3)\}$), along with a single choice of gflow g defined as $1 \mapsto \{2\}$ and $2 \mapsto \{3\}$, which gives the correction sets (only the non-empty such sets are shown):

$$\mathcal{X}_2 = \{1\}; \quad (71)$$

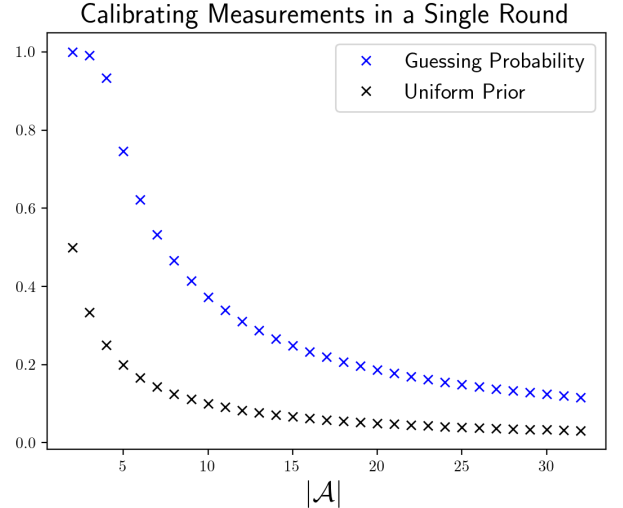


Figure 7: The guessing probability for D_{calibr} in a single round as the size of possible angles set \mathcal{A} varies (shown in blue). The angles of \mathcal{A} are taken to be evenly spaced. The probability of guessing the correct value for the angle off-set θ prior to interacting with the device is shown in black.

$$\mathcal{X}_3 = \{2\}; \quad (72)$$

$$\mathcal{Z}_3 = \{1\}. \quad (73)$$

For the purposes of writing down the comb D_{calibr} for this example, we take the basis $|\pm_{\text{meas}}\rangle\langle\pm_{\text{meas}}|$ as reference and write the graph state ρ_G and the correction operators $U_{\text{corr}(\mathbf{c}), i}$ (recall Equation (53)) with respect to this basis:

$$\rho_G^\theta := R_Z^{\otimes n}(-\theta) \rho_G (R_Z^{\otimes n}(-\theta))^\dagger; \quad (74)$$

$$U_{\text{corr}(\mathbf{c}), i}^\theta := \left(R_Z(-\theta) X_{A_i}^{\bigoplus_{j \in \mathcal{X}_i} c_j} R_Z(-\theta)^\dagger \right) Z_{A_i}^{\bigoplus_{j \in \mathcal{Z}_i} c_j}. \quad (75)$$

Denoting the comb defined from the $U_{\text{corr}(\mathbf{c}), i}^\theta$ in analogy to Equation (55) as $\sigma_{\text{MBQC}}^\theta$ and the (discrete) set of possible (regularly spaced) values for θ by \mathcal{A} , the comb of interest for this example is

$$D_{\text{calibr}} := \sum_{\theta \in \mathcal{A}} P(\theta) |\theta\rangle\langle\theta| \otimes \sigma_{\text{MBQC}}^\theta * \rho_G^\theta. \quad (76)$$

As per usual, we take the prior distribution over θ to be uniform: $P(\theta) = \frac{1}{|\mathcal{A}|}$. The guessing probability values for D_{calibr} for different sizes of \mathcal{A} , ranging from $|\mathcal{A}| = 2$ to $|\mathcal{A}| = 32$, are shown in Figure 7. For $|\mathcal{A}| = 2$, the correct direction can be known with certainty in a single round, and almost so for the case where $|\mathcal{A}| = 3$ ($P_{\text{guess}} \approx 0.992(5)$), but otherwise there is a steep decrease in the guessing probability as the size of \mathcal{A} increases.

6 Discussion

By interacting with a system, possibly via some complicated sequence of actions, one can learn a certain prop-

erty of the system that influences the details of the interaction. By modelling such a situation within the quantum combs formalism, it is possible to leverage the comb min-entropy [26], to quantify how much one can learn about the unknown property in question. Due to the general, and also natural, modelling of both quantum and classical interactions as combs of the form considered above, the methodology showcased here has broad applicability.

In this work, we restricted our attention to a novel set of combs defined by the paradigm of measurement-based quantum computation. In this first instance, we defined a classical comb which models a specific BQC protocol [36] and by so doing, give a proof of partial security based on the comb min-entropy for both a single round of the protocol as well as the multi-round case, extending the security analysis in the existing literature.

We further defined a series of combs that model interactions with an MBQC device under varying levels of knowledge regarding the inner working of the device. This establishes a previously unmade connection between MBQC and quantum causality. By observing that the gflow component from which the MBQC combs are built satisfies the criteria of a quantum causal model, we were able to utilise the comb min-entropy to quantify the optimal strategy for causal discovery in specific cases, including cases where no information about the causal structure could be determined by any strategy. We investigated further examples related to learning the minimal extra information required in order to ensure the correct functioning of the device as a computer.

6.1 Limitations of the Min-Entropy Approach

Despite the broad applicability and operational meaning of the methodology used in this work, there are certain limitations of which one should be made aware. Primarily, when using a numerical SDP solver, size issues quickly start to play a role. For example, in the three-qubit graph state example for the BQC protocol in Section 4.3, as a square matrix, the operator $D_{\text{client}}^{(m)}$ has dimension $|\mathcal{A}|^{3+3m}2^{3m}$ where m is the number of rounds. For the minimal possible choice of angle set, $|\mathcal{A}| = 4$ and for a single round, this already equals 32768. For larger angle sets or greater number of rounds, the size problems became prohibitive, disallowing any numerical calculations of the guessing probability on the available hardware (see Appendix E).

6.2 Future Work

As mentioned above, the generality of the combs framework ensures that the methodology considered in this work can be applied in a wide variety of contexts (keeping in mind the limitations outlined above). We conclude by outlining a couple of avenues for future work.

One feature of many SDP solvers that was not utilised in this work, regards the possibility to return an optimal solution instance (and its dual) along with the optimal value (e.g. the min-entropy) for the problem at hand. Depending on the exact formulation used for the min-entropy (recall Equations (12) to (14)) either the primal solution or its dual will be a matrix representing a strategy for interacting with the system in question. It would be interesting to analyse these matrices in order to infer what the corresponding strategy would be. For example, in Section 5.3, the min-entropy quantified the best strategy for inferring the causal structure in a single round of interaction. The solution that gives the optimal value could in principle be deconstructed into components acting at each node of the quantum causal model. This may help identify a type of quantum instrument or sequence of instruments that are optimal for causal inference in general (rather than just for the specific example).

A second interesting type of analysis that could be performed relates to the effect of noise on the min-entropy. The examples considered in Section 5 all included the preparation of a graph state ρ_G and the operators σ_{MBQC} which were specifically tailored to the graph G . In realistic situations, these preparations and the implementations of the corrections $U_{\text{corr}(\epsilon)}$ could be afflicted by noise. Using the methodology here, one could, for example, investigate the effect that different noise models could have on the guessing probability for determining e.g. the correct measurement planes for the MBQC device. Since adding noise to ρ_G would not change the dimension of the comb to which it is constituent, there is no added computational overhead and so the noise analysis could be conducted for any case in which the noiseless case can be calculated.

7 Acknowledgements

We would like to thank Atul Mantri for useful discussions about the security of the BQC protocol of [36], Simon Milz for insightful comments regarding quantum combs, Joshua Morris for invaluable suggestions regarding semi-definite programming resources, and Sofiene Jerbi for useful conversations regarding gflow and MBQC. We acknowledge support from the Austrian Science Fund (FWF) through DK-ALM: W1259-N27 and SFB BeyondC F7102, and from the University of Innsbruck. This work was also co-funded by the European Union (ERC, QuantAI, Project No. 101055129). Views and opinions expressed are however those of the author(s) only and do not necessarily reflect those of the European Union or the European Research Council. Neither the European Union nor the granting authority can be held responsible for them.

References

- [1] John Preskill. "Quantum Computing in the NISQ era and beyond". In: *Quantum* 2 (2018), p. 79. ISSN: 2521-327X. DOI: [10.22331/q-2018-08-06-79](https://doi.org/10.22331/q-2018-08-06-79). URL: <https://doi.org/10.22331/q-2018-08-06-79>.
- [2] H.-J. Briegel et al. "Quantum Repeaters: The Role of Imperfect Local Operations in Quantum Communication". In: *Phys. Rev. Lett.* 81 (26 1998), pp. 5932–5935. DOI: [10.1103/PhysRevLett.81.5932](https://doi.org/10.1103/PhysRevLett.81.5932). URL: <https://link.aps.org/doi/10.1103/PhysRevLett.81.5932>.
- [3] Rodney Van Meter. *Quantum Networking*. ISTE Ltd/John Wiley and Sons Inc, Hoboken, NJ, 2014. DOI: [10.1002/9781118648919](https://doi.org/10.1002/9781118648919).
- [4] Davide Castelvecchi. "The quantum internet has arrived (and it hasn't)." In: *Nature* 554.7690 (2018), pp. 289–293. DOI: [10.1038/d41586-018-01835-3](https://doi.org/10.1038/d41586-018-01835-3).
- [5] Sheng-Kai Liao et al. "Satellite-relayed intercontinental quantum network". In: *Physical review letters* 120.3 (2018), p. 030501. DOI: [10.1103/PhysRevLett.120.030501](https://doi.org/10.1103/PhysRevLett.120.030501).
- [6] CT Nguyen et al. "Quantum network nodes based on diamond qubits with an efficient nanophotonic interface". In: *Physical review letters* 123.18 (2019), p. 183602. DOI: [10.1103/PhysRevLett.123.183602](https://doi.org/10.1103/PhysRevLett.123.183602).
- [7] Peter C Humphreys et al. "Deterministic delivery of remote entanglement on a quantum network". In: *Nature* 558.7709 (2018), pp. 268–273. DOI: [10.1038/s41586-018-0200-5](https://doi.org/10.1038/s41586-018-0200-5).
- [8] Boris Korzh et al. "Provably secure and practical quantum key distribution over 307 km of optical fibre". In: *Nature Photonics* 9.3 (2015), pp. 163–168. DOI: [10.1038/nphoton.2014.327](https://doi.org/10.1038/nphoton.2014.327).
- [9] Rachel Courtland. "China's 2,000-km quantum link is almost complete". In: *IEEE Spectrum* 53.11 (2016), pp. 11–12. DOI: [10.1109/MSPEC.2016.7607012](https://doi.org/10.1109/MSPEC.2016.7607012).
- [10] Mohamed Elboukhari, Mostafa Azizi, and Abdelmalek Azizi. "Quantum Key Distribution Protocols: A Survey." In: *International Journal of Universal Computer Science* 1.2 (2010). DOI: [10.1109/ICWT.2018.8527822](https://doi.org/10.1109/ICWT.2018.8527822).
- [11] Angela Sara Cacciapuoti et al. "Quantum internet: networking challenges in distributed quantum computing". In: *IEEE Network* 34.1 (2019), pp. 137–143. DOI: [10.1109/MNET.001.1900092](https://doi.org/10.1109/MNET.001.1900092).
- [12] Quantum Internet Alliance. <https://quantum-internet.team>. 2022.
- [13] Antonio Acín et al. "The quantum technologies roadmap: a European community view". In: *New Journal of Physics* 20.8 (2018), p. 080201. DOI: [10.1088/1367-2630/aad1ea](https://doi.org/10.1088/1367-2630/aad1ea). URL: <https://doi.org/10.1088/1367-2630/2Faad1ea>.
- [14] Robert Beals et al. "Efficient distributed quantum computing". In: *Proceedings of the Royal Society A: Mathematical, Physical and Engineering Sciences* 469.2153 (2013), p. 20120686. DOI: [10.1098/rspa.2012.0686](https://doi.org/10.1098/rspa.2012.0686).
- [15] Vasil S Denchev and Gopal Pandurangan. "Distributed quantum computing: A new frontier in distributed systems or science fiction?" In: *ACM SIGACT News* 39.3 (2008), pp. 77–95.
- [16] Rene Allerstorfer et al. *On the Role of Quantum Communication and Loss in Attacks on Quantum Position Verification*. arXiv:2208.04341. 2022. DOI: [10.48550/ARXIV.2208.04341](https://doi.org/10.48550/ARXIV.2208.04341). URL: <https://arxiv.org/abs/2208.04341>.
- [17] Joseph F Fitzsimons. "Private quantum computation: an introduction to blind quantum computing and related protocols". In: *npj Quantum Information* 3.1 (2017), pp. 1–11. DOI: [10.1038/s41534-017-0025-3](https://doi.org/10.1038/s41534-017-0025-3).
- [18] John-Mark A Allen et al. "Quantum common causes and quantum causal models". In: *Physical Review X* 7.3 (2017), p. 031021. DOI: [10.1103/PhysRevX.7.031021](https://doi.org/10.1103/PhysRevX.7.031021).
- [19] Fabio Costa and Sally Shrapnel. "Quantum causal modelling". In: *New Journal of Physics* 18.6 (2016), p. 063032. DOI: [10.1088/1367-2630/18/6/063032](https://doi.org/10.1088/1367-2630/18/6/063032).
- [20] Jonathan Barrett, Robin Lorenz, and Oghnyan Oreshkov. "Quantum causal models". In: *arXiv preprint arXiv:1906.10726* (2019). DOI: [10.48550/arXiv.1906.10726](https://doi.org/10.48550/arXiv.1906.10726).
- [21] Judea Pearl. *Causality*. 2nd ed. Cambridge University Press, 2009. DOI: [10.1017/CBO9780511803161](https://doi.org/10.1017/CBO9780511803161).
- [22] Peter Spirtes et al. *Causation, prediction, and search*. MIT press, 2000. DOI: [10.7551/mitpress/1754.001.0001](https://doi.org/10.7551/mitpress/1754.001.0001).
- [23] Giulio Chiribella, Giacomo Mauro D'Ariano, and Paolo Perinotti. "Theoretical framework for quantum networks". In: *Physical Review A* 80.2 (2009), p. 022339. DOI: [10.1103/PhysRevA.80.022339](https://doi.org/10.1103/PhysRevA.80.022339).
- [24] Giulio Chiribella, G Mauro D'Ariano, and Paolo Perinotti. "Quantum circuit architecture". In: *Physical review letters* 101.6 (2008), p. 060401. DOI: [10.1103/PhysRevLett.101.060401](https://doi.org/10.1103/PhysRevLett.101.060401).
- [25] Felix A Pollock et al. "Non-Markovian quantum processes: Complete framework and efficient characterization". In: *Physical Review A* 97.1 (2018), p. 012127. DOI: [10.1103/PhysRevA.97.012127](https://doi.org/10.1103/PhysRevA.97.012127).
- [26] Giulio Chiribella and Daniel Ebler. "Optimal quantum networks and one-shot entropies". In: *New Journal of Physics* 18.9 (2016), p. 093053. DOI: [10.1088/1367-2630/18/9/093053](https://doi.org/10.1088/1367-2630/18/9/093053).
- [27] Robert Konig, Renato Renner, and Christian Schaffner. "The operational meaning of min-and max-entropy". In: *IEEE Transactions on Information theory* 55.9 (2009), pp. 4337–4347. DOI: [10.1109/TIT.2009.2025545](https://doi.org/10.1109/TIT.2009.2025545).

[28] Mark M Wilde. “From classical to quantum Shannon theory”. In: *arXiv preprint arXiv:1106.1445* (2011). doi: [10.48550/arXiv.1106.1445](https://doi.org/10.48550/arXiv.1106.1445).

[29] Robert Raussendorf and Hans J Briegel. “A one-way quantum computer”. In: *Physical review letters* 86.22 (2001), p. 5188. doi: [10.1103/PhysRevLett.86.5188](https://doi.org/10.1103/PhysRevLett.86.5188).

[30] Hans J Briegel et al. “Measurement-based quantum computation”. In: *Nature Physics* 5.1 (2009), pp. 19–26. doi: [10.1038/nphys1157](https://doi.org/10.1038/nphys1157).

[31] Robert Raussendorf, Daniel E Browne, and Hans J Briegel. “Measurement-based quantum computation on cluster states”. In: *Physical review A* 68.2 (2003), p. 022312. doi: [10.1103/PhysRevA.68.022312](https://doi.org/10.1103/PhysRevA.68.022312).

[32] Robert Raussendorf and Hans Briegel. “Computational model underlying the one-way quantum computer”. In: *arXiv preprint quant-ph/0108067* (2001). doi: [10.48550/arXiv.quant-ph/0108067](https://doi.org/10.48550/arXiv.quant-ph/0108067).

[33] Richard Jozsa. “An introduction to measurement based quantum computation”. In: *NATO Science Series, III: Computer and Systems Sciences. Quantum Information Processing-From Theory to Experiment* 199 (2006), pp. 137–158.

[34] D Gross and J Eisert. “Novel schemes for measurement-based quantum computation”. In: *Physical review letters* 98.22 (2007), p. 220503. doi: [10.1103/PhysRevLett.98.220503](https://doi.org/10.1103/PhysRevLett.98.220503).

[35] Anne Broadbent, Joseph Fitzsimons, and Elham Kashefi. “Universal blind quantum computation”. In: *2009 50th Annual IEEE Symposium on Foundations of Computer Science*. IEEE. 2009, pp. 517–526. doi: [10.1109/FOCS.2009.36](https://doi.org/10.1109/FOCS.2009.36).

[36] Atul Mantri et al. “Flow ambiguity: A path towards classically driven blind quantum computation”. In: *Physical Review X* 7.3 (2017), p. 031004. doi: [10.1103/PhysRevX.7.031004](https://doi.org/10.1103/PhysRevX.7.031004).

[37] Tomoyuki Morimae and Keisuke Fujii. “Blind quantum computation protocol in which Alice only makes measurements”. In: *Physical Review A* 87.5 (2013), p. 050301. doi: [10.1103/PhysRevA.87.050301](https://doi.org/10.1103/PhysRevA.87.050301).

[38] Tomoyuki Morimae. “Verification for measurement-only blind quantum computing”. In: *Physical Review A* 89.6 (2014), p. 060302. doi: [10.1103/PhysRevA.89.060302](https://doi.org/10.1103/PhysRevA.89.060302).

[39] Hans J Briegel and Robert Raussendorf. “Persistent entanglement in arrays of interacting particles”. In: *Physical Review Letters* 86.5 (2001), p. 910. doi: [10.1103/PhysRevLett.86.910](https://doi.org/10.1103/PhysRevLett.86.910).

[40] Marc Hein et al. “Entanglement in graph states and its applications”. In: *Volume 162: Quantum Computers, Algorithms and Chaos*. Proceedings of the International School of Physics “Enrico Fermi”. IOS Press Ebooks, 2006, pp. 115–218. doi: [10.3254/978-1-61499-018-5-115](https://doi.org/10.3254/978-1-61499-018-5-115).

[41] Marc Hein, Jens Eisert, and Hans J Briegel. “Multiparty entanglement in graph states”. In: *Physical Review A* 69.6 (2004), p. 062311. doi: [10.1103/PhysRevA.69.062311](https://doi.org/10.1103/PhysRevA.69.062311).

[42] Mehdi Mhalla et al. “Which graph states are useful for quantum information processing?” In: *Conference on Quantum Computation, Communication, and Cryptography*. Springer. 2011, pp. 174–187. doi: [10.1007/978-3-642-54429-3_12](https://doi.org/10.1007/978-3-642-54429-3_12).

[43] Marc Hein et al. “Entanglement in graph states and its applications”. In: *arXiv preprint quant-ph/0602096* (2006). doi: [10.48550/arXiv.quant-ph/0602096](https://doi.org/10.48550/arXiv.quant-ph/0602096).

[44] Daniel E Browne et al. “Generalized flow and determinism in measurement-based quantum computation”. In: *New Journal of Physics* 9.8 (2007), p. 250. doi: [10.1088/1367-2630/9/8/250](https://doi.org/10.1088/1367-2630/9/8/250).

[45] Vincent Danos and Elham Kashefi. “Determinism in the one-way model”. In: *Physical Review A* 74.5 (2006), p. 052310. doi: [10.1103/PhysRevA.74.052310](https://doi.org/10.1103/PhysRevA.74.052310).

[46] Damian Markham and Elham Kashefi. “Entanglement, flow and classical simulability in measurement based quantum computation”. In: *Horizons of the Mind. A Tribute to Prakash Panangaden*. Springer, 2014, pp. 427–453. doi: [10.1007/978-3-319-06880-0_22](https://doi.org/10.1007/978-3-319-06880-0_22).

[47] Vincent Danos, Elham Kashefi, and Prakash Panangaden. “The measurement calculus”. In: *Journal of the ACM (JACM)* 54.2 (2007), 8–es. doi: [10.1145/1219092.1219096](https://doi.org/10.1145/1219092.1219096).

[48] Maarten Van den Nest, Jeroen Dehaene, and Bart De Moor. “Graphical description of the action of local Clifford transformations on graph states”. In: *Physical Review A* 69.2 (2004), p. 022316. doi: [10.1103/PhysRevA.69.022316](https://doi.org/10.1103/PhysRevA.69.022316).

[49] Maarten Van den Nest, Jeroen Dehaene, and Bart De Moor. “Local unitary versus local Clifford equivalence of stabilizer states”. In: *Physical Review A* 71.6 (2005), p. 062323. doi: [10.1103/PhysRevA.75.032325](https://doi.org/10.1103/PhysRevA.75.032325).

[50] Katja Ried et al. “A quantum advantage for inferring causal structure”. In: *Nature Physics* 11.5 (2015), pp. 414–420. doi: [10.1038/nphys3266](https://doi.org/10.1038/nphys3266).

[51] Joseph F Fitzsimons, Jonathan A Jones, and Vlatko Vedral. “Quantum correlations which imply causation”. In: *Scientific reports* 5.1 (2015), pp. 1–7. doi: [10.1038/srep18281](https://doi.org/10.1038/srep18281).

[52] Giulio Chiribella and Daniel Ebler. “Quantum speedup in the identification of cause–effect relations”. In: *Nature communications* 10.1 (2019), pp. 1–8. doi: [10.1038/s41467-019-09383-8](https://doi.org/10.1038/s41467-019-09383-8).

[53] Jonas M Kübler and Daniel Braun. “Two-qubit causal structures and the geometry of positive qubit-maps”. In: *New Journal of Physics* 20.8 (2018), p. 083015. doi: [10.1088/1367-2630/aad612](https://doi.org/10.1088/1367-2630/aad612).

[54] Stephen D Bartlett, Terry Rudolph, and Robert W Spekkens. “Reference frames, superselection rules, and quantum information”. In: *Reviews of Modern Physics* 79.2 (2007), p. 555. DOI: [10.1103/RevModPhys.79.555](https://doi.org/10.1103/RevModPhys.79.555).

[55] Man-Duen Choi. “Completely positive linear maps on complex matrices”. In: *Linear algebra and its applications* 10.3 (1975), pp. 285–290. DOI: [10.1016/0024-3795\(75\)90075-0](https://doi.org/10.1016/0024-3795(75)90075-0).

[56] Andrzej Jamiołkowski. “Linear transformations which preserve trace and positive semidefiniteness of operators”. In: *Reports on Mathematical Physics* 3.4 (1972), pp. 275–278. DOI: [10.1016/0034-4877\(72\)90011-0](https://doi.org/10.1016/0034-4877(72)90011-0).

[57] Daniel Gottesman. *Stabilizer codes and quantum error correction*. California Institute of Technology, 1997.

[58] Mehdi Mhalla and Simon Perdrix. “Finding optimal flows efficiently”. In: *International Colloquium on Automata, Languages, and Programming*. Springer, 2008, pp. 857–868. DOI: [10.1007/978-3-540-70575-8-70](https://doi.org/10.1007/978-3-540-70575-8-70).

[59] Niel De Beaudrap. “Finding flows in the one-way measurement model”. In: *Physical Review A* 77.2 (2008), p. 022328. DOI: [10.1103/PhysRevA.77.022328](https://doi.org/10.1103/PhysRevA.77.022328).

[60] Renato Renner. “Security of quantum key distribution”. In: *International Journal of Quantum Information* 6.01 (2008), pp. 1–127. DOI: [10.1142/S0219749908003256](https://doi.org/10.1142/S0219749908003256).

[61] Marco Tomamichel, Roger Colbeck, and Renato Renner. “A fully quantum asymptotic equipartition property”. In: *IEEE Transactions on information theory* 55.12 (2009), pp. 5840–5847. DOI: [10.1109/TIT.2009.2032797](https://doi.org/10.1109/TIT.2009.2032797).

[62] Marco Tomamichel. *Quantum information processing with finite resources: mathematical foundations*. Vol. 5. Springer, 2015. DOI: [10.1007/978-3-319-21891-5](https://doi.org/10.1007/978-3-319-21891-5).

[63] Matthew S Leifer and Robert W Spekkens. “Towards a formulation of quantum theory as a causally neutral theory of Bayesian inference”. In: *Physical Review A* 88.5 (2013), p. 052130. DOI: [10.1103/PhysRevA.88.052130](https://doi.org/10.1103/PhysRevA.88.052130).

[64] Christopher Portmann et al. “Causal boxes: quantum information-processing systems closed under composition”. In: *IEEE Transactions on Information Theory* 63.5 (2017), pp. 3277–3305. DOI: [10.1109/TIT.2017.2676805](https://doi.org/10.1109/TIT.2017.2676805).

[65] Ueli Maurer. “Abstract models of computation in cryptography”. In: *IMA International Conference on Cryptography and Coding*. Springer, 2005, pp. 1–12. DOI: [10.1007/11586821-1](https://doi.org/10.1007/11586821-1).

[66] Christopher Portmann and Renato Renner. “Security in quantum cryptography”. In: *Reviews of Modern Physics* 94.2 (2022), p. 025008. DOI: [10.1103/RevModPhys.94.025008](https://doi.org/10.1103/RevModPhys.94.025008).

[67] Atul Mantri, Tommaso F Demarie, and Joseph F Fitzsimons. “Universality of quantum computation with cluster states and (X, Y)-plane measurements”. In: *Scientific reports* 7.1 (2017), pp. 1–7. DOI: [10.1038/srep42861](https://doi.org/10.1038/srep42861).

[68] Giacomo Mauro D’Ariano. “Causality re-established”. In: *Philosophical Transactions of the Royal Society A: Mathematical, Physical and Engineering Sciences* 376.2123 (2018), p. 20170313. DOI: [10.1098/rsta.2017.0313](https://doi.org/10.1098/rsta.2017.0313).

[69] Bernhard Schölkopf et al. “On causal and anticausal learning”. In: *arXiv preprint arXiv:1206.6471* (2012). DOI: [10.48550/arXiv.1206.6471](https://doi.org/10.48550/arXiv.1206.6471).

[70] Christopher J Wood and Robert W Spekkens. “The lesson of causal discovery algorithms for quantum correlations: Causal explanations of Bell-inequality violations require fine-tuning”. In: *New Journal of Physics* 17.3 (2015), p. 033002. DOI: [10.1088/1367-2630/17/3/033002](https://doi.org/10.1088/1367-2630/17/3/033002).

[71] Ognyan Oreshkov, Fabio Costa, and Časlav Brukner. “Quantum correlations with no causal order”. In: *Nature communications* 3.1 (2012), pp. 1–8. DOI: [10.1038/ncomms2076](https://doi.org/10.1038/ncomms2076).

[72] Isaac D. Smith and Marius Krumm. *Min-Entropy and MBQC*. https://github.com/IsaacDSmith/Min-Entropy_and_MBQC.

[73] Steven Diamond and Stephen Boyd. “CVXPY: A Python-embedded modeling language for convex optimization”. In: *Journal of Machine Learning Research* 17.83 (2016), pp. 1–5.

[74] Akshay Agrawal et al. “A rewriting system for convex optimization problems”. In: *Journal of Control and Decision* 5.1 (2018), pp. 42–60.

[75] Brendan O’Donoghue et al. *SCS: Splitting Conic Solver, version 3.2.2*. <https://github.com/cvxgrp/scs>. 2021.

[76] Brendan O’Donoghue et al. “Conic Optimization via Operator Splitting and Homogeneous Self-Dual Embedding”. In: *Journal of Optimization Theory and Applications* 169.3 (2016), pp. 1042–1068. URL: <http://stanford.edu/~boyd/papers/scs.html>.

A Preliminaries Section Supplementary

This appendix houses some supporting discussion for Section 2.

A.1 Motivating Quantum Combs

In this subsection, we briefly motivate the definition of quantum comb given in the main text (Definition 2.1), including why this is an appropriate representation of quantum networks and what the conditions of the definition correspond to. We provide these explanations here for completeness; they are drawn from references such as [23, 24] which should be referred to for further details.

The definition of quantum comb given earlier is as an operator on a tensor product of Hilbert spaces, which represents a series of connected quantum channels. This correspondence between operators on a tensor product of spaces and maps between these spaces, that is, between elements of $\mathcal{L}(\mathcal{H}_A \otimes \mathcal{H}_B)$ and $\mathcal{L}(\mathcal{L}(\mathcal{H}_A), \mathcal{L}(\mathcal{H}_B))$ respectively, makes use of the Choi-Jamiolkowski isomorphism [55, 56]. Since we are most interested in the operator form, we make the following definition.

Definition A.1. For a linear map $\mathcal{E} : \mathcal{L}(\mathcal{H}_A) \rightarrow \mathcal{L}(\mathcal{H}_B)$, its **Choi operator** is defined as:

$$E := (\mathcal{E} \otimes I_{\mathcal{H}_{A'}})(|\Phi^+\rangle\langle\Phi^+|). \quad (77)$$

Here, $\mathcal{H}_{A'} \simeq \mathcal{H}_A$ is a copy of the input space, and $|\Phi^+\rangle := \sum_{i=0}^{d_A-1} |ii\rangle_{A'A}$ is an unnormalised maximally entangled state on $\mathcal{H}_{A'} \otimes \mathcal{H}_A$.

The defining properties of CPTP maps correspond to properties of the Choi operator:

Lemma A.1. *The Choi operator E of a linear map \mathcal{E} satisfies the following properties:*

1. E is positive semi-definite, denoted $E \geq 0$, iff \mathcal{E} is completely positive;
2. E is Hermitian iff \mathcal{E} is Hermitian-preserving;
3. $\text{Tr}_B [E] \leq I_A$ iff \mathcal{E} is trace non-increasing;
4. $\text{Tr}_B [E] = I_A$ iff \mathcal{E} is trace-preserving.

One notices that the first and last items of the above lemma feature in Definition 2.1, however iteratively for the latter item. To arrive at the iterative constraints, consider a simple example of two CPTP maps $\mathcal{E}_1 : \mathcal{L}(\mathcal{H}_{A_1}) \rightarrow \mathcal{L}(\mathcal{H}_{B_1} \otimes \mathcal{H}_C)$ and $\mathcal{E}_2 : \mathcal{L}(\mathcal{H}_{A_2} \otimes \mathcal{H}_C) \rightarrow \mathcal{H}_{B_2}$ with Choi operators E_1 and E_2 respectively. The composition of the two maps over the space H_C , denoted $\mathcal{E}_2 \circ_C \mathcal{E}_1$ is a linear operator from $\mathcal{L}(\mathcal{H}_{A_1} \otimes \mathcal{H}_{A_2})$ to $\mathcal{L}(\mathcal{H}_{B_1} \otimes \mathcal{H}_{B_2})$, and the corresponding Choi operator is given by

$$E = E_1 *_C E_2 \quad (78)$$

where $*_C$ denotes the link product over the space C , which is the analogue of composition in the Choi operator picture. By tracing over B_2 , we get

$$\text{Tr}_{B_2} [E] = \text{Tr}_{B_2} [E_1 *_C E_2] \quad (79)$$

$$= E_1 *_C \text{Tr}_{B_2} [E_2] \quad (80)$$

$$= E_1 *_C (I_C \otimes I_{A_2}) \quad (81)$$

$$= I_{A_2} \otimes \text{Tr}_C [E_1] \quad (82)$$

where we have used the trace-preservation criterion of Lemma A.1. Noting that $\text{Tr}_C [E_1]$ is a positive semi-definite operator, we see that the last line above is indeed of the form of the constraints in Definition 2.1. By tracing also over B_1 , we can use the trace-preservation again to obtain the terminal constraint of normalisation to 1. This reasoning extends to any number of composed maps, which helps demonstrate the conciseness of the comb notation.

The remainder of this appendix subsection provides the proof of Proposition 2.1 given in Section 2.1.

Proof of Proposition 2.1. The proof consists of showing that the sequence of partial trace constraints (Definition 2.1) are satisfied for both the sequence where X is traced over first then $A_n^{\text{out}}, \dots, A_1^{\text{out}}$ and the sequence $A_n^{\text{out}}, \dots, A_1^{\text{out}}, X$. Starting with the former, tracing over X gives

$$\text{Tr}_X[D] = \sum_x P(x) \sigma_x \equiv I_{\mathbb{C}} \otimes \sum_x P(x) \sigma_x. \quad (83)$$

Since the σ_x are normalised combs, and since the set of normalised combs is convex, $\sum_x P(x) \sigma_x$ is also a normalised comb and so the remaining trace conditions are satisfied, thus showing that $D \in \text{Comb}(A_1^{\text{in}} \rightarrow A_1^{\text{out}}, \dots, A_n^{\text{in}} \rightarrow A_n^{\text{out}}, \mathbb{C} \rightarrow X)$.

For the other sequence, define a sequence of operators D_k , $k = 0, \dots, n+1$ via

$$D_k := \sum_x P(x) |x\rangle\langle x| \otimes C_{x,k-1} \quad \forall k = 1, \dots, n+1 \quad (84)$$

$$D_0 := \sum_x P(x) \quad (85)$$

where $C_{x,0}, \dots, C_{x,n}$ denote the positive semi-definite operators that satisfy the comb conditions for σ_x , that is:

$$\sigma_x = C_{x,n}; \quad (86)$$

$$\text{Tr}_{A_j^{\text{out}}}[C_{x,j}] = I_{A_j^{\text{in}}} \otimes C_{x,j-1} \quad \forall j = 1, \dots, n; \quad (87)$$

$$C_{x,0} = 1. \quad (88)$$

It follows that $D_{n+1} = D$, that

$$\text{Tr}_{A_{k-1}^{\text{out}}}[D_k] = \sum_x P(x) |x\rangle\langle x| \otimes \text{Tr}_{A_{k-1}^{\text{out}}}[C_{x,k-1}] \quad (89)$$

$$= \sum_x P(x) |x\rangle\langle x| \otimes I_{A_{k-1}^{\text{in}}} \otimes C_{x,k-2} \quad (90)$$

$$= I_{A_{k-1}^{\text{in}}} \otimes D_{k-1} \quad (91)$$

for all $k = 2, \dots, n+1$, that

$$\text{Tr}_X[D_1] = \text{Tr}_X \left[\sum_x P(x) |x\rangle\langle x| \otimes 1 \right] \quad (92)$$

$$= \sum_x P(x) \quad (93)$$

$$= I_{\mathbb{C}} \otimes D_0 \quad (94)$$

and that $D_0 = 1$. Thus, D is also in $\text{Comb}(\mathbb{C} \rightarrow X, A_1^{\text{in}} \rightarrow A_1^{\text{out}}, \dots, A_n^{\text{in}} \rightarrow A_n^{\text{out}})$. \square

A.2 Equivalent Correction Methods for Measurement Outcomes

Here, we elaborate on the discussion in Section 2.2 regarding the correction of measurement outcomes in MBQC via products of stabilisers K_v of graph state $|G\rangle$. To recap what is written in the main text, the correction for negative measurement outcomes starts by noticing that, due to the restriction of the allowed measurement to the planes of the Bloch sphere, the negative projection operators are related to the positive ones via conjugation by X , Z or their product, which each exist as a factor of a (product of) stabiliser(s). By applying the remainder of an appropriate stabiliser in the case when a negative outcome obtains, a symmetry of the graph state is completed and in effect, a positive projection has been enacted instead.

We demonstrate this with the following example where a vertex $v \in V$ is measured in the XY -plane (the same reasoning applies for the other measurement planes). We let $v' \in V$ be a distinguished neighbour of v and denote all pending measurements on $|G\rangle$ (also in the XY -plane for simplicity) as $|\pm_{\alpha_{\tilde{v}}}\rangle\langle\pm_{\alpha_{\tilde{v}}}|_{\tilde{v}}$ for $\tilde{v} \in V \setminus \{v\}$. The notation $K_{v'}|_{\setminus v}$ denotes the stabiliser $K_{v'}$ with the tensor factor corresponding to v replaced by I_v .

$$\text{Tr} \left[\left(\left| -_{\alpha_v} \rangle\langle -_{\alpha_v} \right|_v \bigotimes_{\tilde{v} \in V \setminus \{v\}} \left| \pm_{\alpha_{\tilde{v}}} \rangle\langle \pm_{\alpha_{\tilde{v}}} \right|_{\tilde{v}} \right) \rho_G \right] = \text{Tr} \left[\left(Z_v^\dagger \left| +_{\alpha_v} \rangle\langle +_{\alpha_v} \right|_v Z_v \bigotimes_{\tilde{v} \in V \setminus \{v\}} \left| \pm_{\alpha_{\tilde{v}}} \rangle\langle \pm_{\alpha_{\tilde{v}}} \right|_{\tilde{v}} \right) \rho_G \right] \quad (95)$$

$$= \text{Tr} \left[\left(|+\alpha_v\rangle\langle +\alpha_v|_v \bigotimes_{\tilde{v} \in V \setminus \{v\}} |\pm_{\alpha_{\tilde{v}}}\rangle\langle \pm_{\alpha_{\tilde{v}}}|_{\tilde{v}} \right) Z_v \rho_G Z_v^\dagger \right] \quad (96)$$

$$= \text{Tr} \left[\left(|+\alpha_v\rangle\langle +\alpha_v|_v \bigotimes_{\tilde{v} \in V \setminus \{v\}} |\pm_{\alpha_{\tilde{v}}}\rangle\langle \pm_{\alpha_{\tilde{v}}}|_{\tilde{v}} \right) K_{v'} |\downarrow_v \rho_G K_{v'}|_{\downarrow_v}^\dagger \right] \quad (97)$$

$$= \text{Tr} \left[\left(|+\alpha_v\rangle\langle +\alpha_v|_v \otimes X_{v'}^\dagger |\pm_{\alpha_{v'}}\rangle\langle \pm_{\alpha_{v'}}| X_{v'}^\dagger \bigotimes_{\tilde{v} \in N_{v'}^G \setminus \{v\}} Z_{\tilde{v}}^\dagger |\pm_{\alpha_{\tilde{v}}}\rangle\langle \pm_{\alpha_{\tilde{v}}}|_{\tilde{v}} Z_{\tilde{v}} \bigotimes_{\hat{v} \in V \setminus (N_{v'}^G \cup \{v'\})} |\pm_{\alpha_{\hat{v}}}\rangle\langle \pm_{\alpha_{\hat{v}}}|_{\hat{v}} \right) \rho_G \right] \quad (98)$$

$$= \text{Tr} \left[\left(|+\alpha_v\rangle\langle +\alpha_v|_v \otimes X_{v'}^\dagger |\pm_{\alpha_{v'}}\rangle\langle \pm_{\alpha_{v'}}| X_{v'}^\dagger \bigotimes_{\tilde{v} \in N_{v'}^G \setminus \{v\}} Z_{\tilde{v}}^\dagger |\pm_{\alpha_{\tilde{v}}}\rangle\langle \pm_{\alpha_{\tilde{v}}}|_{\tilde{v}} Z_{\tilde{v}} \bigotimes_{\hat{v} \in V \setminus (N_{v'}^G \cup \{v'\})} |\pm_{\alpha_{\hat{v}}}\rangle\langle \pm_{\alpha_{\hat{v}}}|_{\hat{v}} \right) \rho_G \right] \quad (99)$$

$$= \text{Tr} \left[\left(|+\alpha_v\rangle\langle +\alpha_v|_v \otimes |\pm_{-\alpha_{v'}}\rangle\langle \pm_{-\alpha_{v'}}| \bigotimes_{\tilde{v} \in N_{v'}^G \setminus \{v\}} |\pm_{\alpha_{\tilde{v}}+\pi}\rangle\langle \pm_{\alpha_{\tilde{v}}+\pi}|_{\tilde{v}} \bigotimes_{\hat{v} \in V \setminus (N_{v'}^G \cup \{v'\})} |\pm_{\alpha_{\hat{v}}}\rangle\langle \pm_{\alpha_{\hat{v}}}|_{\hat{v}} \right) \rho_G \right] \quad (100)$$

where the last line uses the useful correspondence between applying X or Z and the update of measurement angles presented in Equation (10) (with the modulo 2π notation suppressed). Thus, a positive outcome at v is recovered at the cost of applying the remainder of the stabiliser $K_{v'}$ to either the graph state ρ_G (Equation (97)) or the measurement operators on $v' \cup N_{v'}^G \setminus \{v\}$ via a classical change of measurement parameter (Equation (100)). The former perspective is used in Section 5 and the latter is key to the BQC protocol in Section 4. Furthermore, we believe the above discussion can provide a more intuitive understanding of corrections work in MBQC and motivate the definition of gflow (Definition 2.4).

B Min-Entropy Section Supplementary

In Section 3.1, we considered combs of the form

$$D = \sum_x P(x) |x\rangle\langle x| \otimes \sigma_x \in \text{Comb}(A_1^{\text{in}} \rightarrow A_1^{\text{out}}, \dots, A_n^{\text{in}} \rightarrow A_n^{\text{out}}, \mathbb{C} \rightarrow X) \quad (101)$$

where all the $\sigma_x \in \text{Comb}(A_1^{\text{in}} \rightarrow A_1^{\text{out}}, \dots, A_n^{\text{in}} \rightarrow A_n^{\text{out}})$ are classical. The ultimate aim was to provide an interpretation of the guessing probability, $P_{\text{guess}}(X|A^{\text{in}}, A^{\text{out}})$, in terms of Bayesian updating since such an interpretation exists for the state min-entropy (see e.g., [Section 6.1.4, 62]). For completeness, we present this interpretation here and discuss the similarities and differences with the combs case.

Let D be a classical-quantum state on $\mathcal{H}_X \otimes \mathcal{H}_Y$ (i.e. $D \in \text{Comb}(\mathbb{C} \rightarrow Y, \mathbb{C} \rightarrow X)$) such that each $\sigma_x \in \mathcal{L}(\mathcal{H}_Y)$ is classical, that is, they can be written as

$$\sigma_x = \sum_y P(y|x) |y\rangle\langle y| \quad (102)$$

for $\{|y\rangle\}_y$ a common choice of orthonormal basis for \mathcal{H}_Y and for $P(y|x)$ a conditional probability distribution. We can thus write

$$D = \sum_{x,y} P(x) P(y|x) |xy\rangle\langle xy|. \quad (103)$$

Applying Bayes' rule, it follows that

$$D = \sum_{x,y} P(x|y) P(y) |xy\rangle\langle xy|. \quad (104)$$

By maximising over x for each y , we obtain the inequality:

$$D \leq \sum_{x,y} \left[\max_{\tilde{x}} P(\tilde{x}|y) P(y) \right] |xy\rangle\langle xy| \quad (105)$$

$$= I_X \otimes \sum_y \max_{\tilde{x}} P(\tilde{x}|y) P(y) |y\rangle\langle y|. \quad (106)$$

The second tensor factor above is an (in general) unnormalised state on Y , and moreover it can be shown that this unnormalised state is a minimal such state ρ_Y for which $D \leq I_X \otimes \rho_Y$ holds (this follows from the proof of the left-hand inequality of Proposition 3.2). Thus, using the unnormalised version of the min-entropy (recall Equation (13)), we arrive at

$$P_{\text{guess}}(X|Y)_D = \sum_y \max_{\tilde{x}} P(\tilde{x}|y) P(y) \quad (107)$$

and hence also at the desired interpretation of the guessing probability in terms of Bayesian updating: the guessing probability is the maximal Bayesian update for each interaction (denoted by y) averaged over all possible interactions. Clearly, for P_{guess} to take value 1, we must have perfect updates for *every* interaction (in the support of $P(y)$).

It is worthwhile emphasising here that, in the state case, the states σ_x can be considered as combs with trivial input spaces, ie. $\sigma_x \in \text{Comb}(\mathbb{C} \rightarrow Y)$, and consequentially, we are guaranteed that $\sum_y \max_x P(x|y) P(y) |y\rangle\langle y|$ is an unnormalised state. For the general case where the σ_x are classical combs with non-trivial input spaces, we have no analogous guarantee as we will now discuss.

In the main text, we used the conditional Bayes' rule and an independence condition to write the classical-classical comb D as

$$D = \sum_{x, \mathbf{a}^{\text{in}}, \mathbf{a}^{\text{out}}} P(x|\mathbf{a}^{\text{in}}, \mathbf{a}^{\text{out}}) P(\mathbf{a}^{\text{out}}|\mathbf{a}^{\text{in}}) |x, \mathbf{a}^{\text{in}}, \mathbf{a}^{\text{out}}\rangle\langle x, \mathbf{a}^{\text{in}}, \mathbf{a}^{\text{out}}| \quad (108)$$

Similarly to above, we can obtain the inequality:

$$D \leq I_X \otimes \sum_{\mathbf{a}^{\text{in}}, \mathbf{a}^{\text{out}}} \max_x P(x|\mathbf{a}^{\text{in}}, \mathbf{a}^{\text{out}}) P(\mathbf{a}^{\text{out}}|\mathbf{a}^{\text{in}}) |\mathbf{a}^{\text{in}}, \mathbf{a}^{\text{out}}\rangle\langle \mathbf{a}^{\text{in}}, \mathbf{a}^{\text{out}}| \quad (109)$$

However, unlike above, we are not guaranteed that the second tensor factor is an unnormalised classical comb: $\sum_{\mathbf{a}^{\text{in}}, \mathbf{a}^{\text{out}}} \max_x P(x|\mathbf{a}^{\text{in}}, \mathbf{a}^{\text{out}}) P(\mathbf{a}^{\text{out}}|\mathbf{a}^{\text{in}}) |\mathbf{a}^{\text{in}}, \mathbf{a}^{\text{out}}\rangle\langle \mathbf{a}^{\text{in}}, \mathbf{a}^{\text{out}}|$ may fail the required marginalisation conditions due to the dependence on the inputs \mathbf{a}^{in} that persists in the distribution $P(x|\mathbf{a}^{\text{in}}, \mathbf{a}^{\text{out}})$ in the maximum. The trace of this operator (appropriately normalised by the dimension of the input spaces) still provides a lower bound for the guessing probability, just as for the state case above, but the assurance that this bound can be reached is lacking.

To obtain an upper bound, we can construct an operator that removes the dependence on the inputs by also maximising over the \mathbf{a}^{in} , which then trivially satisfies the required marginalisation conditions. The proof of these bounds are given more formally in the following proof of Proposition 3.2. Note that, for notational simplicity, we have replaced \mathbf{a}^{in} by \mathbf{a} and \mathbf{a}^{out} by \mathbf{b} in the following. Also note that the proof makes use of lemmas that are stated and proved after the current proof.

Proof of Proposition 3.2. The lower bound is established by showing that any positive semi-definite operator Γ on $\bigotimes_{i=1}^n \mathcal{H}_{A_i} \otimes \mathcal{H}_{B_i}$ that satisfies $I_X \otimes \Gamma \geq D$ must have trace greater than or equal to $\sum_{\mathbf{a}, \mathbf{b}} \max_x P(x|\mathbf{a}, \mathbf{b}) P(\mathbf{b}|\mathbf{a})$.

Let Γ be any positive semi-definite operator on $\bigotimes_{i=1}^n \mathcal{H}_{A_i} \otimes \mathcal{H}_{B_i}$ such that $I_X \otimes \Gamma \geq D$. By Lemma B.1, it follows that $\text{diag}(I_X \otimes \Gamma) = I_X \otimes \text{diag}(\Gamma) \geq D$. We write

$$I_X \otimes \text{diag}(\Gamma) = \sum_{x, \mathbf{a}, \mathbf{b}} \alpha_{\mathbf{a}\mathbf{b}} |x\mathbf{a}\mathbf{b}\rangle\langle x\mathbf{a}\mathbf{b}|$$

where the $\alpha_{\mathbf{a}\mathbf{b}}$ are all real and non-negative by positive semi-definiteness of Γ . The condition $I_X \otimes \text{diag}(\Gamma) \geq D$ induces a further condition on the α terms: we must have for all \mathbf{a}, \mathbf{b} that, for all x ,

$$\alpha_{\mathbf{a}\mathbf{b}} \geq P(x|\mathbf{a}, \mathbf{b}) P(\mathbf{b}|\mathbf{a})$$

which in particular enforces that

$$\alpha_{\mathbf{a}\mathbf{b}} \geq \max_x P(x|\mathbf{a}, \mathbf{b}) P(\mathbf{b}|\mathbf{a})$$

and it thus follows that

$$\text{Tr}[\Gamma] \geq \sum_{\mathbf{a}, \mathbf{b}} \max_x P(x|\mathbf{a}, \mathbf{b}) P(\mathbf{b}|\mathbf{a}).$$

The upper bound is established by showing that

$$\Upsilon := \sum_{\mathbf{a}, \mathbf{b}} \max_{x, \tilde{\mathbf{a}}} P(x|\tilde{\mathbf{a}}, \mathbf{b}) P(\mathbf{b}|\tilde{\mathbf{a}}) |\mathbf{a}\mathbf{b}\rangle\langle\mathbf{a}\mathbf{b}| \quad (110)$$

is a valid unnormalised comb, since $I_X \otimes \Upsilon \geq D$ clearly holds. Defining f via $f(\mathbf{b}, \mathbf{a}) = \max_{x, \tilde{\mathbf{a}}} P(x|\tilde{\mathbf{a}}, \mathbf{b}) P(\mathbf{b}|\tilde{\mathbf{a}})$, non-negativity is immediate. Moreover, due to the maximum over $\tilde{\mathbf{a}}$, f has no dependence on \mathbf{a} : $f(\mathbf{b}, \mathbf{a}) = f(\mathbf{b}, \mathbf{a}')$ for all \mathbf{a}, \mathbf{a}' . By defining the functions $f^{(k)}$ via

$$f^{(k)}(b_1, \dots, b_k, a_1, \dots, a_k) := \sum_{b_{n+1}, \dots, b_{k+1}} f(\mathbf{b}, \mathbf{a}) \quad (111)$$

for all $k = 1, \dots, n$, the required conditions (non-negativity and the marginalisation conditions - recall Equation (3)) are trivially satisfied due to the non-negativity and independence from \mathbf{a} exhibited by f . The sum over b_1 of $f^{(1)}$ so defined is also clearly positive since $\max_{x, \mathbf{a}} P(x|\mathbf{a}, \mathbf{b}) P(\mathbf{b}|\mathbf{a})$ must be non-zero for some \mathbf{b} , and so Υ is indeed an unnormalised classical comb. \square

The following two lemmas establish that, for any classical comb D , we need only (un)normalised classical combs Γ in the minimum formulations of the min-entropy since if some non-classical comb achieves the minimum, then there exists a related classical comb that does also.

Lemma B.1. *Let A and B be operators on \mathcal{H} , where A is diagonal in a specific basis and B is an arbitrary positive semi-definite operator. If $B - A \geq 0$ then $\text{diag}(B) - A \geq 0$.*

Proof. Let $\mathcal{E} : \mathcal{L}(\mathcal{H}) \rightarrow \mathcal{L}(\mathcal{H})$ be a decohering channel in the basis for which A is diagonal. Since this is in particular a positive map and $B - A$ is positive semi-definite by assumption, it follows that $\mathcal{E}(B - A)$ is also positive semi-definite. Linearity of \mathcal{E} ensures that $\mathcal{E}(B - A) = \mathcal{E}(B) - \mathcal{E}(A) = \text{diag}(B) - A$ giving the result. \square

Lemma B.2. *If Γ is a normalised (resp. unnormalised) quantum comb, then $\text{diag}(\Gamma)$ is a normalised (resp. unnormalised) classical comb.*

Proof. The proof is essentially immediate by definition but the details are spelt out nonetheless. Let Γ be a normalised (resp. unnormalised) quantum comb in $\text{Comb}(A_1 \rightarrow B_1, \dots, A_n \rightarrow B_n)$ and let $C^{(k)}$, $k = 0, \dots, n$ be positive semi-definite operators that satisfy $C^{(n)} = \Gamma$,

$$\text{Tr}_{B_k} \left[C^{(k)} \right] = I_{A_k} \otimes C^{(k-1)} \quad (112)$$

for $k = 1, \dots, n$ and $C^{(0)} = 1$ (resp. $C^{(0)} > 0$). Denoting the $\mathbf{a}\mathbf{b}^{\text{th}}$ diagonal element of Γ by $\alpha_{\mathbf{a}\mathbf{b}}$, we define f via $f(\mathbf{b}, \mathbf{a}) = \alpha_{\mathbf{a}\mathbf{b}}$. Thus, we can write

$$\text{diag}(\Gamma) = \sum_{\mathbf{a}, \mathbf{b}} f(\mathbf{b}, \mathbf{a}) |\mathbf{a}\mathbf{b}\rangle\langle\mathbf{a}\mathbf{b}|. \quad (113)$$

Since Γ is positive semi-definite every $\alpha_{\mathbf{a}\mathbf{b}}$, and hence every $f(\mathbf{b}, \mathbf{a})$, is non-negative. By denoting the diagonal elements of $C^{(k)}$ similarly as $\alpha_{\mathbf{a}_{1:k} \mathbf{b}_{1:k}}$, where $\mathbf{a}_{1:k} := a_1 a_2 \dots a_k$ and similarly for $\mathbf{b}_{1:k}$, we define $f^{(k)}(\mathbf{b}_{1:k}, \mathbf{a}_{1:k}) := \alpha_{\mathbf{a}_{1:k} \mathbf{b}_{1:k}}$ for all $k = 1, \dots, n$ and take $f^{(0)} := C^{(0)}$. Since taking the partial trace and applying $\text{diag}(\cdot)$ commute, that is,

$$\text{diag} \left(\text{Tr}_{B_k} \left[C^{(k)} \right] \right) = \text{Tr}_{B_k} \left[\text{diag}(C^{(k)}) \right] \quad (114)$$

it follows that

$$\text{Tr}_{B_k} \left[\text{diag}(C^{(k)}) \right] = \text{diag}(I_{A_k} \otimes C^{(k-1)}) = I_{A_k} \otimes \text{diag}(C^{(k-1)}). \quad (115)$$

The left-hand side can be written as

$$\sum_{\mathbf{a}_{1:k}, \mathbf{b}_{1:k-1}} \left(\sum_{b_k} \alpha_{\mathbf{a}_{1:k} \mathbf{b}_{1:k}} \right) |\mathbf{a}_{1:k} \mathbf{b}_{1:k-1} \rangle \langle \mathbf{a}_{1:k} \mathbf{b}_{1:k-1}| = \sum_{\mathbf{a}_{1:k}, \mathbf{b}_{1:k-1}} \left(\sum_{b_k} f^{(k)}(\mathbf{b}_{1:k}, \mathbf{a}_{1:k}) \right) |\mathbf{a}_{1:k} \mathbf{b}_{1:k-1} \rangle \langle \mathbf{a}_{1:k} \mathbf{b}_{1:k-1}| \quad (116)$$

and the right-hand side as

$$\sum_{\mathbf{a}_{1:k}, \mathbf{b}_{1:k-1}} \alpha_{\mathbf{a}_{1:k-1} \mathbf{b}_{1:k-1}} |\mathbf{a}_{1:k} \mathbf{b}_{1:k-1} \rangle \langle \mathbf{a}_{1:k} \mathbf{b}_{1:k-1}| = \sum_{\mathbf{a}_{1:k}, \mathbf{b}_{1:k-1}} f^{(k-1)}(\mathbf{b}_{1:k-1}, \mathbf{a}_{1:k-1}) |\mathbf{a}_{1:k} \mathbf{b}_{1:k-1} \rangle \langle \mathbf{a}_{1:k} \mathbf{b}_{1:k-1}| \quad (117)$$

which establishes the required marginalisation condition on the $f^{(k)}$: $\sum_{b_k} f^{(k)}(\mathbf{b}_{1:k}, \mathbf{a}_{1:k}) = f^{(k-1)}(\mathbf{b}_{1:k-1}, \mathbf{a}_{1:k-1})$ for $k = 2, \dots, n$ as well as the edge case of $\sum_{b_1} f^{(1)}(b_1, a_1) = f^{(0)}$. \square

The following is the proof of Lemma 3.1 which states that the min-entropy for multi-round combs, i.e. of the form $D^{(m)}$, is non-increasing as the number of rounds m increases.

Proof of Lemma 3.1. Let $\lambda \in \mathbb{R}$ and $\Gamma \in \text{Comb}((A_1^{\text{in}})^{(1)} \rightarrow (A_1^{\text{out}})^{(1)}, \dots, (A_n^{\text{in}})^{(m)} \rightarrow (A_n^{\text{out}})^{(m)})$ be such that $I_X \otimes \lambda \Gamma \geq D^{(m)}$ and that $-\log(\lambda)$ gives the min-entropy for $D^{(m)}$. Let $\Gamma' \in \text{Comb}((A_1^{\text{in}})^{(1)} \rightarrow (A_1^{\text{out}})^{(1)}, \dots, (A_n^{\text{in}})^{(l)} \rightarrow (A_n^{\text{out}})^{(l)})$ be given by

$$\Gamma' := \frac{1}{\prod_{t=l+1}^m \dim(\mathbf{A}^{\text{in}})^{(t)}} \text{Tr}_{\mathbf{A}^{(l+1)} \dots \mathbf{A}^{(m)}} [\Gamma] \quad (118)$$

where $\dim(\mathbf{A}^{\text{in}})^{(t)} := \prod_{k=1}^n \dim(A_k^{\text{in}})^{(t)}$ and the subscripts $\mathbf{A}^{(j)}$ in the trace indicate that the trace is over all subspace related to $\sigma_x^{(j)}$, i.e. $(\mathcal{H}_{A_1^{\text{in}}})^{(j)}, (\mathcal{H}_{A_1^{\text{out}}})^{(j)}, \dots, (\mathcal{H}_{A_n^{\text{in}}})^{(j)}, (\mathcal{H}_{A_n^{\text{out}}})^{(j)}$.

It remains only to show that $I_X \otimes \lambda \Gamma' \geq D^{(l)}$. It suffices to show that

$$\frac{1}{\prod_{t=l+1}^m \dim(\mathbf{A}^{\text{in}})^{(t)}} \text{Tr}_{\mathbf{A}^{(l+1)} \dots \mathbf{A}^{(m)}} [D^{(m)}] = D^{(l)}. \quad (119)$$

Starting from the left-hand side:

$$\frac{1}{\prod_{t=l+1}^m \dim(\mathbf{A}^{\text{in}})^{(t)}} \text{Tr}_{\mathbf{A}^{(l+1)} \dots \mathbf{A}^{(m)}} [D^{(m)}] = \frac{1}{\prod_{t=l+1}^m \dim(\mathbf{A}^{\text{in}})^{(t)}} \sum_x P(x) |x\rangle \langle x| \otimes \text{Tr}_{\mathbf{A}^{(l+1)} \dots \mathbf{A}^{(m)}} \left[\bigotimes_{j=1}^m \sigma_x^{(j)} \right] \quad (120)$$

$$= \frac{1}{\prod_{t=l+1}^m \dim(\mathbf{A}^{\text{in}})^{(t)}} \sum_x P(x) |x\rangle \langle x| \otimes \left(\prod_{k=l+1}^m \dim(\mathbf{A}^{\text{in}})^{(k)} \right) \bigotimes_{j=1}^l \sigma_x^{(j)} \quad (121)$$

$$= D^{(l)} \quad (122)$$

where we have used the fact that each $\sigma_x^{(j)}$ is a comb, so $\text{Tr}[\sigma_x^{(j)}]$ is equal to the product of input space dimensions by definition. So, it holds that $I_X \otimes \lambda \Gamma' \geq D^{(l)}$, which entails that

$$H_{\min}(X | \mathbf{A}^{(1)}, \dots, \mathbf{A}^{(l)})_{D^{(l)}} \geq -\log(\lambda) = H_{\min}(X | \mathbf{A}^{(1)}, \dots, \mathbf{A}^{(m)}) \quad (123)$$

thus proving that the min-entropy is non-increasing with increasing round number. \square

C Blind Quantum Computing Protocol Supplementary

This appendix contains supporting results for the blindness theorems of Section 4 and for the accompanying examples.

C.1 Single Round Theorem Supporting Results

The proof of Theorem 4.2 makes use of the following lemma which demonstrates that for α', α, c' and g fixed, there is at most one r such that Equation (35) is satisfied for each i .

Lemma C.1. *If there exists an r such that $P(\alpha'|c', \alpha, r, g) = 1$ for all other variables fixed, then it is unique, otherwise $P(\alpha'|c', \alpha, r, g) = 0$.*

Proof. Since $P(\alpha'|c', \alpha, r, g)$ is a deterministic distribution, it takes values either 0 or 1. Let r be such that $P(\alpha'|c', \alpha, r, g) = 1$. Recalling Equation (35) and the fact that a total order is imposed on communication, we have that for each i

$$\alpha'_i := (-1)^{\bigoplus_{j \in \mathcal{X}_i} c'_j \oplus r_j} \alpha_i + \left(r_i \oplus \bigoplus_{j \in \mathcal{Z}_i} c'_j \oplus r_j \right) \pi \bmod 2\pi \quad (124)$$

where \mathcal{X}_i and \mathcal{Z}_i are necessarily subsets of $\{1, \dots, i-1\}$. In particular, this means that

$$\alpha'_1 = \alpha_1 + r_1 \pi \bmod 2\pi \quad (125)$$

and hence there is a unique value for r_1 given α and α' are fixed. The result then follows by induction: since c' and g are fixed, for fixed values $r_{1:i-1}$ the quantities $\bigoplus_{j \in \mathcal{X}_i} c'_j \oplus r_j$ and $\bigoplus_{j \in \mathcal{Z}_i} c'_j \oplus r_j$ are determined for each i , and thus there is a unique r_i for which Equation (124) holds. \square

We can now give the proof of the theorem.

Proof of Theorem 4.2. From Proposition 3.2, we know that

$$H_{\min}(\mathbf{A}, \mathbf{O} | \mathbf{A}', \mathbf{C}')_{D_{\text{client}}} \geq -\log \left[\sum_{\alpha'} \max_{\alpha, O, c'} P(\alpha, O | \alpha', c') P(\alpha' | c') \right]. \quad (126)$$

Instead of dealing directly with $P(\alpha, O | \alpha', c') P(\alpha' | c')$, it is easier to revert back to the form before the Bayes' rule was applied. That is, we aim to find

$$\sum_{\alpha'} \max_{\alpha, O, c'} P(\alpha, O) P(\alpha' | c', \alpha, O). \quad (127)$$

Using the uniformity assumptions for choosing the computation, gflow and one-time pads, as well as the definition of $P(\alpha' | c', \alpha, O)$ in the previous subsection, we have

$$P(\alpha, O) P(\alpha' | c', \alpha, O) = \frac{1}{|\mathcal{A}|^n |\mathcal{O}|} \sum_{g \sim O, r} \frac{P(\alpha' | c', \alpha, r, g)}{|g \sim O| 2^n} \quad (128)$$

where $g \sim O$ indicates that the gflow is defined for the output set O and $|g \sim O|$ denotes the number of all such gflows. Recalling that $P(\alpha' | c', \alpha, r, g)$ is a deterministic distribution, it can be shown (Lemma C.1) that for fixed g , α and c' there is at most one r for which $P(\alpha' | c', \alpha, r, g) = 1$. Thus,

$$\max_{\alpha, O, c'} \sum_{g \sim O, r} \frac{P(\alpha' | c', \alpha, r, g)}{|g \sim O| 2^n} \quad (129)$$

can be interpreted as selecting the α , O and c' for which α' is reportable from α for the greatest number of pairs (g, r) for gflows $g \sim O$. This quantity is clearly upper-bounded by a situation where α' is reportable under all gflows, hence

$$\max_{\alpha, O, c'} \sum_{g \sim O, r} \frac{P(\alpha' | c', \alpha, r, g)}{|g \sim O| 2^n} \leq \frac{1}{2^n} \quad (130)$$

which holds for all α' . Thus, returning to Equation (127):

$$\sum_{\alpha'} \max_{\alpha, O, c'} P(\alpha, O) P(\alpha' | c', \alpha, O) \leq \sum_{\alpha'} \frac{1}{|\mathcal{A}|^n |\mathcal{O}| 2^n} \quad (131)$$

$$= \frac{1}{|\mathcal{O}| 2^n} \quad (132)$$

which proves the theorem. \square

It is worthwhile making some further comments regarding the interpretation of Equation (129) and the related inequality Equation (130) in the proof above. Firstly, it is possible to find a simple example, namely that given in the main text (see also below), for which Equation (130) is equality for every α' . That is, for every α' , there exists an α , O and c' that α' is reportable from α for every gflow $g \sim O$. Said another way, the pre-images of α' under the gflows $g \sim O$ (for some fixed c' and as r varies) have non-empty mutual intersection. Since the pre-image of each gflow has a fixed size (this follows from Lemma C.1), a larger mutual intersection corresponds to a smaller total set of angles α from which α' can be reported. Since α is one part of the secret information, it is intuitive that a smaller set of possible α given the evidence α', c' corresponds to a lower min-entropy. This also suggests that, to improve security, considering a graph where the corresponding gflows have smaller mutual intersection is beneficial.

Obtaining equality in Equation (130) for all α', c' accordingly means that equality is also achieved in Equation (47), however, it is unlikely that this bound is obtained in general. The above discussion highlights how much is dependent on the specific properties of gflows for the graph chosen for the protocol. Since (to the best knowledge of the authors') there is no characterisation of gflows in terms of graph-theoretic properties, and since the given example achieves the lower bound, it is unlikely that a better lower bound than that given in the theorem can be given in general.

C.2 BQC Minimum Example

This appendix provides further details regarding the minimal example given in the main text (recall Figure 4) which obtains the lower bound in Theorem 4.2. We begin by demonstrating that $O = \{2, 3\}$ is indeed the only choice of output set for which gflows compatible with the total order exist.

Lemma C.2. *For G as in Figure 4 with partial order $1 < 2 < 3$ and the XY-plane the only allowed measurement plane, $O = \{2, 3\}$ is the only non-trivial output set for which there exist $I \subset \{1, 2, 3\}$ such that a gflow compatible with the total order exists. Moreover, there are just two possible gflows, g_1 and g_2 , defined by*

$$g_1 : 1 \mapsto \{2\}, \quad (133)$$

$$g_2 : 1 \mapsto \{3\}, \quad (134)$$

where g_1 is compatible with (I, O) for I equal to $\{1\}$, $\{3\}$ or $\{1, 3\}$ and g_2 is compatible with (I, O) for $I = \{1\}$, $\{2\}$ and $\{1, 2\}$, for O as above.

Proof. We begin by demonstrating $O = \{2, 3\}$ is the only valid non-trivial output set (note that we do not consider the trivial output set $O = \{1, 2, 3\}$ since this does not allow for any computation). Due to the total order and measurement plane restriction, 3 must be in the output set, since if this was not the case, then $3 \in O^c$ meaning that any gflow would map 3 to $\{1\}$, $\{2\}$ or $\{1, 2\}$. In any of these cases, we would require that $3 < 1$ or $3 < 2$ which contradicts the compatibility with total order. Thus $\{1\}$, $\{2\}$ and $\{1, 2\}$ cannot be output sets.

Suppose either $\{3\}$ or $\{1, 3\}$ was a valid output set. Any gflow compatible with either output must then map 2 to some subset of $\{1, 2, 3\}$, however no such set exists for which some contradiction does not arise, as follows. If 2 maps to $\{1\}$, $2 < 1$ which is a contradiction to the total order. If 2 maps to $\{2\}$, $\{1, 2\}$ or $\{2, 3\}$, the gflow requirement $2 \notin g(2)$ is contradicted. If 2 maps to $\{3\}$, $1 \in \text{Odd}(g(2))$ implying $2 < 1$, contradicting the total order. If 2 maps to $\{1, 3\}$, then $2 \notin \text{Odd}(g(2))$ which contradicts a gflow requirement.

This leaves $\{2, 3\}$ as the only remaining possible output set. We now show it does indeed support gflow and characterise them. For output set $O = \{2, 3\}$, the domain of any gflow map is $O^c = \{1\}$, so we can begin to characterise valid gflows by where they map 1. Due to the XY-plane restriction, we can't have $1 \in g(1)$, so a valid gflow cannot map 1 to $\{1\}$, $\{1, 2\}$ or $\{1, 3\}$. Since $\text{Odd}(\{2, 3\}) = \{2, 3\}$ and since we require $1 \in \text{Odd}(g(1))$, no valid gflow maps 1 to $\{2, 3\}$. This leaves just the options $1 \mapsto \{2\}$ and $1 \mapsto \{3\}$. Both of these are valid gflows since in both cases, $1 \notin g(1)$ is satisfied and the corresponding implications for the partial order, $1 < 2$ and $1 < 3$ respectively, are compatible with

the total order. Similarly, for both maps $1 \in \text{Odd}(g(1))$ is satisfied ($\text{Odd}(\{2\}) = \{1, 3\}$ and $\text{Odd}(\{3\}) = \{1, 2\}$) and the again the implications for the partial order are compatible with the total order.

Denote by g_1 the gflow that maps 1 to $\{2\}$ and by g_2 the gflow that maps 1 to $\{3\}$. Since a gflow is a map from O^c to $\mathcal{P}(I^c)$, g_1 is compatible with all sets I for which $\{2\} \in \mathcal{P}(I^c)$, i.e. $I = \{1\}, \{3\}$ and $\{1, 3\}$, and similarly, g_2 is compatible with $I = \{1\}, \{2\}$ and $\{1, 2\}$. \square

Returning to the discussion of the BQC protocol for the example, it is useful to explicitly write out the correction sets given by g_1 and g_2 (only those that are non-empty are shown):

$$\begin{aligned}\mathcal{X}_2^{g_1} &= \mathcal{Z}_3^{g_1} = \{1\}; \\ \mathcal{Z}_2^{g_2} &= \mathcal{X}_3^{g_2} = \{1\}.\end{aligned}$$

Let \mathcal{A} be any agreed upon set of angles that satisfies Equation (34). For a single round of the protocol, if g_1 is chosen by the client, then the reported angles are given by

$$\alpha'_1 = \alpha_1 + r_1\pi \bmod 2\pi, \quad (135)$$

$$\alpha'_2 = (-1)^{r_1 \oplus c'_1} \alpha_2 + r_2\pi \bmod 2\pi, \quad (136)$$

$$\alpha'_3 = \alpha_3 + (r_3 \oplus r_1 \oplus c'_1)\pi \bmod 2\pi, \quad (137)$$

where $\alpha_1, \alpha_2, \alpha_3 \in \mathcal{A}$ are the chosen (and secret) angles for the computation, c'_1 is the classical message reported by the server after the first measurement and $\mathbf{r} = r_3 r_2 r_1 \in \{0, 1\}^3$ is the one-time pad. If g_2 is used instead, the angles are reported as

$$\alpha'_1 = \alpha_1 + r_1\pi \bmod 2\pi, \quad (138)$$

$$\alpha'_2 = \alpha_2 + (r_2 \oplus r_1 \oplus c'_1)\pi \bmod 2\pi, \quad (139)$$

$$\alpha'_3 = (-1)^{r_1 \oplus c'_1} \alpha_3 + r_3\pi \bmod 2\pi. \quad (140)$$

Note that the only classical message relevant to this example is c'_1 . Let $\boldsymbol{\alpha}'$ and \mathbf{c}' be reported in a single round of the protocol. We can write the pre-image of $\boldsymbol{\alpha}'$ under g_1 given \mathbf{c}' by inverting Equations (135) to (137) (we drop the $\bmod 2\pi$ notation and leave it implicit):

$$\alpha_1 = \alpha'_1 + r_1\pi; \quad (141)$$

$$\alpha_2 = (-1)^{r_1 \oplus c'_1} \alpha'_2 + r_2\pi; \quad (142)$$

$$\alpha_3 = \alpha'_3 + (r_3 \oplus r_1 \oplus c'_1)\pi. \quad (143)$$

Restricting our focus to a subset of the pre-image defined by $r_1 = c'_1$, that is, the angles

$$\alpha_1 = \alpha'_1 + c'_1\pi, \quad (144)$$

$$\alpha_2 = \alpha'_2 + r_2\pi, \quad (145)$$

$$\alpha_3 = \alpha'_3 + r_3\pi, \quad (146)$$

one observes that $\boldsymbol{\alpha}'$ can be reported from any one of these angles under g_2 given \mathbf{c}' , namely by the one-time pads $\hat{\mathbf{r}} = \hat{r}_3 \hat{r}_2 \hat{r}_1 = r_3 r_2 c'_1$ (as can be shown via simple substitution into Equations (138) to (140)). Since this holds for any $\boldsymbol{\alpha}'$ and \mathbf{c}' , we have thus shown both that the bound Equation (130) in the proof of Theorem 4.2 above is in fact equality for every $\boldsymbol{\alpha}'$ and moreover that the maximum is obtained for every \mathbf{c}' . Recalling the discussion after Proposition 3.2, this means that we have found the guessing probability (equivalently min-entropy) exactly for this example and that any strategy used by the server is equally informative. These results are corroborated numerically (see Appendix E for details of the implementation using an SDP solver): the min-entropy is given as $-\log_2(0.125) = 3$, which is consistent with $|\mathcal{O}| = 1$ and $n = 3$ for this example (this result was obtained for different choices of \mathcal{A} : for $|\mathcal{A}| = 4$ and for $|\mathcal{A}| = 8$).

We now consider two rounds of the protocol in order to calculate the guessing probability for $D_{\text{client}}^{(2)}$, which, for this example, can be written as

$$D_{\text{client}}^{(2)} = \sum_{\boldsymbol{\alpha}, O} \frac{1}{|\mathcal{A}|^n |\mathcal{O}|} |\boldsymbol{\alpha}, O\rangle \langle \boldsymbol{\alpha}, O| \otimes \sigma_{\boldsymbol{\alpha}, O}^{(1)} \otimes \sigma_{\boldsymbol{\alpha}, O}^{(2)} \quad (147)$$

$$= \sum_{\alpha} \frac{1}{|\mathcal{A}|^3} |\alpha\rangle\langle\alpha| \otimes \sum_{\substack{\alpha'^{(1)}, \alpha'^{(2)}, g^{(1)}, g^{(2)}, \\ c'^{(1)}, c'^{(2)}, r^{(1)}, r^{(2)}}} \frac{1}{2^8} P(\alpha'^{(1)}|c'^{(1)}, \alpha, r^{(1)}, g^{(1)}) P(\alpha'^{(2)}|c'^{(2)}, \alpha, r^{(2)}, g^{(2)}) \left| \alpha'^{(1)} c'^{(1)} \alpha'^{(2)} c'^{(2)} \right\rangle \langle \dots | \quad (148)$$

where $g^{(j)}$ take values in $\{g_1, g_2\}$ where g_1 and g_2 are as above, and where we have used $P(g^{(j)}) = \frac{1}{2}$ and $P(\mathbf{r}^{(j)}) = \frac{1}{2^3}$. For a choice of angle set $\mathcal{A} = \{\frac{\pi}{5}, \frac{\pi}{3}, \frac{-\pi}{3} + \pi, \frac{-\pi}{5} + \pi, \frac{\pi}{5} + \pi, \frac{\pi}{3} + \pi, \frac{-\pi}{3}, \frac{-\pi}{5}\}$, the guessing probability for $D_{\text{client}}^{(2)}$ takes value between 0.140625 and 0.28125 as computed via numeric methods (see [72]) and as explained in the following. Note that various other choices of angle set give the same or similar results.

These bounds are derived directly from Proposition 3.2 for the specific comb under consideration. The lower bound (which includes the normalisation over the input spaces) can be written as

$$\sum_{\substack{\alpha'^{(1)}, \alpha'^{(2)}, \\ c'^{(1)}, c'^{(2)}}} \frac{1}{|\mathcal{A}|^3 2^6} \max_{\alpha} \sum_{\substack{g^{(1)}, g^{(2)}, \\ r^{(1)}, r^{(2)}}} \frac{1}{2^8} P(\alpha'^{(1)}|c'^{(1)}, \alpha, r^{(1)}, g^{(1)}) P(\alpha'^{(2)}|c'^{(2)}, \alpha, r^{(2)}, g^{(2)}). \quad (149)$$

Due to the redundancy of $(c'_2)^{(j)}$ and $(c'_3)^{(j)}$ (they don't appear in Equations (135) to (140)), this reduces to

$$\sum_{\substack{\alpha'^{(1)}, \alpha'^{(2)}, \\ (c'_1)^{(1)}, (c'_1)^{(2)}}} \frac{1}{|\mathcal{A}|^3 2^2} \max_{\alpha} \sum_{\substack{g^{(1)}, g^{(2)}, \\ r^{(1)}, r^{(2)}}} \frac{1}{2^8} P(\alpha'^{(1)}|(c'_1)^{(1)}, \alpha, r^{(1)}, g^{(1)}) P(\alpha'^{(2)}|(c'_1)^{(2)}, \alpha, r^{(2)}, g^{(2)}). \quad (150)$$

The upper bound is given by

$$\sum_{\alpha'^{(1)}, \alpha'^{(2)}} \frac{1}{|\mathcal{A}|^3} \max_{\alpha, (c'_1)^{(1)}, (c'_1)^{(2)}} \sum_{\substack{g^{(1)}, g^{(2)}, \\ r^{(1)}, r^{(2)}}} \frac{1}{2^8} P(\alpha'^{(1)}|(c'_1)^{(1)}, \alpha, r^{(1)}, g^{(1)}) P(\alpha'^{(2)}|(c'_1)^{(2)}, \alpha, r^{(2)}, g^{(2)}). \quad (151)$$

Computing these quantities for \mathcal{A} above via the code in the repository [72] gives the results as listed above.

C.3 Multi-round Blindness Supplementary

For this section, it is useful to have the following notation. Let a graph G on vertices V be given and $O \subset V$ a choice of output set. For a given $\alpha \in \mathcal{A}^n$, define the set $\mathcal{A}_{\alpha, O} := \{\alpha + (0, \dots, 0, b_{o_1}, \dots, b_{o_{|O|}}) \pi \bmod 2\pi : b_{o_i} \in \{0, 1\}\}$ where the zero entries of $(0, \dots, 0, b_{o_1}, \dots, b_{o_{|O|}})$ correspond to $V \setminus O$ and the labels o_i correspond to the elements of O . We define an equivalence relation \sim_O by $\alpha \sim_O \tilde{\alpha}$ for $\tilde{\alpha} \in \mathcal{A}_{\alpha, O}$. The set obtained by quotienting \mathcal{A}^n by the equivalence relation, i.e. \mathcal{A}^n / \sim_O has $\frac{|\mathcal{A}|^n}{2^{|O|}}$ elements.

Lemma C.3. Consider $\sum_{g \sim O, \mathbf{r}} P(g|O) p(\mathbf{r}) \sigma_{\text{BQC}}^{\alpha, \mathbf{r}, g}$ as in Equation (38) with $P(g|O)$ and $P(\mathbf{r})$ both uniform. Then, for all $\tilde{\alpha} \sim_O \alpha$:

$$\sum_{g \sim O, \mathbf{r}} P(g|O) P(\mathbf{r}) \sigma_{\text{BQC}}^{\alpha, \mathbf{r}, g} = \sum_{g \sim O, \mathbf{r}} P(g|O) P(\mathbf{r}) \tilde{\sigma}_{\text{BQC}}^{\tilde{\alpha}, \mathbf{r}, g} \quad (152)$$

Proof. We begin by noting that, by definition of gflow, for any $g \sim O$, no element of O is in the domain of g . This means that, for all $i \in O$, $i \notin \mathcal{X}_k$ and $i \notin \mathcal{Z}_k$ for all $k \in V$. The consequence of this being that for any r_i for $i \in O$, the only equation for α'_i (recall Equation (35)) that contains r_i is when $k = i$. This results in the following symmetry:

$$\alpha'_i = (-1)^{\bigoplus_{j \in \mathcal{X}_i} c'_j \oplus r_j} \alpha_i + (r_i \oplus \bigoplus_{j \in \mathcal{Z}_i} c'_j \oplus r_j) \pi \bmod 2\pi = (-1)^{\bigoplus_{j \in \mathcal{X}_i} c'_j \oplus r_j} (\alpha_i + \pi) + ((r_i \oplus 1) \oplus \bigoplus_{j \in \mathcal{Z}_i} c'_j \oplus r_j) \pi \bmod 2\pi \quad (153)$$

Thus, for fixed gflow g and classical messages \mathbf{c}' , if α' is reportable from α for one-time pads \mathbf{r} , i.e. $P(\alpha'|c', \alpha, \mathbf{r}, g) = 1$, then α' is reportable from $\alpha + (0, \dots, 0, b_{o_1}, \dots, b_{o_{|O|}}) \pi$ for one-time pads $\mathbf{r} + (0, \dots, 0, b_{o_1}, \dots, b_{o_{|O|}}) \pi$, i.e. $P(\alpha'|c', \alpha +$

$(0, \dots, 0, b_{o_1}, \dots, b_{o_{|O|}}) \pi, \mathbf{r} + (0, \dots, 0, b_{o_1}, \dots, b_{o_{|O|}}) \pi, g) = 1$. In light of Lemma C.1, and with the assumption that $P(\mathbf{r})$ is uniform, this in particular means that

$$\sum_{\mathbf{r}} P(\boldsymbol{\alpha}' | \mathbf{c}', \boldsymbol{\alpha}, \mathbf{r}, g) P(\mathbf{r}) = \sum_{\mathbf{r}} P(\boldsymbol{\alpha}' | \mathbf{c}' \cdot \boldsymbol{\alpha} + (0, \dots, 0, b_{o_1}, \dots, b_{o_{|O|}}) \pi, \mathbf{r}, g) P(\mathbf{r}) \quad (154)$$

and so

$$\sum_{g \sim O, \mathbf{r}} P(g|O) P(\mathbf{r}) \sigma_{\text{BQC}}^{\boldsymbol{\alpha}, \mathbf{r}, g} = \sum_{\substack{g \sim O, \mathbf{r}, \\ \boldsymbol{\alpha}', \mathbf{c}'}} P(g|O) P(\mathbf{r}) P(\boldsymbol{\alpha}' | \mathbf{c}', \boldsymbol{\alpha}, \mathbf{r}, g) |\boldsymbol{\alpha}' \mathbf{c}' \rangle \langle \boldsymbol{\alpha}' \mathbf{c}'| \quad (155)$$

$$= \sum_{\substack{g \sim O, \mathbf{r}, \\ \boldsymbol{\alpha}', \mathbf{c}'}} P(g|O) P(\mathbf{r}) P(\boldsymbol{\alpha}' | \mathbf{c}', \boldsymbol{\alpha} + (0, \dots, 0, b_{o_1}, \dots, b_{o_{|O|}}) \pi, \mathbf{r}, g) |\boldsymbol{\alpha}' \mathbf{c}' \rangle \langle \boldsymbol{\alpha}' \mathbf{c}'| \quad (156)$$

$$= \sum_{g \sim O, \mathbf{r}} P(g|O) P(\mathbf{r}) \sigma_{\text{BQC}}^{\boldsymbol{\alpha} + (0, \dots, 0, b_{o_1}, \dots, b_{o_{|O|}}) \pi, \mathbf{r}, g} \quad (157)$$

□

In the notation of Equation (43), the above lemma states that $\sigma_{\boldsymbol{\alpha}, O} = \sigma_{\tilde{\boldsymbol{\alpha}}, O}$ for all $\tilde{\boldsymbol{\alpha}} \sim_O \boldsymbol{\alpha}$ which is the notation used in the following proof.

Proof of Theorem 4.3. For this proof, we work with the maximisation formulation for the guessing probability, and moreover in the form given by maximising over pairs of dual combs and CPTP maps (\hat{E}, \mathcal{F}) as given in Equation (15). That is, we consider

$$\max_{\hat{E}, \mathcal{F}} \text{Tr}_{\mathbf{A}, \mathbf{O}, \mathbf{A}', \mathbf{O}'} \left[(I_{\mathbf{A}, \mathbf{O}} \otimes \mathcal{F}) \left(D_{\text{client}}^{(m)} \hat{E}^T \right) \left(\sum_{\boldsymbol{\alpha}, O} |\boldsymbol{\alpha}, O, \boldsymbol{\alpha}, O \rangle \langle \boldsymbol{\alpha}, O, \boldsymbol{\alpha}, O|_{\mathbf{A}, \mathbf{O}, \mathbf{A}', \mathbf{O}'} \right) \right] \quad (158)$$

where $\hat{E} \in \text{Comb}(\mathbb{C} \rightarrow \mathbb{C}, (A'_1)^{(1)} \rightarrow (C'_1)^{(1)}, \dots, (A'_n)^{(m)} \rightarrow (C'_n)^{(m)}, \mathbb{C} \rightarrow B)$ is a normalised dual comb and $\mathcal{F} : \mathcal{H}_B \rightarrow \mathcal{H}_{\mathbf{A}'} \otimes \mathcal{H}_{\mathbf{O}'} \cong \mathcal{H}_{\mathbf{A}} \otimes \mathcal{H}_{\mathbf{O}}$ is a CPTP map. The transpose T is over all spaces $\mathbf{A}'_1, \mathbf{C}'_1, \dots, \mathbf{A}'_n, \mathbf{C}'_n$.

Let (\hat{E}, \mathcal{F}) be any such pair. Writing $D_{\text{client}}^{(m)}$ as $\sum_{\boldsymbol{\alpha}, O} P(\boldsymbol{\alpha}, O) |\boldsymbol{\alpha}, O \rangle \langle \boldsymbol{\alpha}, O| \otimes_{j=1}^m \sigma_{\boldsymbol{\alpha}, O}^{(j)}$, we get

$$\begin{aligned} & \text{Tr}_{\mathbf{A}, \mathbf{O}, \mathbf{A}', \mathbf{O}'} \left[(I_{\mathbf{A}, \mathbf{O}} \otimes \mathcal{F}) \left(D_{\text{client}}^{(m)} \hat{E}^T \right) \left(\sum_{\boldsymbol{\alpha}, O} |\boldsymbol{\alpha}, O, \boldsymbol{\alpha}, O \rangle \langle \boldsymbol{\alpha}, O, \boldsymbol{\alpha}, O|_{\mathbf{A}, \mathbf{O}, \mathbf{A}', \mathbf{O}'} \right) \right] \\ &= \sum_{\boldsymbol{\alpha}, O} \langle \boldsymbol{\alpha}, O |_{\mathbf{A}, \mathbf{O}} \langle \boldsymbol{\alpha}, O |_{\mathbf{A}', \mathbf{O}'} \left[\sum_{\boldsymbol{\alpha}, O} P(\boldsymbol{\alpha}, O) |\boldsymbol{\alpha}, O \rangle \langle \boldsymbol{\alpha}, O| \otimes \mathcal{F} \left(\left(\bigotimes_{j=1}^m \sigma_{\boldsymbol{\alpha}, O}^{(j)} \right) \hat{E}^T \right) \right] |\boldsymbol{\alpha}, O \rangle_{\mathbf{A}, \mathbf{O}} |\boldsymbol{\alpha}, O \rangle_{\mathbf{A}', \mathbf{O}'} \end{aligned} \quad (159)$$

By the fact that \hat{E} is a (normalised) dual comb, $\left(\bigotimes_{j=1}^m \sigma_{\boldsymbol{\alpha}, O}^{(j)} \right) \hat{E}^T$ is a (normalised) state in \mathcal{H}_B . Moreover, since $\bigotimes_{j=1}^m \sigma_{\boldsymbol{\alpha}, O}^{(j)} = \bigotimes_{j=1}^m \sigma_{\tilde{\boldsymbol{\alpha}}, O}^{(j)}$ for all $\tilde{\boldsymbol{\alpha}} \sim_O \boldsymbol{\alpha}$ by Lemma C.3, $\left(\bigotimes_{j=1}^m \sigma_{\boldsymbol{\alpha}, O}^{(j)} \right) \hat{E}^T$ is the same state for each $\tilde{\boldsymbol{\alpha}} \in \mathcal{A}_{\boldsymbol{\alpha}, O}$, and hence so is $\mathcal{F} \left(\left(\bigotimes_{j=1}^m \sigma_{\boldsymbol{\alpha}, O}^{(j)} \right) \hat{E}^T \right)$. For simplicity, let us replace the notation $\mathcal{F} \left(\left(\bigotimes_{j=1}^m \sigma_{\boldsymbol{\alpha}, O}^{(j)} \right) \hat{E}^T \right)$ by $\rho_{\sim_O \boldsymbol{\alpha}}$. With this notation and invoking the assumption on $P(\boldsymbol{\alpha}, O)$, Equation (159) becomes

$$\begin{aligned} & \sum_{\boldsymbol{\alpha}, O} \langle \boldsymbol{\alpha}, O |_{\mathbf{A}, \mathbf{O}} \langle \boldsymbol{\alpha}, O |_{\mathbf{A}', \mathbf{O}'} \left(\sum_{\boldsymbol{\alpha}, O} \frac{P(O)}{|\mathcal{A}|^n} |\boldsymbol{\alpha}, O \rangle \langle \boldsymbol{\alpha}, O| \otimes \rho_{\sim_O \boldsymbol{\alpha}} \right) |\boldsymbol{\alpha}, O \rangle_{\mathbf{A}, \mathbf{O}} |\boldsymbol{\alpha}, O \rangle_{\mathbf{A}', \mathbf{O}'} \\ &= \frac{1}{|\mathcal{A}|^n} \sum_{\boldsymbol{\alpha}, O} P(O) \langle \boldsymbol{\alpha}, O |_{\mathbf{A}', \mathbf{O}'} \rho_{\sim_O \boldsymbol{\alpha}} |\boldsymbol{\alpha}, O \rangle \end{aligned} \quad (160)$$

$$= \frac{1}{|\mathcal{A}|^n} \sum_O P(O) \sum_{\boldsymbol{\alpha} \in \mathcal{A}^n / \sim_O} \sum_{\tilde{\boldsymbol{\alpha}} \sim_O \boldsymbol{\alpha}} \langle \tilde{\boldsymbol{\alpha}}, O |_{\mathbf{A}', \mathbf{O}'} \rho_{\sim_O \boldsymbol{\alpha}} |\tilde{\boldsymbol{\alpha}}, O \rangle \quad (161)$$

where we are abusing notation slightly by denoting by α the equivalence class $[\alpha] \in \mathcal{A}^n / \sim_O$. Since $\rho_{\sim_O \alpha}$ is a normalised state for every α, O and the term $\sum_{\tilde{\alpha} \sim_O \alpha} \langle \tilde{\alpha}, O |_{\mathbf{A}', \mathbf{O}'} \rho_{\sim_O \alpha, O} | \tilde{\alpha}, O \rangle$ can be interpreted as part of the trace over $\rho_{\sim_O \alpha}$, we thus have

$$\sum_{\tilde{\alpha} \sim_O \alpha} \langle \tilde{\alpha}, O |_{\mathbf{A}', \mathbf{O}'} \rho_{\sim_O \alpha, O} | \tilde{\alpha}, O \rangle \leq 1 \quad (162)$$

Thus,

$$\frac{1}{|\mathcal{A}|^n} \sum_O P(O) \sum_{\alpha \in \mathcal{A}^n / \sim_O} \sum_{\tilde{\alpha} \sim_O \alpha} \langle \tilde{\alpha}, O |_{\mathbf{A}', \mathbf{O}'} \rho_{\sim_O \alpha} | \tilde{\alpha}, O \rangle \leq \frac{1}{|\mathcal{A}|^n} \sum_O P(O) \sum_{\alpha \in \mathcal{A}^n / \sim_O} 1 \quad (163)$$

$$= \frac{1}{|\mathcal{A}|^n} \sum_O \frac{P(O) |\mathcal{A}|^n}{2^{|O|}} \quad (164)$$

$$= \frac{1}{|\mathcal{O}|} \sum_O \frac{P(O)}{2^{|O|}} \quad (165)$$

Since this holds for any pair (\hat{E}, \mathcal{F}) , it in particular also holds for the one that maximises the trace, so

$$\max_E \text{Tr}_{\mathbf{A}, \mathbf{O}, \mathbf{A}', \mathbf{O}'} \left[D_{\text{client}}^{(m)} E^T \left(\sum_{\alpha, O} |\alpha, O, \alpha, O\rangle \langle \alpha, O, \alpha, O|_{\mathbf{A}, \mathbf{O}, \mathbf{A}', \mathbf{O}'} \right) \right] \leq \sum_O \frac{P(O)}{2^{|O|}} \quad (166)$$

proving the theorem. \square

D Grey Box MBQC Supplementary

D.1 Correctness of σ_{MBQC}^g

Proposition D.1. *Let g be a gflow for (G, I, O, ω) where G is a graph on vertices V , let σ_{MBQC}^g be defined as in Equation (55), and let $\mathcal{M}_{\alpha_i, i, \omega(i)}^{c_i}$ denote the c_i measurement outcome of the measurement channels defined in Equation (56) ($c_i = 0$ for positive outcome and $c_i = 1$ for the negative outcome). Then*

$$\left(\bigotimes_{i \in V \setminus O} \mathcal{M}_{\alpha_i, i, \omega(i)}^{c_i} \right) * \sigma_{\text{MBQC}}^g * \rho_G \quad (167)$$

is the same state for all $\mathbf{c} = c_1 \dots c_{|V \setminus O|}$.

Proof. The proposition is a consequence of the fact that σ_{MBQC}^g is defined directly from gflow, and essentially follows the same reasoning as that presented in Appendix A.2 but written in the combs formalism and for general measurement planes. We write out the details in part to highlight that no issues arise with the choice of ordering of X and Z operators in Equation (53). We proceed by showing that the state produced by any series of measurement outcomes is the same as that produced by all positive measurement outcomes (which encodes the computation for the MBQC):

$$\left(\bigotimes_{i \in V \setminus O} \mathcal{M}_{\alpha_i, i, \omega(i)}^{c_i} \right) * \sigma_{\text{MBQC}}^g * \rho_G = \left(\bigotimes_{i \in V \setminus O} \mathcal{M}_{\alpha_i, i, \omega(i)}^0 \right) * \sigma_{\text{MBQC}}^g * \rho_G \quad (168)$$

Consider first only a single measurement channel for qubit $i \in V \setminus O$, which obtains the negative outcome:

$$\mathcal{M}_{\alpha_i, i, \omega(i)}^1 * \sigma_{\text{MBQC}}^g * \rho_G = \left(|1\rangle\langle 1| \otimes |-\alpha_i\rangle\langle -\alpha_i|_{\omega(i)} \right) * \sigma_{\text{MBQC}}^g * \rho_G \quad (169)$$

By the definition of gflow, we are guaranteed that

$$|-\alpha_i\rangle\langle -\alpha_i|_{\omega(i)} \equiv K_{g(i)}|_i^\dagger |+\alpha_i\rangle\langle +\alpha_i|_{\omega(i)} K_{g(i)}|_i \quad (170)$$

where $K_{g(i)}|_i$ denotes the operator which appears as the tensor factor of i in the stabiliser $K_{g(i)}$. Thus, using the properties of the link product and also that $K_{g(i)}|_i^\dagger \equiv K_{g(i)}|_i^T$ (in fact $K_v^\dagger = K_v^T$ for all stabilisers K_v), we have

$$\left(|1\rangle\langle 1| \otimes |-\alpha_i\rangle\langle -\alpha_i|_{\omega(i)}\right) * \sigma_{\text{MBQC}}^g * \rho_G = \left(|1\rangle\langle 1| \otimes K_{g(i)}|_i^\dagger |+\alpha_i\rangle\langle +\alpha_i|_{\omega(i)} K_{g(i)}|_i\right) * \sigma_{\text{MBQC}}^g * \rho_G \quad (171)$$

$$= \left(|1\rangle\langle 1| \otimes |+\alpha_i\rangle\langle +\alpha_i|_{\omega(i)}\right) * K_{g(i)}|_i \sigma_{\text{MBQC}}^g K_{g(i)}|_i^\dagger * \rho_G \quad (172)$$

By contracting the link product over C_i and writing σ_{MBQC}^g in the form of Equation (55), we get

$$|+\alpha_i\rangle\langle +\alpha_i|_{\omega(i)} * \left(\sum_{\mathbf{a}, \mathbf{b}, \mathbf{c}|_{\setminus i}} K_{g(i)}|_i U_{\text{corr}(1\mathbf{c}|_{\setminus i})} |\mathbf{a}\rangle\langle \mathbf{b}| U_{\text{corr}(1\mathbf{c}|_{\setminus i})}^\dagger K_{g(i)}|_i^\dagger \otimes |\mathbf{c}|_{\setminus i} \mathbf{a}\rangle\langle \mathbf{c}|_{\setminus i} \mathbf{b}\right) * \rho_G \quad (173)$$

where the sum over $\mathbf{c}|_{\setminus i}$ indicates the sum over basis element of all the \mathcal{H}_{C_j} for $j \neq i$ and $1\mathbf{c}|_{\setminus i}$ denotes the binary string \mathbf{c} with the entry corresponding to C_i a 1 and the other entries given by $\mathbf{c}|_{\setminus i}$. By the definition of the correction sets \mathcal{X}_j and \mathcal{Z}_j , as well as the definition of $U_{\text{corr}(\mathbf{c})}$, we can write

$$U_{\text{corr}(1\mathbf{c}|_{\setminus i})} = (-1)^{f(\mathbf{c}|_{\setminus i})} U_{\text{corr}(0\mathbf{c}|_{\setminus i})} K_{g(i)}|_{\setminus i} \quad (174)$$

where the exponent $f(\mathbf{c}|_{\setminus i})$ encodes the coefficient that arises from commuting the factors of $K_{g(i)}|_{\setminus i}$ through the other factors of $U_{\text{corr}(1\mathbf{c}|_{\setminus i})}$ and where $U_{\text{corr}(0\mathbf{c}|_{\setminus i})}$ denotes the correction operator with $c_i = 0$. In particular, this means that

$$K_{g(i)}|_i U_{\text{corr}(1\mathbf{c}|_{\setminus i})} = (-1)^{f(\mathbf{c}|_{\setminus i})+t_i} U_{\text{corr}(0\mathbf{c}|_{\setminus i})} K_{g(i)}|_i K_{g(i)}|_{\setminus i} \quad (175)$$

$$= (-1)^{f(\mathbf{c}|_{\setminus i})+t_i} U_{\text{corr}(0\mathbf{c}|_{\setminus i})} K_{g(i)} \quad (176)$$

where t_i encodes the coefficient arises from commuting $K_{g(i)}|_i$ through $U_{\text{corr}(0\mathbf{c}|_{\setminus i})}$. Since the same coefficient arises from the conjugate term (i.e. $U_{\text{corr}(1\mathbf{c}|_{\setminus i})}^\dagger K_{g(i)}|_i^\dagger$), the net result is that no -1 factor can appear. That is, we have

$$K_{g(i)}|_i U_{\text{corr}(1\mathbf{c}|_{\setminus i})}(\cdot) U_{\text{corr}(1\mathbf{c}|_{\setminus i})}^\dagger K_{g(i)}|_i^\dagger = U_{\text{corr}(0\mathbf{c}|_{\setminus i})} K_{g(i)}(\cdot) K_{g(i)}^\dagger U_{\text{corr}(0\mathbf{c}|_{\setminus i})}^\dagger \quad (177)$$

The cancelling of any phase factor arising from commuting X and Z factors in $U_{\text{corr}(\mathbf{c})}$ is the reason why the ordering in Equation (53) is justified. Continuing from Equation (173), we have

$$|+\alpha_i\rangle\langle +\alpha_i|_{\omega(i)} * \left(\sum_{\mathbf{a}, \mathbf{b}, \mathbf{c}|_{\setminus i}} U_{\text{corr}(0\mathbf{c}|_{\setminus i})} K_{g(i)} |\mathbf{a}\rangle\langle \mathbf{b}| K_{g(i)}^\dagger U_{\text{corr}(0\mathbf{c}|_{\setminus i})}^\dagger \otimes |\mathbf{c}|_{\setminus i} \mathbf{a}\rangle\langle \mathbf{c}|_{\setminus i} \mathbf{b}\right) * \rho_G \quad (178)$$

$$= |+\alpha_i\rangle\langle +\alpha_i|_{\omega(i)} * \left(\sum_{\mathbf{a}, \mathbf{b}, \mathbf{c}|_{\setminus i}} U_{\text{corr}(0\mathbf{c}|_{\setminus i})} |\mathbf{a}\rangle\langle \mathbf{b}| U_{\text{corr}(0\mathbf{c}|_{\setminus i})}^\dagger \otimes |\mathbf{c}|_{\setminus i} \mathbf{a}\rangle\langle \mathbf{c}|_{\setminus i} \otimes K_{g(i)} |\mathbf{a}\rangle\langle \mathbf{b}| K_{g(i)}^\dagger\right) * \rho_G \quad (179)$$

$$\equiv \left(|0\rangle\langle 0| \otimes |+\alpha_i\rangle\langle +\alpha_i|_{\omega(i)}\right) * K_{g(i), A'} \sigma_{\text{MBQC}}^g K_{g(i), A'}^\dagger * \rho_G \quad (180)$$

$$= \mathcal{M}_{\alpha_i, i, \omega(i)}^0 * \sigma_{\text{MBQC}}^g * K_{g(i)} \rho_G K_{g(i)}^\dagger \quad (181)$$

$$= \mathcal{M}_{\alpha_i, i, \omega(i)}^0 * \sigma_{\text{MBQC}}^g * \rho_G \quad (182)$$

where the extra subscript A' on the operators in Equation (180) indicate that they act on the appropriate spaces A'_j rather than A_j as before, and can thus be transferred to the ρ_G via the properties of the link product (which also uses the fact that $K_{g(i)}^\dagger = K_{g(i)}^T$). We have also made use of properties of the Choi operator in Equation (179) to transfer the $K_{g(i)}$ from the A -spaces to the A' -spaces in the first place.

Since the left-hand side of Equation (168) contains a tensor product of terms $\mathcal{M}_{\alpha_i, i, \omega(i)}^{c_i}$, we can apply the same reasoning as above to each factor for which $c_i = 1$ which thus establishes that Equation (168) does indeed hold for any measurement outcomes \mathbf{c} . This means that once all the link products are evaluated, which in particular includes the trace over all spaces except for $\bigotimes_{i \in O} \mathcal{H}_{A_i}$, the same state is produced on the output space. \square

D.2 Gflow-Induced Quantum Causal Models

This subsection provides some further details regarding the the quantum causal model (QCM) induced by gflow for MBQC and thus supports Section 5.2 in the main text. Firstly, we confirm here that gflow does indeed define a DAG, which is a requirement for showing Proposition 5.1. Thereafter we provide a table that elucidates the comparisons between the components of the QCM defined for MBQC and the components of classical causal models as presented eg., by Pearl in [21].

Proposition D.2. *Let (G, I, O, ω) be such that a gflow exists and let $(g, <)$ be a choice of such a gflow. The directed graph \overline{G} on vertex set V and edge set defined from the gflow via*

$$E := \{(i, j) \in V \times V \mid j \in V, i \in \mathcal{X}_j \cup \mathcal{Z}_j\}$$

is acyclic.

Proof. Suppose for a contradiction that \overline{G} is not acyclic, that is, there exists a directed path $v_0 \rightarrow v_1 \rightarrow \dots \rightarrow v_k = v_0$ for some sequence of vertices v_0, \dots, v_k . By the definition of the edge set of \overline{G} , it follows that either $v_{i+1} \in g(v_i) \setminus \{v_i\}$ or $v_i \neq v_{i+1} \in \text{Odd}(g(v_i))$. In either case $v_i < v_{i+1}$ in the ordering of the given gflow. Thus, $v_0 < v_k = v_0$ by transitivity of the order, which gives the desired contradiction as the order is strict by definition. \square

Classical causal models are typically presented as consisting of a set of observed variables $V = \{V_1, \dots, V_n\}$ (those within the model), a set of unobserved variables $U = \{U_1, \dots, U_n\}$ (those determined by factors outside of the model), a DAG that specifies which variables (both unobserved and observed) that have a causal influence on a given observed variable, and set of functions $F = \{f_i : \text{Pa}(V_i) \cup U_i \rightarrow V_i\}_{i=1}^n$ that map from the parents of a variable to the variable itself. These functions are often called structural equations and uniquely specify the values for the observed variables given values of the unobserved variables. A probabilistic causal model further includes a distribution $P(U)$ over the unobserved variables. Using this terminology, the following table outlines the correspondence between classical causal models and the QCM σ_{MBQC}^g defined in Section 5.2.

Comparing the QCM σ_{MBQC}^g to Classical Causal Models				
Classical Causal Model MBQC QCM σ_{MBQC}^g	Unobserved Variable U_i Input Space $\mathcal{H}_{A'_i}$	Observed Variable V_i Quantum Node $\mathcal{H}_{A_i} \otimes \mathcal{H}_{C_i}$	$f_i : \text{Pa}(V_i) \cup U_i \rightarrow V_i$ $\rho_{A_i C_{j:j \in \text{Pa}(i)}, A'_i}$	DAG \overline{G}

D.3 Causal Equivalence of Gflows

Proof of Proposition 5.2. Consider

$$\left(\bigotimes_{j=1}^{|V \setminus O|} |c_j\rangle\langle c_j|_{C_j} \right) * \sigma_{\text{MBQC}}^g * \rho_G \quad (183)$$

for some $g \sim (G, I, O, \omega)$. Evaluating the link product over the C_j gives

$$\left(\sum_{\mathbf{a}, \mathbf{b}} U_{\text{corr}(\mathbf{c})}^g |\mathbf{a}\rangle\langle \mathbf{b}| (U_{\text{corr}(\mathbf{c})}^g)^\dagger \otimes |\mathbf{a}\rangle\langle \mathbf{b}| \right) * \rho_G = \left(\sum_{\mathbf{a}, \mathbf{b}} |\mathbf{a}\rangle\langle \mathbf{b}| \otimes |\mathbf{a}\rangle\langle \mathbf{b}| \right) * U_{\text{corr}(\mathbf{c})}^g \rho_G (U_{\text{corr}(\mathbf{c})}^g)^\dagger \quad (184)$$

where $\mathbf{c} = c_1 \dots c_{|V \setminus O|}$. To prove the proposition, it suffices to show that all the $U_{\text{corr}(\mathbf{c})}^g$ as g varies are mutually related by stabilisers of G for each \mathbf{c} , up to a phase (which is cancelled by the corresponding conjugate phase from the adjoint $(U_{\text{corr}(\mathbf{c})}^g)^\dagger$).

Let $g, g' \sim (G, I, O, \omega)$ be arbitrary. By definition of $U_{\text{corr}(\mathbf{c})}$, we have

$$U_{\text{corr}(\mathbf{c})}^g \propto \prod_{j=1}^{|V \setminus O|} K_{g(j)}^{c_j} |_{\setminus j} \quad (185)$$

$$U_{\text{corr}(\mathbf{c})}^{g'} \propto \prod_{j=1}^{|V \setminus O|} K_{g'(j)}^{c_j} |_{\setminus j} \quad (186)$$

where \propto denotes that a -1 phase may arise from commuting X and Z operators to arrive at the above form of the operator in terms of $K_{g(j)}$ from the canonical form of $U_{\text{corr}(\mathbf{c})}^g$ (respectively $U_{\text{corr}(\mathbf{c})}^{g'}$) as in Equation (54) and Equation (53). Despite that $K_{g(j)}$ and $K_{g'(j)}$ may be different stabilisers, by the fact that both g and g' observe the same measurement planes, the j th tensor factor of each is the same. Thus,

$$U_{\text{corr}(\mathbf{c})}^g \propto \left(\bigotimes_{l=1}^{|V \setminus O|} K_{g(l)}^{c_l} |_l \right) \prod_{j=1}^{|V \setminus O|} K_{g(j)} \quad (187)$$

$$= \left(\bigotimes_{l=1}^{|V \setminus O|} K_{g(l)}^{c_l} |_l \right) \prod_{j=1}^{|V \setminus O|} K_{g'(j)} K_{g'(j)} K_{g(j)} \quad (188)$$

$$= \left(\bigotimes_{l=1}^{|V \setminus O|} K_{g'(l)}^{c_l} |_l \right) \left(\prod_{j=1}^{|V \setminus O|} K_{g'(j)} \right) \left(\prod_{i=1}^{|V \setminus O|} K_{g'(i)} K_{g(i)} \right) \quad (189)$$

$$\propto U_{\text{corr}(\mathbf{c})}^{g'} \left(\prod_{i=1}^{|V \setminus O|} K_{g(i)} K_{g'(i)} \right) \quad (190)$$

The restriction to only those gflows $g \sim (G, I, O, \omega)$ that have mutually compatible partial orders that is made in the statement of the proposition is required when considering σ_{MBQC}^g with a total order on input and output spaces. \square

D.4 Gflow Catalogue

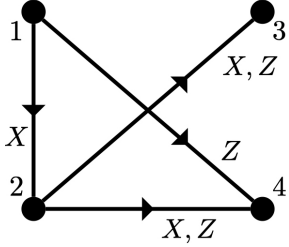
Figure 8, Figure 9, and Figure 10 depict the DAGs corresponding to the 15 different gflows for the four-vertex graph considered in Section 5 and depicted in Figure 6a, grouped by the assigned measurement plane for the second qubit (the first is always measured in the XY -plane). The details of the gflow and corresponding $U_{\text{corr}(\mathbf{c})}$ for each DAG are given in the caption.

E Details of SDP Implementation

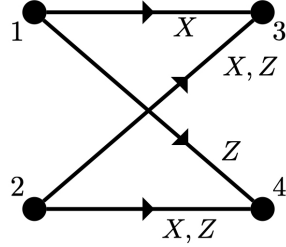
The numerical calculations of the guessing probabilities throughout this work made use of the convex optimisation library CVXPY [73, 74]. We primarily used the Splitting Conic Solver (SCS) [75, 76]. Our code is provided at [72]. Calculations were run on an HP Z4 G4 9980XE workstation.

To provide some indication of the limitations of the numerical approach in its current form, to complement those detailed in Section 6.1, we document here some of hurdles we faced when calculating guessing probabilities. For the BQC examples, we generated the classical combs as 1-dimensional objects representing the corresponding diagonals. Despite this, size issues played a role when storing the combs even before calling the SDP solver: D_{client} for a single round and for any \mathcal{A} of size greater than 12 and $D_{\text{client}}^{(2)}$ for \mathcal{A} of size greater than 4 caused problems. The guessing probability for $D_{\text{client}}^{(1)}$ for $|\mathcal{A}| = 4$ was calculated within a day, whereas for $|\mathcal{A}| = 8$, it took on the order of a week and required approximately 110GB of RAM. Attempting to calculate the guessing probability for $D_{\text{client}}^{(2)}$ with $|\mathcal{A}| = 4$ exceeded the available RAM of the machine.

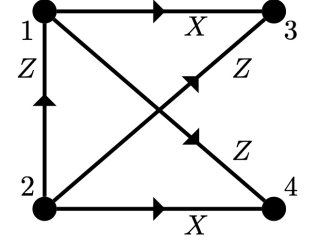
For the Grey Box MBQC examples, the guessing probabilities for all single round combs could be calculated quickly (on the order of minutes) however all multi-round combs again caused size problems. Typically, the primary bottleneck occurred when enforcing the comb constraints (i.e. sequential partial trace constraints) on the variable in the SDP solver, which tended to dominate the runtime of the algorithm. Otherwise, some size error would occur during the Cone Matrix Stuffing reduction phase of the solver (see the CVXPY documentation for details).



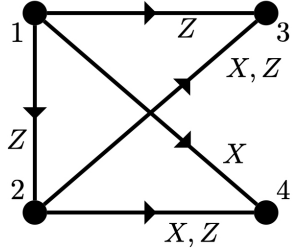
(a) $g_1 : 1 \mapsto \{2\}, 2 \mapsto \{3, 4\}$,
 $U_{\text{corr}(c)}^{g_1} = X_2^{c_1} \otimes X_3^{c_2} Z_3^{c_2} \otimes X_4^{c_2} Z_4^{c_1 c_2}$



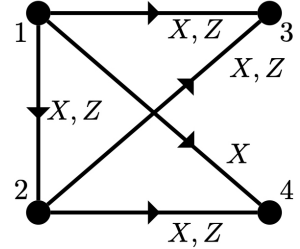
(b) $g_2 : 1 \mapsto \{3\}, 2 \mapsto \{3, 4\}$,
 $U_{\text{corr}(c)}^{g_2} = X_3^{c_1 c_2} Z_3^{c_2} \otimes X_4^{c_2} Z_4^{c_1 c_2}$



(c) $g_3 : 1 \mapsto \{3\}, 2 \mapsto \{4\}$,
 $U_{\text{corr}(c)}^{g_3} = Z_1^{c_2} \otimes X_3^{c_1} Z_3^{c_2} \otimes X_4^{c_2} Z_4^{c_1}$

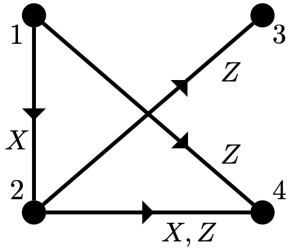


(d) $g_4 : 1 \mapsto \{4\}, 2 \mapsto \{3, 4\}$,
 $U_{\text{corr}(c)}^{g_4} = Z_2^{c_1} \otimes X_3^{c_2} Z_3^{c_1 c_2} \otimes X_4^{c_1 c_2} Z_4^{c_2}$

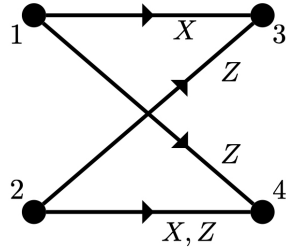


(e) $g_5 : 1 \mapsto \{2, 3, 4\}, 2 \mapsto \{3, 4\}$,
 $U_{\text{corr}(c)}^{g_5} = X_2^{c_1} Z_2^{c_1} \otimes X_3^{c_1 c_2} Z_3^{c_1 c_2} \otimes X_4^{c_1 c_2} Z_4^{c_2}$

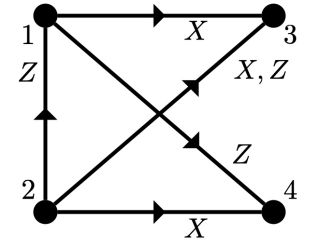
Figure 8: (a) - (e) display the directed acyclic graphs and correction operators for the gflows g_1, \dots, g_5 respectively which are compatible with (G, I, O, ω) where $\omega(1) = \omega(2) = XY$. The corresponding captions detail the gflows themselves and the associated $U_{\text{corr}(c)}$. The partial order for g_1, g_2, g_4 and g_5 is given by $1 < 2$, and that for g_3 is $2 < 1$.



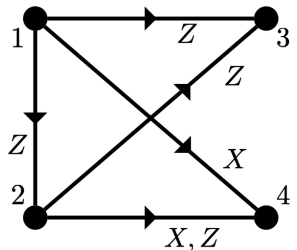
(a) $g_6 : 1 \mapsto \{2\}, 2 \mapsto \{2, 4\}$,
 $U_{\text{corr}(c)}^{g_6} = X_2^{c_1} \otimes Z_3^{c_2} \otimes X_4^{c_2} Z_4^{c_1 c_2}$



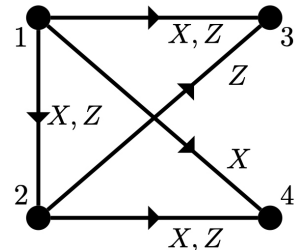
(b) $g_7 : 1 \mapsto \{3\}, 2 \mapsto \{2, 4\}$,
 $U_{\text{corr}(c)}^{g_7} = X_3^{c_1} Z_3^{c_2} \otimes X_4^{c_2} Z_4^{c_1 c_2}$



(c) $g_8 : 1 \mapsto \{3\}, 2 \mapsto \{2, 3, 4\}$,
 $U_{\text{corr}(c)}^{g_8} = Z_1^{c_2} \otimes X_3^{c_1 c_2} Z_3^{c_2} \otimes X_4^{c_2} Z_4^{c_1}$

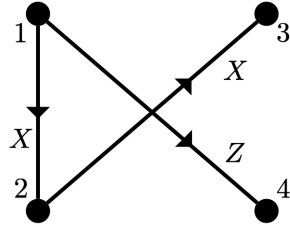


(d) $g_9 : 1 \mapsto \{4\}, 2 \mapsto \{2, 4\}$,
 $U_{\text{corr}(c)}^{g_9} = Z_2^{c_1} \otimes Z_3^{c_1 c_2} \otimes X_4^{c_1 c_2} Z_4^{c_2}$

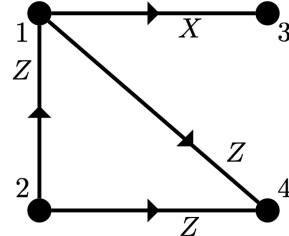


(e) $g_{10} : 1 \mapsto \{2, 3, 4\}, 2 \mapsto \{2, 4\}$,
 $U_{\text{corr}(c)}^{g_{10}} = X_2^{c_1} Z_2^{c_1} \otimes X_3^{c_1} Z_3^{c_1 c_2} \otimes X_4^{c_1 c_2} Z_4^{c_2}$

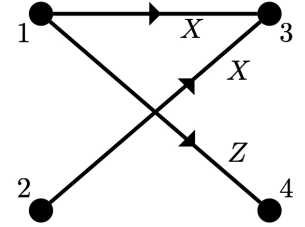
Figure 9: (a) - (e) display the directed acyclic graphs and correction operators for the gflows g_6, \dots, g_{10} respectively which are compatible with (G, I, O, ω) where $\omega(1) = XY$ and $\omega(2) = XZ$. The corresponding captions detail the gflows themselves and the associated $U_{\text{corr}(c)}$. The partial order for g_6, g_7, g_9 and g_{10} is given by $1 < 2$, and that for g_8 is $2 < 1$.



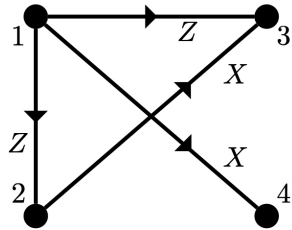
(a) $g_{11} : 1 \mapsto \{2\}, 2 \mapsto \{2, 3\}$,
 $U_{\text{corr}(c)}^{g_{11}} = X_2^{c_1} \otimes X_3^{c_2} \otimes Z_4^{c_1}$



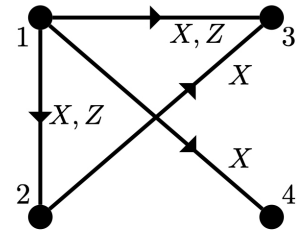
(b) $g_{12} : 1 \mapsto \{3\}, 2 \mapsto \{2\}$,
 $U_{\text{corr}(c)}^{g_{12}} = Z_1^{c_2} \otimes X_3^{c_1} \otimes Z_4^{c_1 c_2}$



(c) $g_{13} : 1 \mapsto \{3\}, 2 \mapsto \{2, 3\}$,
 $U_{\text{corr}(c)}^{g_{13}} = X_3^{c_1 c_2} \otimes Z_4^{c_1}$



(d) $g_{14} : 1 \mapsto \{4\}, 2 \mapsto \{2, 3\}$,
 $U_{\text{corr}(c)}^{g_{14}} = Z_2^{c_1} \otimes X_3^{c_2} Z_3^{c_1} \otimes X_4^{c_1}$



(e) $g_{15} : 1 \mapsto \{2, 3, 4\}, 2 \mapsto \{2, 3\}$,
 $U_{\text{corr}(c)}^{g_{15}} = X_2^{c_1} Z_2^{c_1} \otimes X_3^{c_1 c_2} Z_3^{c_1} \otimes X_4^{c_1}$

Figure 10: (a) - (e) display the directed acyclic graphs and correction operators for the gflows g_{11}, \dots, g_{15} respectively which are compatible with (G, I, O, ω) where $\omega(1) = XY$ and $\omega(2) = YZ$. The corresponding captions detail the gflows themselves and the associated $U_{\text{corr}(c)}$. The partial order for g_{11}, g_{13}, g_{14} and g_{15} is given by $1 < 2$, and that for g_{12} is $2 < 1$.

F Whose Prior?

Throughout this work, we have considered combs of the form $\sum_x P(x) |x\rangle\langle x| \otimes \sigma_x$. As made particularly apparent in Section 3.1 (in conjunction with Appendix B), the distribution $P(x)$ can be considered as a prior distribution and the min-entropy for such a comb can be interpreted in terms of a maximum over posterior distributions. One might then ask, *whose* prior is it? The natural answer seems to be that it is the prior of the agent interacting with the system in each case: the server in the BQC protocol or the user of the MBQC device. As such, the operators D_{client} , D_{gflow} , D_{mp} or D_{calibr} can be considered as a model of the client internal to the server in the former case, or as models of the MBQC device internal to the user in the latter three cases. With this interpretation, it is interesting to reconsider D_{gflow} and D_{mp} : they essentially consist of the same components but via a slight difference in their composition, which is to say, a slight difference in the internal representation of the system by the agent, the agent learns about a different property of the system.

From a practical point of view, the presence of the prior distribution, as in any Bayesian updating, also allows for the inputting of specific knowledge of the problem into the calculation of the min-entropy. Throughout, we have typically taken prior distributions to be uniform in order to simplify the numerics, however this need not be the case. For example, in the BQC example, the assumption that the client chooses a computation uniformly at random is not necessarily a reasonable one - most known quantum algorithms have specific structure which would correspond to the requirement that certain entries of α to specific values. This does, however, seem to pose a slight dilemma - since changing the prior changes the value for the min-entropy, is it really acceptable to have a proof of security for a protocol that depends on the (subjective) prior of the server?